DOE F 4650.2
(10-91)
(All Other Editions Are Obsolete)

OMB Control No.
1910-1400
(OMB Burden Disclosure Statement on Back)

Office of Science (SC

Face Page

TITLE OF PROPOSED RESEARCH:

1. CATALOG OF FEDERAL DOMESTIC ASSISTANCE #
   81.049

2. CONGRESSIONAL DISTRICT:
   Applicant Organization's District: _____
   Project Site's District: _____

3. I.R.S. ENTITY IDENTIFICATION OR SSN:

4. AREA OF RESEARCH OR ANNOUNCEMENT TITLE/#:

5. HAS THIS RESEARCH PROPOSAL BEEN SUBMITTED
   TO ANY OTHER FEDERAL AGENCY?
   YES   NO

   PLEASE LIST _____

6. DOE/OER PROGRAM STAFF CONTACT (if known):

7. TYPE OF APPLICATION:
   New   Renewal
   Continuation   Revision
   Supplement

8. ORGANIZATION TYPE:
   Local Govt.   State Govt.
   Non-Profit   Hospital
   Indian Tribal Govt.   Individual
   Other   Inst. of Higher Educ.
   For-Profit
     Small Business   Disadvan. Business
     Women-Owned   8(a)

9. CURRENT DOE AWARD # (IF APPLICABLE):

10. WILL THIS RESEARCH INVOLVE:
   10A. Human Subjects   No   If yes
        Exemption No. _____ or
        IRB Approval Date _____
        Assurance of Compliance No: _____
   10A. Vertebrate Animals   No   If yes
        IACUC Approval Date _____ or
        Animal Welfare Assurance No: _____

11. AMOUNT REQUESTED FROM DOE FOR ENTIRE
    PROJECT PERIOD $ _____

12. DURATION OF ENTIRE PROJECT PERIOD:
    _____ to _____
    MM/DD/YY   MM/DD/YY

13. REQUESTED AWARD START DATE
    _____
    MM/DD/YY

14. IS APPLICANT DELINQUENT ON ANY FEDERAL DEBT?
    Yes (attach an explanation)   No

15. PRINCIPAL INVESTIGATOR/PROGRAM DIRECTOR
    * NAME _____
    TITLE _____
    ADDRESS _____
    _____
    _____
    PHONE NUMBER _____

16. ORGANIZATION'S NAME _____
    ADDRESS _____
    _____
    _____
    _____

    CERTIFYING REPRESENTATIVE'S
    * NAME _____
    TITLE _____
    PHONE NUMBER _____

SIGNATURE OF PRINCIPAL INVESTIGATOR/ PROGRAM DIRECTOR
(please type in full name if electronically submitted)
*Date _____

PI/PD ASSURANCE: I agree to accept responsibility for the scientific conduct of the project and to provide the required progress reports if an award is made as a result of this submission. Willful provision of false information is a criminal offense. (U.S. Code, Title 18, Section 1001).

SIGNATURE OF ORGANIZATION'S CERTIFYING REPRESENTATIVE
(please type in full name if electronically submitted)
*Date _____

CERTIFICATION and ACCEPTANCE: I certify that the statements herein are true and complete to the best of my knowledge, and accept the obligation to comply with DOE terms and conditions if an award is made as the result of this submission. A willfully false certification is a criminal offense. (U.S. Code, Title 18, Section 1001).

Los Alamos

Los Alamos National Laboratory
Los Alamos, New Mexico 87545

FIELD WORK PROPOSAL
FOR DOE PROGRAMS

1. Work Proposal Number SCFY05E870	1.A Program Code E870	2. Revision Number	3. Date Prepared 7/11/05	MTA	AA

4. Work Proposal Title Compressional Heating of a Compact Toroid Plasma to Fusion Conditions	5. Budget and Reporting Code AT5015020

6. Work Proposal Term (Include Months/Days/Years) Begin 10/01/05 End 09/30/09	7. Is this work proposal included in the institutional Plan? X Yes No

8. DOE Program Manager Francis Thio	Telephone Number 301-903-4678
9. Operations Office Work Proposal	Telephone Number
10. Contractor Program Manager Glen A. Wurden	Telephone Number 505-667-5633
11.A Contractor Principal Investigator Thomas P. Intrator	Telephone Number 505-665-2927

Headquarters Organization OFES	12. Operations Office ALBUQUERQUE	13. Contractor Name LOS ALAMOS NATIONAL LABORATORY
14. DOE Organization CODE SC-55	15. Operations Office Code AL	16. Code 03

17. Work Proposal Description

We propose a four-year (FY06-09) program to demonstrate compressional heating of a compact toroid plasma within a converging flux-conserving boundary to fusion conditions, also known as magnetized target fusion (MTF). MTF is a potentially low cost path to fusion energy that is intermediate in plasma regime between magnetic (MFE) and inertial fusion energy. We will demonstrate MTF by using a field-reversed configuration (FRC) as our magnetized target plasma and an imploding metal liner for compression. These choices take advantage of significant past scientific and technical accomplishments in MFE and Defense Programs research and should yield substantial plasma performance $n\tau > 10^{13}$ s·cm^{-3}, T > 5 keV) using an available pulsed-power implosion facility at modest cost. We have recently achieved the required FRC pressure and are within a factor of 2-3 of the required FRC lifetime. The proposed work will demonstrate stable translation of the target FRC into a static liner followed by the construction and operation of the first integrated liner-on-plasma compression experiments. This proposal responds to MFE Goal 2 of the Integrated Program Planning Activity for the DOE Fusion Energy Sciences Program, as well as several stated goals in the recent FESAC Priorities Panel report. The national MTF effort is a collaboration between multiple institutions including LANL, AFRL, LLNL, General Atomics, U. Washington, U. New Mexico, U. Wisconsin-Madison, and U. Nevada-Reno.

18. Contractor Work Proposal Manager (Signature) *Glen A. Wurden*	Date 7/11/05	19. Operations Office Review Official (Signature)	Date

20. Detail Attachments (See Attachments)

x	a.	Facility Requirements	x	e.	Approach	☐ l.	Environmental Assessment
x	b.	Publications	x	f.	Technical Progress	x j.	Explanation of Milestones
x	c.	Purpose	x	g.	Future Accomplishments	☐ k.	Other (Specify)
x	d.	Background	x	h.	Relationships to Other Projects		

Los Alamos

Los Alamos National Laboratory
Los Alamos, New Mexico 87545

<div align="right">

**FIELD WORK PROPOSAL
FOR DOE PROGRAMS**

</div>

OBLIGATIONS AND COSTS

Pg. 2

Contractor Name	Work Proposal Number	Program Code	Revision Number	Date Prepared
Los Alamos National Laboratory	SCFY05E870	E870		07/11/05

21. Staffing (in staff years)	PRIOR YEARS (optional)	FY- 2005 (BY-2)	(BY-1) FY - 2006 President's	Revised	(BY) FY - 2007 Guidance	Request	
a. Scientific		3.3	2.95	0.00	2.95	0.00	
b. Other Direct		2.4	2.33	0.00	2.33	0.00	
c. Total Direct		5.7	5.28	0.00	5.28	0.00	
22. Operating Expense (in thousands) a. Total Obligations (BA)		1,417	1,500	0	1,540	0	
b. Total Costs (BO)		1,447	1,500	0	1,540	0	
23. Equipment (in thousands) a. Equipment Obligations (BA)		0	0	0	0	0	
b. Equipment Costs (BO)		0	0	0	0	0	

24. Five Year Plan (in thousands) constant BY $	(BY+1) FY- 2008	(BY+2) FY- 2009	(BY+3) FY- 2010	(BY+4) FY- 2011	TOTAL TO COMPLETE
a. Total Operating Obligations	1,590	1,640	0	0	
b. Total Operating Costs	1,590	1,640	0	0	
c. Total Equipment Obligations	0	0	0	0	
d. Total Equipment Costs	0	0	0	0	

25. Milestone Schedules (Tasks) (optional) See attached	PROPOSED SCHEDULE	AUTHORIZED SCHEDULE

Reporting Requirements (Description)
See attached

Form 1647 (01/96)

Compressional Heating of a Compact Toroid Plasma to Fusion Conditions

SC Program: LAB 05-09 Research in Innovative Approaches to Fusion Energy Sciences

Name of Laboratory: Los Alamos National Laboratory

PI: Thomas P. Intrator (Technical Staff Member)

PI mailing address: P-24 Plasma Physics Group, MS E526, Los Alamos, NM 87545

PI phone: 505-665-2927

PI fax: 505-665-3552

PI email: `intrator@lanl.gov`

Lab official: Glen A. Wurden (LANL Fusion Energy Sciences Program Manager)

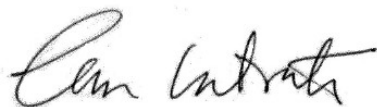Lab official fax: 505-665-3552

Lab official phone: 505-667-5633

Lab official email: `wurden@lanl.gov`

Requested funding: FY06: $1.5M; FY07: $1.54M; FY08: $1.59M; FY09: $1.64M;
Total: $6.27M

Use of human subjects: NO

Use of vertebrate animals: NO

PI signature and date:

7/14/05

Lab official signature and date:

7/14/05

Contents

1 Executive summary

We propose to carry out a four-year project that was successfully renewed for FY04–07 to demonstrate compressional (PdV) heating of a compact toroid plasma within a converging flux conserving boundary to fusion conditions, also known as "magnetized target fusion" (MTF). MTF could be a reduced-cost path to fusion energy that takes advantage of a plasma regime between magnetic (MFE) and inertial fusion energy (IFE).

Our proposed physics demonstration of MTF will utilize a field-reversed configuration (FRC) compact toroid magnetized plasma and an imploding metal liner to compress the plasma. Integrated liner-on-plasma compression experiments will be done using the 9 MJ Shiva-Star pulsed power facility at AFRL (Air Force Research Laboratory in Albuquerque, NM). This strategy takes advantage of significant past scientific and technical accomplishments in MFE and Defense Programs research and should yield substantial fusion plasma performance ($n\tau > 10^{13}$ s·cm^{-3}, $T > 5$ keV) at very modest cost. Among candidate magnetized targets, the choice of the FRC confers the following key advantages:

- High power density $\rightarrow \beta \approx 1$, advanced fuel potential
- Simply connected topology $\rightarrow$ no center stack
- Simple magnetic configuration $\rightarrow$ no toroidal field, no linked magnets
- Natural axial divertor $\rightarrow$ heat exhaust handling capability
- Small size $\rightarrow$ reduced cost

Accomplishments in previous funding cycles include the successful design and construction of an experimental facility to form high density target FRC's suitable for translation and MTF implosion. The facility, FRX-L (Field Reversed Experiment-Liner), is located at LANL. FRX-L has successfully formed FRC's meeting the required temperature ($T_i + T_e \approx 300$ eV) design goal for proceeding to translation/implosion experiments for MTF, and we have achieved FRC density ($n \sim 5 \times 10^{16}$ cm^{-3}) and lifetimes (12–15 μs) within a factor of two of what is required. We expect to reach these targets during our ongoing experimental campaigns, which have the benefit of a recently upgraded crowbar switch that reduces θ-coil current modulation and therefore minimizes FRC compression/decompression which was previously terminating our FRC's prematurely. During the present funding cycle, which unfortunately suffered a 4–6 month setback due to a LANL-wide shutdown (July–December, 2004), we also have nearly completed a full engineering design of a translation/implosion MTF experiment that will be built and operated at the Shiva-Star pulsed power facility at AFRL. This experiment, to be called Shiva-FRC, will be the first integrated liner-on-plasma MTF experiment with modern diagnostics and the capability for reaching significant equivalent fusion gain ($Q \sim 0.01$).

During the proposed funding cycle (FY06–09), we will deliver the following results:

- Via recent pulsed-power upgrades, we will increase the lifetime and density of our high pressure FRC's beyond that of previous data taken in 2004 and 2005.
- Demonstrate and diagnose the stable translation of a target FRC into a static "mock" liner.
- Implement our design for the first integrated liner-on-plasma compression experiments at AFRL.

7

- Conduct the first integrated liner-on-plasma MTF experiments with modern diagnostics and the capability for achieving significant equivalent fusion gain ($Q \sim 0.01$).
- Provide understanding for key physics issues for the integrated MTF experiments, via experimental data and comparisons with theoretical/numerical modeling of our collaborators.

Our proposal responds directly to recommendations in reports resulting from two recent Fusion Energy Sciences planning activities: (1) report of the Integrated Program Planning Activity (IPPA) for the DOE Fusion Energy Sciences Program, Report DOE/SC-0028,[1] and (2) report to FESAC by the Panel on Program Priorities, "Scientific Challenges, Opportunities and Priorities for the U.S. Fusion Energy Sciences Program."[2] MFE Program Goal 2 of the IPPA document states "Resolve outstanding scientific issues and establish reduced-cost paths to more attractive fusion energy systems by investigating a broad range of innovative magnetic confinement configurations." The purpose of our MTF project is exactly this, to resolve scientific issues leading to a physics demonstration of a low-cost, high-gain, innovative approach to magnetic fusion. Section 3.2.4.4 of the IPPA report states explicitly "Resolve key issues of target formation, translation, and physics for magnetized target fusion." These tasks are exactly what our project is doing and proposes to finish doing. Our project also responds to several recommendations of the FESAC Priority Panel report. MTF responds most directly to topical question 7 (T7), "How can high energy density plasmas be assembled and ignited in the laboratory?" As elaborated under T7, we are trying to understand "the energy confinement and stability properties, as well as the interaction between the hot plasma and the imploding liner" . . . which are the "key scientific issues to be resolved for imploding magnetically insulated plasmas." Additionally, our project contributes indirectly to the resolution of many of the other fifteen topical questions. For example, our efforts to form, study, and optimize a high density FRC (as our MTF target) contribute to the macroscopic plasma physics questions T1–T3 concerning the impact of magnetic field structure on plasma confinement, maximum pressure limits in laboratory plasmas, and how to harness plasma self-organization to improve fusion performance; and also to the multi-scale transport question T5 concerning how fields and flow are generated in plasmas, as expected to occur in our high density FRC's. During our liner-on-plasma experiments, we will contribute valuable data and new understanding for T10 concerning boundary effects of a hot plasma interacting with its surroundings. Indeed, this is one of the key outstanding scientific issues to resolve if we are to determine MTF's viability for compressing a magnetized plasma to fusion conditions. Finally, if we are successful in achieving modest fusion power via MTF, we will motivate future experiments that will contribute to the fusion engineering science questions T13–T15 concerning the challenges of integrating a complex engineering system with harsh fusion environments.

For the next 4–8 years, this project's most significant contribution to burning plasmas and ITER will be to maintain excellent small-scale science, provide a high visibility recruitment tool, and keep the public's attention on potential near-term alternative fusion energy successes. This project led by LANL benefits from collaborations with AFRL, LLNL, General Atomics, U. Washington, U. New Mexico, U. Wisconsin–Madison, and U. Nevada-Reno.

---

[1] http://www.ofes.fusion.doe.gov/FusionDocuments/IPPAFinalDec00.pdf

[2] http://www.ofes.fusion.doe.gov/more_html/FESAC/PP_Rpt_Apr05R.pdf

2   Abstract

We propose a four-year (FY06–09) program to demonstrate compressional (PdV) heating of a compact toroid plasma within a converging flux-conserving boundary to fusion conditions, also known as magnetized target fusion (MTF). MTF is a potentially low cost path to fusion energy that is intermediate in plasma regime between magnetic (MFE) and inertial fusion energy. We will demonstrate MTF by using a field-reversed configuration (FRC) as our magnetized target plasma and an imploding metal liner for compression. These choices take advantage of significant past scientific and technical accomplishments in MFE and Defense Programs research and should yield substantial plasma performance ($n\tau > 10^{13}$ s·cm^{-3}, $T > 5$ keV) using an available pulsed-power implosion facility at modest cost. We have recently achieved the required FRC pressure and are within a factor of 2–3 of the required FRC lifetime. The proposed work will demonstrate stable translation of the target FRC into a static liner followed by the construction and operation of the first integrated liner-on-plasma compression experiments. This proposal responds to MFE Goal 2 of the Integrated Program Planning Activity for the DOE Fusion Energy Sciences Program, as well as several stated goals in the recent FESAC Priorities Panel report. The national MTF effort is a collaboration between multiple institutions including LANL, AFRL, LLNL, General Atomics, U. Washington, U. New Mexico, U. Wisconsin-Madison, and U. Nevada-Reno.

3   Background

3.1   Magnetized target fusion (MTF)

Magnetized Target Fusion (MTF) is a subset of magneto-inertial fusion (MIF), which includes all pulsed high-pressure approaches to fusion involving inertial confinement of a magnetized plasma. MIF concepts include laser-heated solenoid plasmas, cryogenic fiber Z-pinches, flow-stabilized Z-pinches, and the composite Z-θ pinch. MTF specifically requires an imploding pusher to compress and PdV heat a magnetized target plasma, such as a spheromak or field-reversed configuration (FRC), to fusion conditions, as schematically illustrated in Fig. 1. MTF involves plasma regimes intermediate ($n \sim 10^{19}$–10^{20} cm^{-3} and $T \sim 5$ keV) between magnetic fusion energy (MFE) and inertial fusion energy (IFE) and seeks to capitalize on the advantages of this intermediate regime (Kirkpatrick *et al.*, 1995; Siemon *et al.*, 1999; Ryutov & Siemon, 2001). Various flux conserving materials have been considered for the imploding pusher, including metal liners, gaseous or plasma pushers (Thio *et al.*, 1999), and compressible liquid shells (Turchi *et al.*, 1976; Turchi *et al.*, 1980).

3.2   Motivation: A potential low cost route to fusion

Density is one of the few adjustable free parameters in the design of a fusion system, particularly when seeking a lower cost development path (Siemon *et al.*, 1999). The fusion energy production per unit volume P_{fusion} scales as density squared, $P_{\text{fusion}} = n^2 \langle \sigma v \rangle E_{\text{f}}$, where n is the density [m^{-3}], $\langle \sigma v \rangle$ the fusion reaction rate [m^3/s], and E_{f} the energy per fusion reaction. The losses per unit volume can be characterized with a loss time τ_{E} so that $P_{\text{loss}} = nT/\tau_{\text{E}}$, where T is the characteristic ion temperature. The ratio $P_{\text{fusion}}/P_{\text{loss}}$ is $Q = n\tau_{\text{E}} \langle \sigma v \rangle E_{\text{f}}/T$, which depends only upon T and the Lawson product $n\tau_{\text{E}}$. If we assume that the fusion
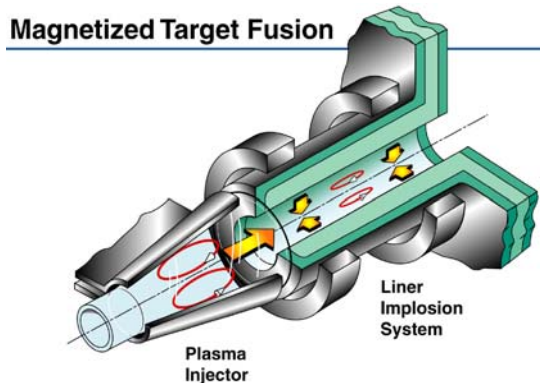
Figure 1: Schematic of the MTF concept, including a plasma injector with translation stage and a liner implosion stage to compress the target plasma to fusion conditions.
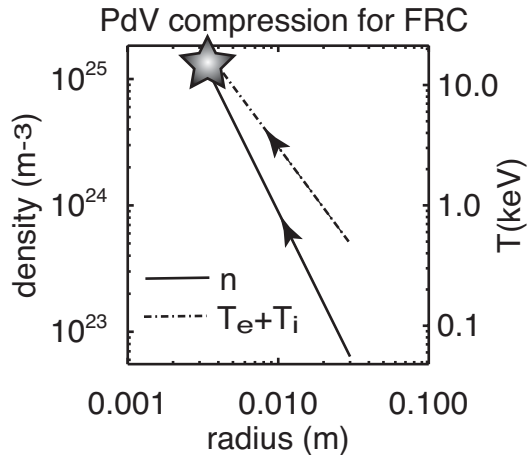
Figure 2: Trajectory for the FRC as the converging flux conserving boundary does work on the plasma. Compressed radius is on the horizontal axis, density and temperature on the vertical axis. The scaling laws invoked are $V \sim r^{2.4}$, $\beta \approx 1$, $PV^{\gamma} = \text{constant}$.

systems have (probably anomalous) diffusive losses χ, then the energy confinement time is $\tau_{\mathrm{E}} = \frac{R^2}{\chi}$. Since system cost and size scale approximately with plasma energy E_{p}, we can roughly estimate cost as

$$E_{\mathrm{p}} \approx nTR^3 \approx \frac{\chi^{3/2}}{n^{1/2}} \left(\frac{T^{5/3}Q}{\langle \sigma v \rangle E_{\mathrm{f}}} \right)^{3/2}. \tag{1}$$

For a D-T fusion scenario, the right hand term on the right hand side of Eq. (1) is relatively constant because $T \approx 10$ keV, $Q \gtrsim 1$, and $\langle \sigma v \rangle E_{\mathrm{f}}$ is fixed. Thermal diffusivity χ is important but relatively difficult to improve. Only density remains as the variable that we can use to influence the energy of a fusion system. Compared with MFE research, the necessity of reducing χ is relaxed because MTF operates at much higher densities than the MFE approach. Using conventional magnet technology and engineering for steady-state power handling, the "conventional MFE density" typically is in the range of 10^{14} cm^{-3}. Inertial fusion scenarios are conceived as working with pulsed systems at much higher density and no magnetic field. A pulsed approach like MTF that takes advantage of magnetic thermal insulation could have much larger density than MFE and smaller χ than ICF.

3.3 FRC as a target plasma

MTF invokes the compression of a magnetized target plasma to fusion conditions. Compact toroids such as the spheromak (Jarboe, 1994) and FRC (Tuszewski, 1988a) have been identified as candidate target plasmas for MTF because of several potentially favorable features: (1) closed field line topology, (2) simply connected, *i.e.*, no internal material objects to inhibit compression within a liner, and (3) ease of translation from the plasma formation region into a liner for compression. Conventional FRC scaling laws predict that the compressed

Figure 3: Schematic of FRC including poloidal magnetic field, toroidal current, θ-pinch coil, cusp/mirror coils, and closed/open magnetic surfaces.

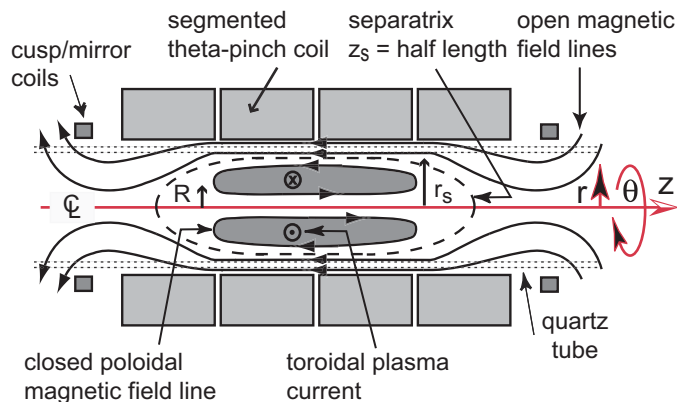equilibrium should have a lifetime on the order one microsecond, which is approximately the dwell time as the external inward pressure stagnates against the FRC internal pressure. As the flux conserver shell does work on the FRC, it decreases the volume and increases the density and temperature, as shown in Fig. 2. We have chosen the FRC as the candidate that can best survive formation, translation, and compression (Wurden *et al.*, 1998), while offering some unique advantages over other possible targets.

The FRC is an elongated, self-organized compact toroid state that ideally has only toroidal plasma current and poloidal magnetic field. In Fig. 3 we indicate the FRC as a closed-field-line torus inside a separatrix with an open-field-line sheath outside the separatrix. In an FRC equilibrium, plasma pressure balances with magnetic field pressure radially and magnetic field-line tension axially. For an ideal straight cylinder it has been shown (Barnes & Seyler, 1979; Armstrong *et al.*, 1981) that average pressure, $P = nT = n(T_e + T_i)$, inside the separatrix normalized to the external magnetic field pressure is

$$\langle \beta \rangle = 1 - \frac{x_s^2}{2}, \tag{2}$$

where $x_s = r_s/r_c$, r_c is the coil or wall radius, $\beta = nT/(B_{ext}^2/2\mu_0)$, and B_{ext} the external separatrix magnetic field. The FRC has $\langle \beta \rangle \sim 1$. Active worldwide FRC research has resulted in significant experimental and theoretical progress, resulting in stable plasmas with good confinement properties.

The FRC offers many potential advantages as an MTF target plasma, including the promise of robust, closed flux surfaces that maintain their topology during compression, as has been observed (Tuszewski, 1988a) in compression, translation (Rej *et al.*, 1986), stability experiments (Tuszewski *et al.*, 1991a), and theoretical models (Milroy & Brackbill, 1982). Formation of an FRC using high-voltage θ-pinch technology is well established, and the plasma characteristics of the FRC (*i.e.*, stability, transport, and impurity content) in the density and temperature range of interest are reasonably well characterized. Early FRC's formed by reversed-field θ-pinches exceed our target density (McLean *et al.*, 1967; Kaleck *et al.*, 1967; Kaleck *et al.*, 1969; Eberhagen & Grossmann, 1971), but the diagnostic methods and theoretical understanding were less complete in the 1960's-70's. Other desirable features include:

- The FRC has been shown to exhibit resiliency during translation and deformation.

- Because of field line tension, the FRC undergoes axial contraction during radial compression (Tuszewski *et al.*, 1991b). A cylindrical adiabatic implosion (r_c contracts) obeying Eq. (2) and conserving particles yields an FRC volume that scales as $r_c^{2.4}$, *i.e.*, more strongly than 2D compression given by r_c^2 (Spencer *et al.*, 1983). A full 3D compression could be achieved with shaped liners.

- FRC's are formed inductively and are largely free of impurity line radiation.

- The open field lines outside the separatrix act as a natural divertor that isolates plasma loss flux from wall boundaries.

The latter two attributes may substantially reduce impurity concerns, an outstanding issue for MTF.

3.4 FRC scientific issues

Formation with large toroidal electric field: For MTF, the FRC plasma must survive long enough to translate into the liner volume for implosion. Once it is compressed, fusion energy breakeven $Q = 1$ at expected implosion convergence factors requires sufficient plasma pressure. The key physics governing both lifetime and pressure is determined by magnetic flux retention during the FRC formation process. FRC formation via θ-pinch (Taccetti *et al.*, 2003) uses an initial bias magnetic field (0.3–0.5 T) that is frozen-in during pre-ionization (PI) and then is radially shocked by another reversed much larger main bank field (3–5 T). The radial jump in poloidal magnetic field induces a plasma toroidal image current, and field line reconnection at the ends forms closed flux surfaces. Formation (2–3 μs) and translation ($v_A \sim 10 - 15$ cm/μs) into the liner region can be accomplished (Rej *et al.*, 1986) in a few μs, a time short compared to the expected FRC lifetime (20–25 μs). We will show the results (see Fig. 18) of recent 2-D MHD MOQUI simulations (Milroy & Brackbill, 1982) that indicate FRC compression could be underway 10 μs after formation.

Our FRC formation experiment, FRX-L (Field Reversed Experiment-Liner), uses a θ-pinch formation method that takes advantage of a large toroidal electric field ($E_\theta \leq 1$ kV/cm) which increases the radial $E_\theta \times B_Z$ implosion velocity and consequently the Green-Newton (Green & Newton, 1966; Tuszewski, 1988a; Hoffman *et al.*, 1986) magnetic field B_{GN}. The FRC geometry is sketched in Fig. 3. This field corresponds to equal Alfvén and $E \times B$ drift speeds at the edge, *i.e.*, $v_A = E_\theta/B_{ext}$, such that

$$B_{GN} = E_\theta^{1/2}(\mu_0 nm)^{1/4}. \tag{3}$$

In practical units $B_{GN}(\text{kG}) = 1.88[E_\theta(\text{kV/cm})]^{1/2}[A_i p_0(\text{mTorr})]^{1/4}$ where A_i is the ion mass in proton units, and for FRX-L operation at $p_0 \approx 40 - 80$ mTorr, $B_{GN} \approx 0.4$–0.6 T. A high B_{GN} is desirable because B_{GN} limits the maximum trapped flux and hence the maximum plasma pressure in a θ-pinch formed FRC. Increasing magnetic lift-off field B_{LO} that is trapped (when the main field reverses and the FRC "lifts off" the wall) relative to B_{GN} can also increase resistive heating relative to the usual radial shock heating. The desired initial temperature ($T_i \approx T_e \approx 250$ eV) and trapped flux correspond to a bias field $B_{bias} = 0.3$–0.7 T. There is experimental evidence (Armstrong *et al.*, 1982; Kutuzov *et al.*, 1981) that a pressure-bearing sheath forms which slows the flux loss during formation from convective to
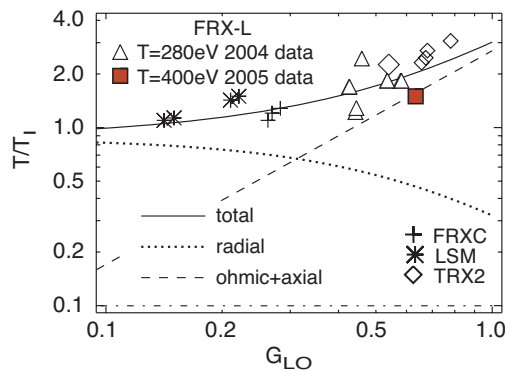
Figure 4: Total particle temperature in equilibrium, expressed as the fraction $T/T_{\rm I}$ where $T_{\rm I}$ is the implosion reference temperature. FRX-L data from years 2004 and 2005 are compared with other FRC experiments.
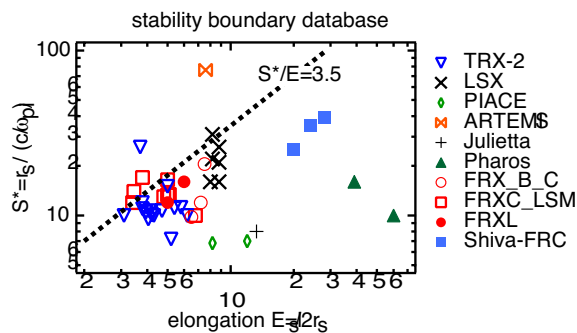
Figure 5: Survey of FRC experimental data showing that most FRC's are in the range $S^*/E \lesssim 3.5$. "Shiva-FRC" is the projected Shiva-Star compressed FRC.

diffusive, and therefore simple estimates of $B_{\rm LO}$ that is trapped are unduly pessimistic for $B_{\rm bias}/B_{\rm GN} > 0.5$ where we operate FRX-L.

Formation with large lift-off flux: The ratio $G_{\rm LO} = B_{\rm LO}/B_{\rm GN}$ is an important quantity that determines the relative amounts of radial shock and Ohmic heating during formation. Operation with large $G_{\rm LO}$ produces stronger flux dissipational heating and is a desired regime for FRX-L. The combination of radial shock heating, axial implosion, and Ohmic heating becomes effective for smaller size FRC's. We show in Fig. 4 the inferred total temperature $T = T_{\rm e} + T_{\rm i}$ from FRX-L magnetic data. Total particle temperature in equilibrium is expressed as the fraction $T/T_{\rm I} = (\sqrt{3}/2)(1 + 1.7G_{\rm LO}^{1.5})^{-1} + 2.7G_{\rm LO}^{1.2}$, where $T_{\rm I}$ is the implosion reference temperature. The first term on the right hand side corresponds to radial shock heating which dominates for small $G_{\rm LO}$. The second term, corresponding to resistive and axial shock heating, can double or triple the final temperature for large $G_{\rm LO}$ approaching unity. FRX-L data at $G_{\rm LO} \approx 0.5$–0.6 is compared with other FRC experiments. One experimental goal is to further enhance $G_{\rm LO}$ and Ohmic heating. We have already shown (Intrator *et al.*, 2004) that the FRX-L resistivity responsible for Ohmic dissipation is anomalously large.

Stability: The domain of good FRC stability is illustrated emprirically in S^*-E parameter space, as shown in Fig. 5, where the radial size is parameterized in units of ion skin depth, $S^* = r_{\rm s}/(c/\omega_{\rm pi})$, and elongation $E = l_{\rm s}/(2r_{\rm s})$ ($S^* \approx 13$ and $E \approx 6$ for FRX-L). Most FRC experiments are in the regime $S^*/E \lesssim 3.5$. This may correspond to FRC tilt stability limits, *e.g.*, gyroviscous finite Larmor radius model (Ishida *et al.*, 1992), or kinetic (Barnes *et al.*, 1986) or Grad-Shafranov calculations in the long thin limit (Barnes, 2002).

The typical FRC is not MHD-like but kinetically dominated, where the size in units of ion gyro radius is

$$s = \int_R^{r_{\rm s}} \frac{r\,{\rm d}r}{r_{\rm s}\rho_{\rm i}} \sim \frac{r_{\rm s}}{\langle \rho_{\rm i} \rangle} \sim \frac{S^*}{10}, \tag{4}$$

and $\rho_{\rm i}$ is the local ion gyroradius. For FRX-L, $s < 2$, although turbulent FRC's with $s < 8$

13

have been formed (Slough & Hoffman, 1993; Hoffman & Slough, 1993b). Whether the experimental stability limit in Fig. 5 arises from global modes (*e.g.*, internal tilt), localized modes (*e.g.*, interchange), or just coincides with technical limitations in FRC formation remains to be seen. Preliminary calculations have suggested that fusion yield is very sensitive to the exact value of S^*/E. An important physics issue for both MTF and conventional FRC's is to determine the practical upper limit for S^*/E. Fortunately, interesting liner compression experiments with significant fusion yield are possible with $S^*/E < 3.5$, consistent with our conservative empirical constraint on FRC formation, translation, and compression. Much better results might be obtained with higher S^*/E values, and thus determining the S^*/E stability limit for MTF-grade plasmas is an important experimental issue.

Another open issue is the toroidal mode number $n = 2$ rotational instability which terminates many FRC experiments, including FRX-L. The main concern is that during liner compression, $n = 2$ modes may terminate the FRC, as was observed during flux compression experiments (Rej *et al.*, 1992). On the other hand, increased trapped flux also increases the lifetime, and for translation experiments (Rej *et al.*, 1986) the $n = 2$ mode proved rather harmless, especially for cases with values of $x_s \sim 0.6$–0.7. Unlike flux compression, wall compression proceeds with fairly constant x_s values. The edge gradient parameter

$$\alpha = \omega_{\text{rotn}}/\omega_{\text{Di}} > 1.2\text{–}1.4 \tag{5}$$

where ω_{rotn} and ω_{Di} are rotational and ion diamagnetic drift frequencies respectively, indicates the threshold for rotational instability. We plan to address this issue as part of our collaboration with University of Washington (J. Slough) during formation by increased trapped flux and multipole stabilization.

Transport: While empirical FRC scaling is well documented, transport properties are not well understood from the perspective of fundamental physics. A key question is whether FRC confinement in past experiments with $T_e < 500$ eV and $T_i < 3$ keV will apply near peak compression where $T_e \sim T_i \sim 5$ keV is anticipated. Will thermal losses remain mostly convective, or will non-convective losses dominate? Electron thermal conduction may prove to be a limiting factor. Impurity radiation is another key issue for MTF that we discuss in the next section. It is also possible that ion thermal conduction may become a dominant energy loss mechanism if ion temperature gradients comparable to r_s arise from a cold boundary. Control of x_s may prove essential to avoid large T_i gradients. On the other hand, increasing x_s to values approaching unity may increase thermal conduction but suppress density-gradient driven convective losses. In the robust FRC domain $S^*/E < 3.5$, the FRC energy confinement time is empirically observed to be approximately half the particle confinement time (Siemon *et al.*, 1986; Tuszewski, 1988a; Hoffman & Slough, 1993b),

$$\tau_E(\mu s) \sim 0.5\tau_N \sim \frac{0.5R^2}{\rho_{\text{ie}}(\text{cm})}, \tag{6}$$

where R is the major (field null) radius and ρ_{ie} (≈ 0.3–0.6 cm for FRX-L) is the ion gyroradius calculated using the internal T_i and external separatrix magnetic field. Typically, particle and internal flux confinement times τ_N and τ_ϕ, respectively, are comparable, with τ_E approximately half this. Recent FRX-L shots already show lifetimes (10–12 μs) that are more than half of the empirical scaling (20 μs). Since our r_s is of the order of the ion-ion collision length, collisional FRX-L regimes may affect the physics of transport in ways

that have not yet been considered. The R^2/ρ_{ie} relation may be related to (among others) anomalous resistivity due to lower-hybrid drift instability, Bohm scaling, or drift dissipative mode. Most FRC experiments indicate that τ_E is dominated by particle loss (Tuszewski, 1988a; Steinhauer, 1992; Slough *et al.*, 1995). Non-convective thermal losses are smaller in most FRC experiments and appear mostly in the electron channel, presumably from a combination of thermal conduction and impurity radiation.

FRC radial pressure balance for $\beta \approx 1$ yields $\rho_{ie} \sim n^{-1/2}$ so that s and S^* scale as $Rn^{1/2}$. The observed energy confinement time will then scale with $\tau_E \sim R^2 n^{1/2}$, and $n\tau_E \sim R^2 n^{3/2}$. The present FRX-L plasma has $n\tau_E \approx 5 \times 10^{10}$ s·cm^{-3} before compression. The empirical scaling law

$$n\tau_E \sim \frac{s^3}{R}, \tag{7}$$

where s is approximately constant during wall compression, suggests that large values of $n\tau_E$ can be achieved for a compressed plasma inside a liner with small values of R. Achieving $n\tau_E \sim 10^{13}$ s·cm^{-3} would prove that high density is advantageous, provided a fundamental understanding of this density scaling is achieved.

Impurity radiation: Even small concentrations of high-Z impurities may yield significant radiation power losses. It is likely that the most serious impurity concerns will relate to liner-plasma interactions during compression, although the impact of line radiation on FRC formation will also need assessment. Most FRC's produced by the field-reversed θ-pinch technique show relatively clean plasmas. This is presumably because of the inductive plasma formation during which wall contact is limited to only a few hundred nano-seconds during field reversal. Afterward, the FRC separatrix is well-separated radially and axially from the walls. FRC formation is the cleanest among magnetically confined plasmas. Low radiation losses have been occasionally measured or inferred in FRC's to be 5–10% of total energy losses (Tuszewski, 1988a). Somewhat higher radiative loss fractions have been measured in the slower formation LSX experiment (Slough *et al.*, 1992). In all cases, $Z_{eff} \approx 1$–1.5 have been inferred. Line radiation is consistent with either $< 1\%$ oxygen or $\sim 0.04\%$ Si concentrations, the dominant quartz wall species. The impurity content of FRX-L is comparable to previous FRC experiments. Large PI fields increase quartz impurity release, but large gas fill pressures and high FRC densities suppress impurity influx and concentrations.

Fundamental FRC physics: Although the proposed research is focused on achieving MTF using an FRC, it will also offer a strong plasma science component. The FRC configuration is unique among magnetic configurations, as described in Sec. 3.3. Consequently, the FRC is a valuable platform for exploring fundamental plasma physics which results in and supports these properties. One example is to understand the effect of strong flows on plasma equilibria and stability. Another is to explore the validity of generalized relaxation principles which may govern FRC formation and equilibria, such as minimum dissipation theory (Montgomery & Phillips, 1990; Bhattacharyya *et al.*, 2001; Steinhauer & Ishida, 1997). Some of these fundamental plasma physics questions reach beyond MHD single fluid models and may also be related to geophysical and astrophysical phenomena.

3.5 Liner implosion technical issues

The broad utility of high-energy liners in Defense Programs and high energy density physics has led to significant investment in liner physics studies and technology advancement that

will be useful for MTF. A flux conserving shell (liner) will be used to implode the MTF target. The interactions of the liner with the plasma interior involve physics and engineering questions that also need to be investigated during the integrated liner-on-plasma experiment. Related background and technical issues are found in the Appendices and the AFRL companion proposal (Dr. Jim Degnan, PI). In late 2004, AFRL successfully tested two shaped deformable aluminum liners (with 8 cm diameter holes at each end) that are the same as the one we plan to use for FRC implosion experiments at Shiva-Star.

3.6 Theory and computation

Evaluation of MTF will benefit from a strong synergism between experimental and theoretical/computational efforts. The computational focus area most in need of experimental benchmarks is the interaction of the FRC with the imploding liner, including the behavior (*e.g.*, stability) of the FRC as it implodes. Modeling of the FRC physics is reasonably successful from a phenomenological standpoint but fundamental questions remain at the basic physics level, especially for collisional regimes. Not much has been done yet to study how to integrate these issues into MTF scenarios.

Early estimates of impurity effects on implosion dynamics (Armstrong, 1987) and a 0-D code developed by (Rej & Tuszewski, 1984) can be used to evaluate power balance and impurity generation. Other codes at LANL (MHRDR), LLNL (TRAC-II), and AFRL (MACH-2) have predicted many of the observations of the Russian MAGO plasma formation scheme, which has many of the properties required for a pre-implosion target plasma (Lindemuth *et al.*, 1995). The 1D RAVEN and 2D radiation MHD (RMHD) codes have been used at LANL to understand and interpret liner implosion data in the parameter regime required for MTF (Faehl *et al.*, 1997). The MOQUI code has been used to design FRC experiments and to understand FRC formation and translation (Milroy & Brackbill, 1982). The strong synergism between MTF and ongoing imploding liner research funded by DOE Defense Programs means that MTF will benefit from advancements expected via the ASCI initiative. Fully 3D codes, which can model the combined liner-plasma dynamics of MTF, are expected to become operational during the time frame of this proposal. Hot plasma interactions with a cold liner wall are rich in physical phenomena and should be a focus of the theory-modeling effort. Computational modeling of the integrated experiments will be an essential component of understanding the complex physics of plasma stability and wall interactions.

Further development of the theory and modification of computational tools would be very useful to the MTF experimental campaign but are not presently funded in our proposal due to fiscal constraints.

3.7 MTF reactor considerations

We believe that low cost single shot demonstrations will be useful before choosing a reactor scheme. A few investigations of MTF-based reactor concepts have been carried out, and we emphasize that there are potentially viable MTF reactor scenarios deserving more dedicated future studies. Because this proposal deals primarily with demonstrating scientifically how to reach fusion conditions by compressing a magnetically confined compact toroid, discussion of MTF reactor considerations appear in the Appendices. Power plant, sacrificial cartridge,

cartridge remanufacture, and direct conversion issues are discussed in work by one of our subcontractors (Dr. Ron Miller) in Appendix B.

4   Accomplishments

The FRC experimental parameters obtained in the previous funding cycles warrant moving toward the translation and implosion experiments, with two exceptions: a relatively short lifetime ($\sim 10\,\mu$s) and low probability of forming an FRC that would remain static under our diagnostics centered around the θ-coil. Consequently, the focus of our present experimental campaigns has been to enhance performance in these two areas, which has resulted in the following accomplishments:

1. improved reproducibiliy of good FRC's via PI/main bank timing experiments
2. improved FRC formation due to upgraded crowbar switch which has minimized magnetic field ringing and premature deterioration of FRC's
3. increased equilibrium n, $T_e + T_i$, and plasma pressure, although we have not finished optimization of FRC lifetime (via PI/main bank timing and using cusp/mirror coil to form axially static FRC's)
4. modeled time-dependent cusps and field penetration of flux-excluder plates to understand why the FRC does not always remain static under the θ-coil
5. use an analytic model and MOQUI simulations to design FRC translation experiment
6. produced an engineering design for full integrated experiment, including magnetics, CAD drawings, pulse power access, etc.

The accomplishments of the past two years, despite a 6-month LANL shutdown, have placed us in an excellent position to pursue the translation and implosion experimental phases. Section 4.3 describes our FY04–05 accomplishments in more detail.

4.1   Summary of first funding cycle (FY00–03)

Table 1 summarizes the accomplishments through the end of the first funding cycle. During the first four-year research cycle, we made major progress in creating a high density FRC target for MTF. Prior to the first funding cycle, the LANL/AFRL MTF effort was seeded with \$0.5M from internal LANL Laboratory Directed Research and Development (LDRD) funds and a matching amount from OFES. We used this to successfully implode two aluminum liners onto vacuum at AFRL, demonstrating parameters appropriate for our proposed liner-on-plasma experiment. Years one through three of the previous funding cycle were consumed by the design, construction, testing, and integration of FRX-L, a high voltage, high current, pulsed-power high density FRC formation experiment. Substantial student effort facilitated the addition of cusp/mirror coils to each end of the θ-coil along with capacitor banks and control systems. Triggered magnetic reconnection during the FRC formation led to FRC equilibria with high reproducibility, substantial trapped poloidal flux, and thus long lifetime (limited by the $n = 2$ rotational instability). Details of the facility and first physics results from the previous funding cycle were reported in several peer-reviewed publications (Wurden *et al.*, 2001; Taccetti *et al.*, 2003; Zhang *et al.*, 2004; Intrator *et al.*, 2004; Zhang *et al.*, 2005).

Accomplishments through FY03 June	shot #	start date	duration (mo.)
liner shots on Shiva-Star		1/99	6
design control systems		7/00	4
fabricate/install θ-coil, banks, vacuum		12/00	5
explore PI configurations		6/01	3
design/install crowbar		10/01	4
first main bank shots	522	10/01	1
first plasma with PI		1/02	3
first FRC		1/02	3
single chord interferometer online	658	1/02	1
FRC with $n = 2$ instability	799	2/02	1
design/implementation of fast pre-fire detection		2/02	3
fabricate/install cusp/mirror bank systems		6/02	4
first shots with cusp/mirror	1501	9/02	
reliable high density FRC formation		10/02	3
publication of first results (APS, RSI)		11/02	
experimental campaigns to scan parameters		11/02	6
APS-DPP invited talk (Intrator)		11/03	

Table 1: Accomplishments through FY03.

4.2 Summary of second funding cycle to date (FY04–05)

Since FY04, we have successfully demonstrated (Wurden *et al.*, 2004) the requisite FRC temperature for proceeding to translation/implosion, but FRC density, pressure, and life-time are all within a factor of 2 for MTF translation/implosion. Table 2 summarizes the accomplishments thus far in the second funding cycle.

Accomplishments FY04 through June 2005	shot	start date	duration (mo.)
reproducible FRC's (80% success rate)	3000	5/04	2
increased FRC lifetime (12–15 μs)	3085	5/04	6
ICC Workshop invited talk (Intrator)		5/04	
1st generation translation/implosion design complete		6/04	6
IEEE invited talk (Zhang)		6/04	
LANL shut-down		7/04	6
IAEA presentation (Wurden)		9/04	
invited talk 16th ANS TOFE conference (Wurden)		9/04	
US-Japan CT Workshop (Intrator organizer)		9/04	
shaped liner implosions onto vacuum (AFRL)		10/04	3
Resumption of operations after LANL shut-down		1/05	
Improved crowbar installation/troubleshooting	3624	1/05	2
2nd generation translation/implosion design complete		2/05	4
Operation at ± 40 kV main bank	3684	4/05	3
Improved high $\langle nT \rangle$ FRC's w/new crowbar	3688	5/05	2

Table 2: Accomplishments FY04 through June, 2005.

Our recent experimental progress has followed from exploration of trigger timing scenarios, bias field interaction with flux excluder plate position, and hardware improvements in crowbar operation. If the FRC expands beyond the θ-coil region, closed flux surfaces open up, which leads to unacceptably large particle and energy losses. An improved crowbar switch (Grabowski *et al.*, 2002) has enabled operation with greatly reduced field ripple. Best parameters so far for formation (and equilibrium) density $> 7 \times 10^{16}$ cm^{-3} (5×10^{16} cm^{-3}), temperature $T = T_\mathrm{e} + T_\mathrm{i} > 600$ eV (400 eV), excluded flux > 3 mWb (1 mWb), and internal flux ≈ 0.7 mWb (0.5 mWb), as shown in Sec. 4.3. Increased lifetime and Ohmic heating require increasesd trapped FRC equilibrium flux. We have had some success in previous campaigns via incremental improvements in the pulsed power systems to increase the bias and PI fields, increases of gas pre-fill pressure, and optimizing the timing sequence.

4.3 Experimental results

To prepare for translation and fast compressional heating, we require FRC density $n \sim 10^{17}$ cm^{-3}, temperature $T_\mathrm{e} + T_\mathrm{i} \approx 300$ eV, and energy confinement time $\tau_\mathrm{E} > 10$ μs. For pressure balance with a given external magnetic confining field B_ext and constant $\beta \approx$ unity, the plasma pressure and Ohmic heating scales with internal trapped poloidal flux. Thus the key is to increase trapped magnetic flux during FRC formation.

4.3.1 FRC preionization (PI) and formation

A key goal is to optimize the PI and formation sequence to produce the best FRC's for translation and implosion. The inductively coupled θ-PI method that we use is very clean ($Z_\mathrm{eff} \approx 1$ historically) compared to a Z-pinch axial current discharge PI approach with internal electrodes. Figure 6 shows six traces from six axial positions of wavelength-resolved spectra for a PI shot, showing that the PI shot is very clean. The θ-PI method provides a high ($\approx 100\%$) level of ionization especially at high fill pressure (40–80 mTorr). This approach tends to trap less than half (Armstrong *et al.*, 1981b) of the initial bias field. We have implemented this with a high voltage bank to get high enough peak current to cancel out the bias field, *i.e.*, create zero crossings for bias with a low enough capacitance to maintain a fast ring frequency (Niblett & Green, 1959; Kever, 1962; Green, 1962; Green & Newton, 1966; Commisso *et al.*, 1980). Zero crossing is necessary for gas breakdown.
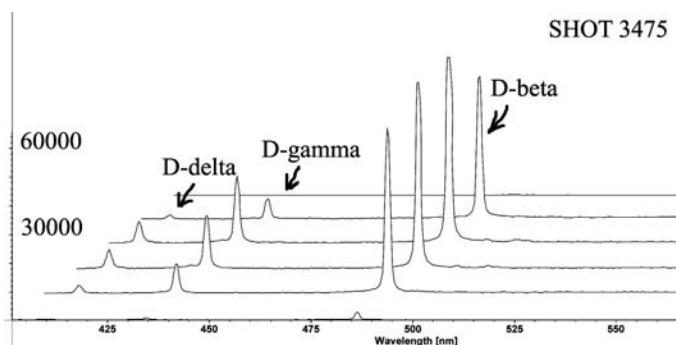

Figure 6: Wavelength-resolved spectra for six axial positions in the FRC during the PI phase of FRC formation, showing that the plasma is free of impurity emission.

FRC's are sensitive to the trigger and rise time of the magnetic fields during the initial formation process. We use the trapped flux and lifetime of the eventual FRC equilibrium as a figure of merit to evaluate all the permutations we tried for FRC formation. As seen in Fig. 7, the θ-PI startup technique rings the θ-pinch coil at high frequency, inducing a large toroidal E_θ field which breaks down the gas and freezes in the bias field before the main bank fires. Figure 8 shows a plot of one figure of merit for a series of shots, *i.e.*, the equilibrium FRC stable lifetime in μs versus time delay after PI trigger. The bottom panel shows the magnetic bias field on the same time scale as it is modulated by the PI current in the θ-coil. The "sweet spot" for formation occurs near the time that maximum B_{bias} is measured outside the quartz tube. This data could be consistent with either nearly zero delay between outside and inside magnetic field diffusion so that B_{bias} is large inside the tube at this instant, or approximately one cycle (3 μs) later. More data at different PI frequencies are needed to clarify this point.

4.3.2 High density FRC's

Recent data with improved crowbar operation, as shown in Fig. 9, exhibit increased trapped flux, density, and temperature. This crowbar circuit behavior is as good as anything achieved in past LANL experiments in the 1980's, such as FRX-A, B, and C. The 2–3 MPa (20–30 Atm) plasma pressure corresponding to this shot is substantial, , *i.e.*, a $\beta \approx 1$ confinement pressure exerted by a 2–3 T magnetic field. Operation with the previous crowbar circuit periodically decompressed the FRC inside the θ-coil, with B_Z as low as 1.5 T. The modulation of B_{ext} due to the original crowbar switch can also be seen in Fig. 7. Flux loss may occur when the length of the FRC separatrix exceeds the coil length (36 cm) and there is no longer a flux conserving radial boundary to confine the equilibrium.

In Fig. 9 the central (solid line) and off-axis (dotted line) chords show the classic $n = 2$ rotational instability at $t = 22$–26 μs that triggers the demise of many FRC's. Off-axis density traces show a decrease as the central chord density increases, consistent with an oval shape spinning about the Z-axis. In data prior to the crowbar improvements Abel inverted (8-chord) interferometer data show significant density surviving crowbar modulated decompressions, as shown in Fig. 10. Peak formation density for recent shots exceeds 7×10^{16} cm^{-3}, and equilibrium density is $\approx 4 \times 10^{16}$ cm^{-3}.

Visible spectra (all views are radial) from a main bank shot (2 μs time-slice) are shown in Fig. 11. Multiple oxygen impurity charge states, from OII through OVI are present. The OVI lines require 80 eV energies to populate the lower level and are only present in the inner two chords (under the θ-coils). Buildup of continuum radiation is noticeable during the FRC equilibrium phase, and the dominant impurity line during this time is OV, as shown in Fig. 12.

Incremental pulsed power improvements, exploration of the operating parameters, and significant improvement of the crowbar circuit have resulted in ≈ 2000 shots with $\approx 40\%$ main bank shots and $> 15\%$ "typical" good shots. We are presently exploring operational regimes to increase the FRC lifetime, with which trapped flux should scale.

4.3.3 Engineering and design

Pulsed power systems: We designed and built improvements to the pulsed power hard-
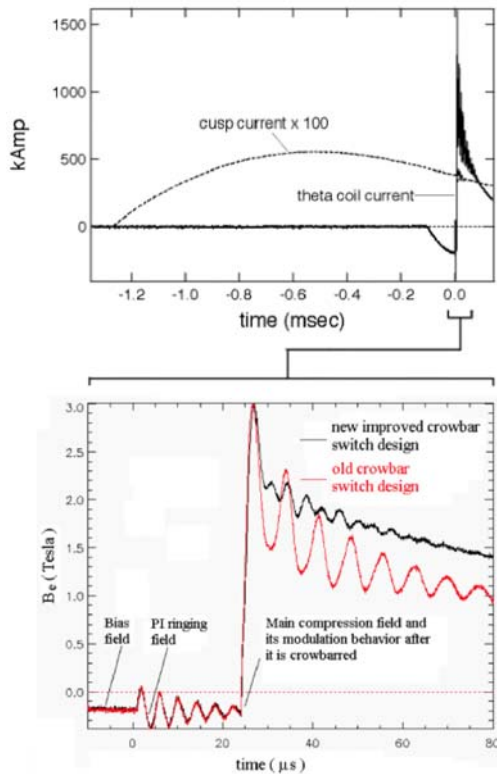
Figure 7: (top) Long time scale current in the θ and cusp/mirror coils. The cusp current creates a $B_{\rm Z}$ opposite to $B_{\rm bias}$. The main bank fires at $t = 0$ μs and rings while the crowbar forces the current to monotonically decay with its L/R time. (bottom) Waveforms from one of the magnetic probes (located on the top of θ-coil segment B) recorded during a shot with the old crowbar switch (red) and with the new crowbar switch (black).
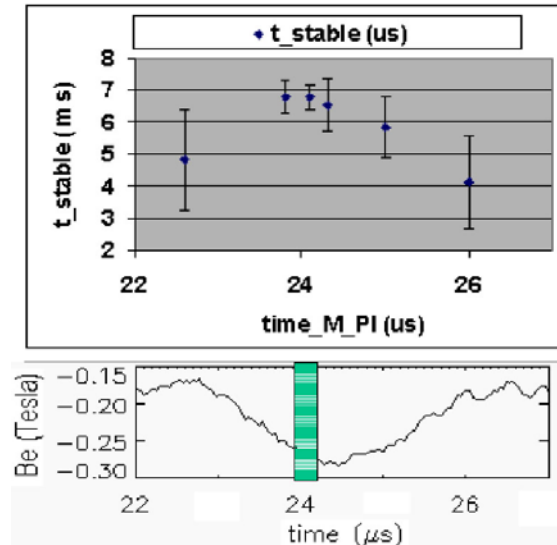
Figure 8: Plot of FRC stable lifetime (top) and magnetic field (bottom) versus time. The dependence of the stable lifetime on the phase of the PI waveform shows that the longest lifetimes are achieved just before the maximum $B_{\rm bias}$ is measured outside the quartz tube.

ware. In particular, we have redesigned the crowbar switch and cable header on the main bank in such a way as to dramatically reduce both the modulation of the θ-coil current and the resultant FRC decompression and recompression that appears after the crowbar switch is triggered. The "ideal" crowbar circuit has no switch inductance and no shared volume between the source loop and the load loop, as this represents a mutual inductance or coupling between the two loops. With the previous crowbar switch arrangement sketched in Fig. 13, there was a significant shared volume between the main bank-to-crowbar and crowbar-to-θ-coil loops. As the main bank current oscillated through this shared volume or mutual inductance in the main bank to crowbar loop, it induced a voltage upon the crowbar-to-θ-coil loop, which in turn produced the observed modulation on the θ-coil current. With the new crowbar switch and cable header arrangement shown in Fig. 14, the shared volume between the two loops has been virtually eliminated, although at the expense of some added
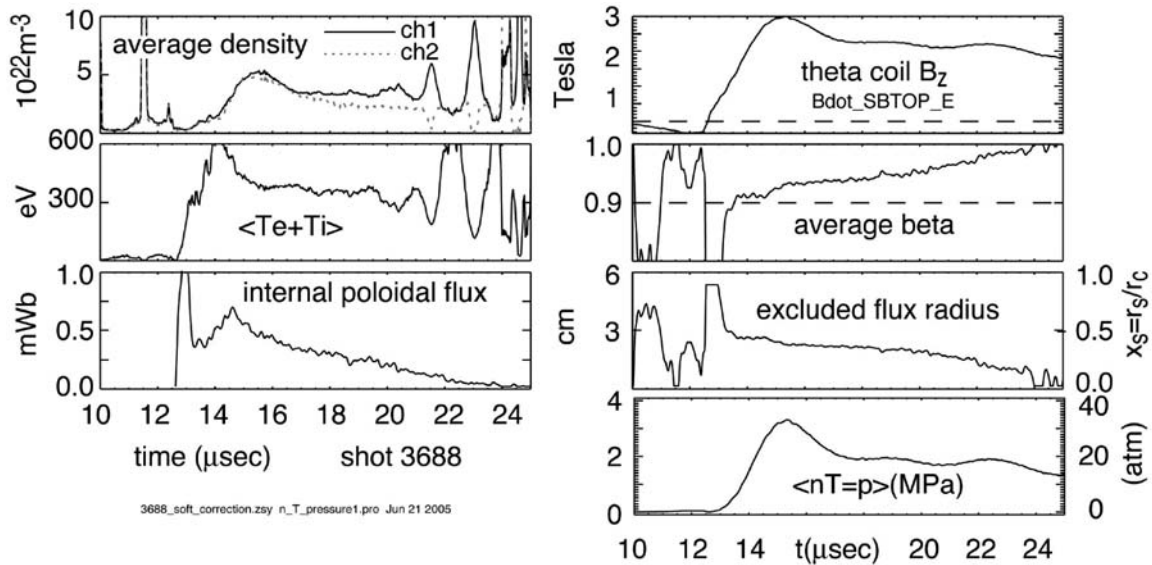
Figure 9: Recent data (June, 2005) with upgraded crowbar show greatly reduced modulation of θ-coil B_Z as well as increased trapped flux, density, and temperature. Plasma pressure is 2–3 MPa or 20–30 Bars.
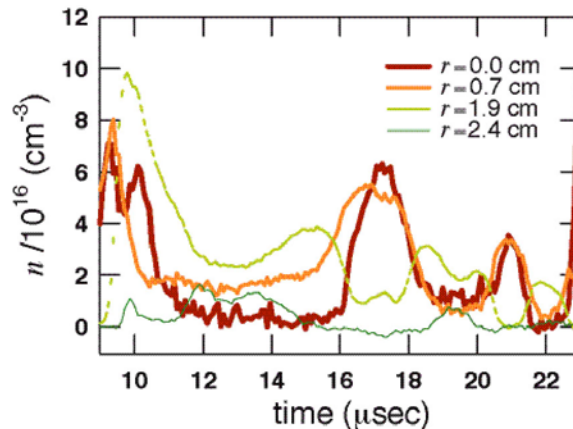
Figure 10: Abel-inverted density versus time for different radii, indicating a hollow spatial density profile as expected for a good FRC. (Note: data from before the crowbar upgrade.)

inductance to the crowbar-to-θ-coil loop. Any remaining influence that the oscillating main bank current has on the crowbarred θ-coil current is now due only to the voltage induced along the shared (linear) path through the crowbar switch. While the added inductance in the crowbar-to-θ-coil loop results in a modest reduction in the peak current initially delivered by the main bank, the fact that it is "downstream" of the crowbar switch helps to still further reduce the effect of the voltage across the crowbar switch inductance (from the main bank current) on the crowbarred θ-coil current. The plot of the axial magnetic field in the θ-coil region shown in Fig. 7 provides a comparison of the performance of both the previous and the new crowbar switches. The drop in field density following the initial peak is only 27% with the new crowbar switch, compared to 46% with the old crowbar switch, and it is obvious that the modulation after this initial drop is much improved. This drop is somewhat
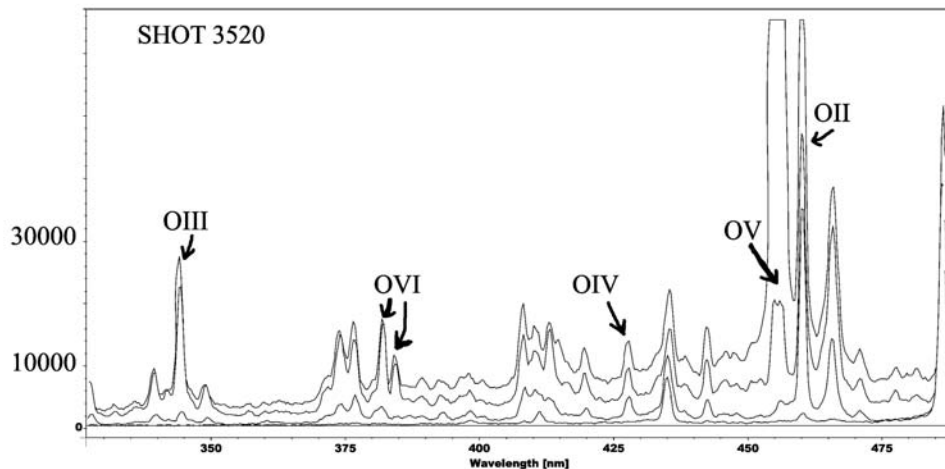
Figure 11: Visible line spectra are shown for a main bank shot for four axial locations (located from one end of the machine, progressively deeper towards the middle of the θ-coils). Oxygen is the dominant impurity. Note that the Ov line was saturated under the θ-coils.
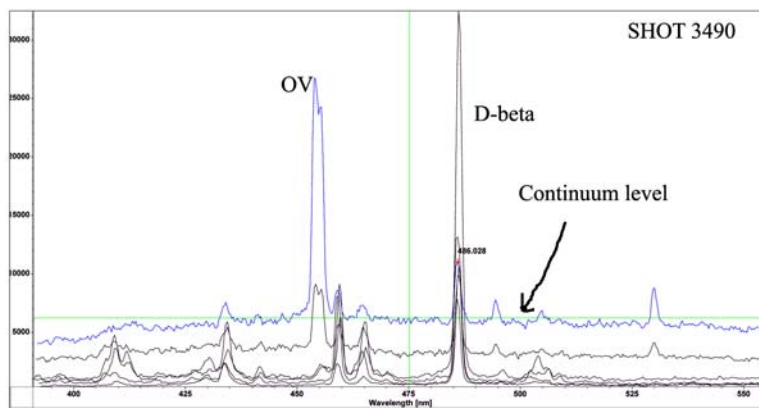
Figure 12: Continuum radiation builds up on the central chords during high density FRC equilibrium phase. The deuterium line (D_β) is suppressed in the center relative to the edge.

dependent on the extent of the trigger delay following the θ-coil current maximum.

Design of FRC translation experiment: Our experimental goal is to develop and operate the FRC translation experiment with the simplest possible technology and with implosion capability built in from the start. Implementation of this experiment is expected to take most of FY06.

We need to translate the FRC out of the formation region in a time comparable or longer than the formation time, where $t_{\text{form}} \approx 3$ μs for FRX-L. The axial force density can be regarded as due to the axial magnetic pressure gradient $(\mathrm{d}/\mathrm{d}Z)(B_Z^2/2\mu_0)$, or force per unit length $I_{\text{tor}} \times B_R$. We can achieve this with

1. conical θ-coil (FRX-C, and many other experiments),
2. fast pulsed mirrors (FRX-A).
3. sequentially triggered coils (Slough & Hoffman, 1997).
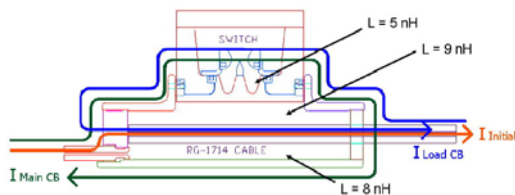
Figure 13: Current paths and inductances in the previous main bank crowbar switch and cable header arrangement. Note the shared inductance (volume) of ≈ 14 nH. The significant modulation of B_{ext} by the crowbar switch has recently been reduced significantly, as shown in Fig. 14.
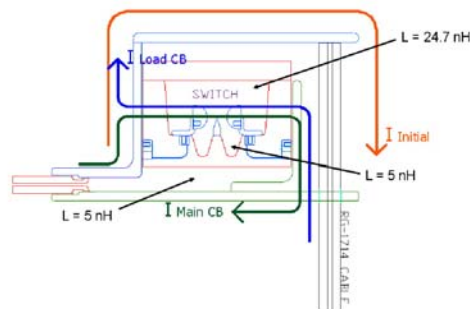
Figure 14: Current paths and inductances in the new main bank crowbar switch and cable header arrangement. There are now no shared current paths between the main bank and θ-coil loops.

Pulsed and sequential magnets have the advantage that one can control the formation separately from the translation timing but have the disadvantage of requiring high voltage pulsed magnet circuits. We will choose option 1.

We need sufficient expulsion force to get the FRC out quickly, but too much conical angle will impart toroidal magnetic field and spheromak characteristics to the FRC. At LANL, the FRX-C experiment had (Rej *et al.*, 1986) a stepped pseudo-conical θ-pinch coil with four sections (effective cone half angle $\alpha_{\text{cone}} = 1.4$ deg.). This apparently was a much smaller α_{cone} than previous translation experiments. Historically conical θ-coils have been used to generate spheromak-like plasmas. We are choosing $\alpha_{\text{cone}} = 1.4$ based on the work of (Wira & Pietrzyk, 1990) and the experience of FRX-C (Rej *et al.*, 1986). The FRX-C translation data shows an FRC emerging from the formation region and bouncing several times between the far end mirror and the θ-coil. This data was taken during "low compression" mode, *i.e.*, $B_{\text{bias}} \approx 1$ kG, $B_{\theta} \approx 5$ kG, $B_{\text{translation}} \approx 2.5$ kG. The reduction in field was on the order of 50% between the θ-coil and translation region. The reported translation speed was near the Alfvén speed evaluated with the reduced guide field and reduced density at 50% of the formation density. For peak acceleration at the most reduced translation magnetic field, translation speed was observed to be limited to the ion acoustic speed ($c_{\text{s}} = \gamma \langle T_{\text{e}} + T_{\text{i}} \rangle / m_{\text{i}}$).

The FRX-C data and analyses showed that if the acceleration and expulsion time was twice the formation time, the translation proceeded well. By this we mean that the final translating FRC seemed to persist with very similar confinement properties to the standard well-formed static FRC. For acceleration times of the order of the formation time, the formation process would be distorted by the acceleration forces. This would make it difficult to predict formation characteristics and perhaps make the FRC much more spheromak-like.

The FRC in the translation region experiences adiabatic expansion as B_{Z} decreases, *i.e.*, x_{s} will increase. Also the coil-generated vacuum magnetic field will get compressed as the FRC excludes the flux in the translation region. This results in at least three constraints:

1. The compressed B_{Z} must be significantly less than the compressed θ-coil field so that translation can proceed
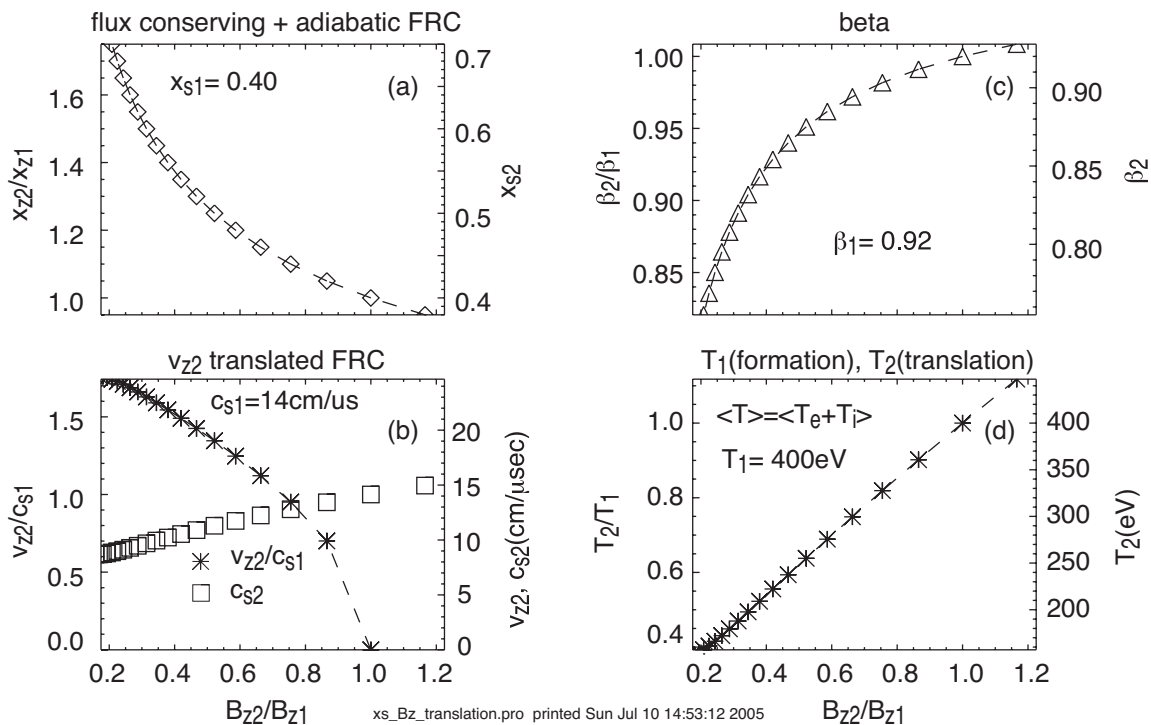
Figure 15: Adiabatic and flux conserving predictions for (a) separatrix radius x_s, (b) translation velocity v_{z2}, (c) β, and (d) $T = T_e + T_i$. Formation parameters are indicated by subscript 1 and translation parameters by subscript 2. The present design point is at $B_{z2}/B_{z1} = 0.7$. B_{z1}, B_{z2} are vacuum magnetic fields in the formation and translation regions, respectively.

2. The expanded FRC must fit inside the translation vacuum vessel

3. The expanded FRC must fit inside the liner region.

We design the magnet systems to furnish a given vacuum magnetic field. Using well known relations, Fig. 15 predicts the translated FRC parameters in terms of the applied B_{Z0} vacuum field in the formation and translation regions. This is slightly different from the way these scaling laws are usually expressed in terms of FRC compressed B_{eq} at the wall. This scaling for the elongated FRC neglects profile effects, assumes radial equilibrium $nT \approx B_{eq}^2/2\mu_0$, conservation of particles, $nV \approx$ constant, adiabatic relation $nT \approx V^{-5/3}$, constant ϵ during compression [see *e.g.*, Sec. 3.3.1 of (Tuszewski, 1988a)].

This model allows us to predict the state of the FRC in the translation region as a function of initial FRC parameters and how much reduction in translation B_Z field we desire. The conclusion is that the 5.5 cm radius vacuum vessel looks like it has plenty of room for the translation experiment, even with the mock liner inserted inside it.

A sketch of the major design elements is shown in Fig. 16. Our engineering design for the integrated formation, translation, and implosion experiment is in its second generation and is being refined to improve the magnetic field shaping. Magnetic fields are 3–5 T, and some parts must be designed to be expendable on each implosion. Other components are below the blast shield and will be recycled. Indicated on the figure are a conical θ-coil that is 8 cm longer than the present FRXL coil and a cusp/mirror coil on the small end of the θ-coil. A low inductance cable header and θ-coil assembly can be flooded inside a plastic bag with

Parameter	Design spec.	FRX-L achieved
coil E_θ (kV/cm)	1	0.85
coil radius (cm)	5.0	6.2
separatrix radius (cm)	2.5	2.5
coil length (cm)	36	36
separatrix length (cm)	35	30
B_{ext} (T)	5	2.0-2.5
B_{bias} (kG)	4	3
B_{GN} (kG)	6.6	5.6
p_0 gas fill (mTorr)	80	50
peak density (10^{17} cm^{-3})	1.0	0.5
$T_{\text{e}} + T_{\text{i}}$ (keV)	0.6	0.4-0.5
plasma energy (kJ)	7	2
τ_{N} (μs)	28	12
particle inventory (10^{19})	5	2-3
Φ_{bias} (mWb)	4	3
Φ_{LO} (mWb)	4	2
Φ_{int} internal flux (mWb)	1.0	0.5
S^*	25	12
s	2.9	0.5–1.6
E	7	5
S^*/E	3.5	2.4

Table 3: Summary of FRX-L design specifications and achieved parameters.

SF_6 to reduce the risk of air side flashover in locations where dielectric stress is substantial. Multipole stabilization Ioffe bars will be inserted in axially bored holes in the θ-coil. Guide field coils in the translation region create a far field that also acts as cusp/mirror field during formation.

4.3.4   FRC reproducibility and lifetime

Several campaigns have been undertaken to explore the experimental knobs available to us. Surveys of fill pressure have been carried for $20 < p_0 < 300$ mTorr, but most shots have been done at 50 mTorr. The PI bank voltage has been pushed to 55 kV. The bias field has been increased to ≈ 0.3 T. FRC lifetimes, shown in Fig. 17, are mostly in the range of ≈ 10 μs but extend as long as 18 μs. The conclusion was we needed a better crowbar circuit to avoid large particle and flux losses early in the shot. The crowbar was fabricated during the LANL shutdown of 2004 and installed immediately thereafter. Scans were resumed, and progress has been rapid as field and fluxes are increased. We would like to increase both the initial bias and PI field by approximately 50% and trap considerably more flux in the FRC. The average shot parameters are summarized in Table 3.
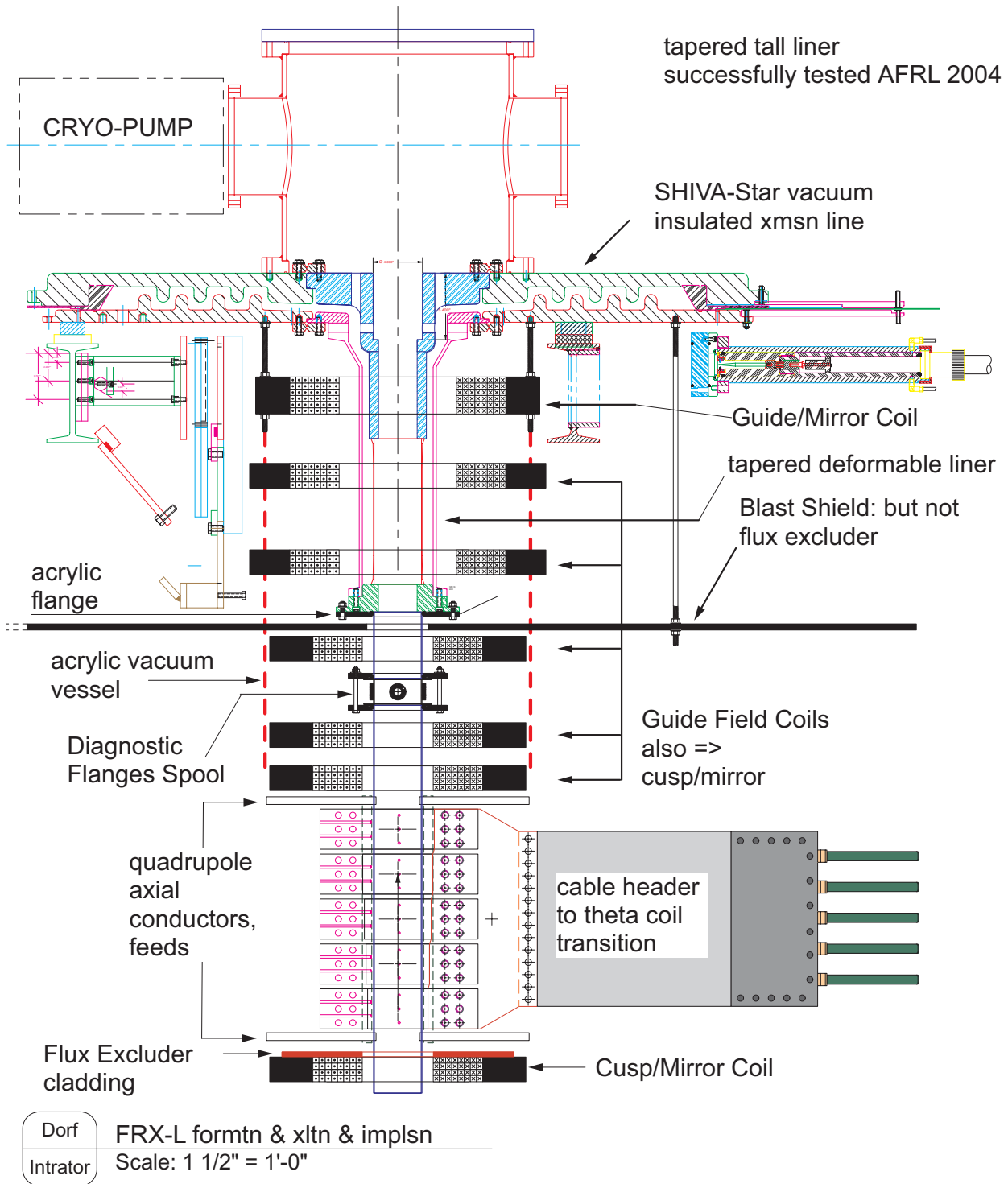
Figure 16: Design for the integrated formation, translation, and implosion experiment. Key design elements include a conical θ-coil, guide field, and magnetic mirror on the implosion end. Also note the cusp/mirror coil on the small end of the θ-coil, a low inductance cable header, a θ-coil assembly that can be flooded with SF_6, and quadrupole stabilization Ioffe bars inserted in axially bored holes in the θ-coil.
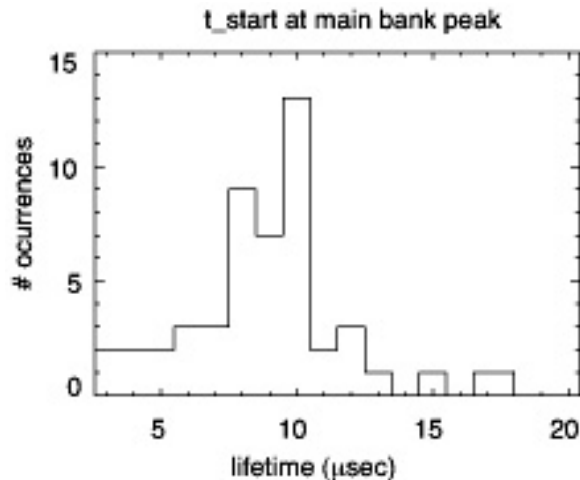
Figure 17: Histogram showing lifetimes of a 35 shot campaign. Lifetime is measured from the main bank peak current.

4.4 MOQUI simulations of FRC formation and translation

We have carried out simulations of the FRC formation, expulsion from a conical θ-coil region, translation, and the eventual bounce from the far end mirror field. We used MOQUI (Milroy & Brackbill, 1982) to sift through many design combinations. We settled on FRC formation inside a conical θ-coil with a small (1.4 deg. half angle), with magnetic profiles that correspond to magnet coil sets and power supplies that are relatively uncomplicated. After formation, translation requires a few microseconds from the formation to the "implosion" sections of the experiment. J. Park has carried out a survey of possible FRC formation and translation options. Figure 18 shows the time history of FRC formation in a conical θ-coil, propulsion, and then translation to the right.

4.5 Student programs

The student program in the P-24 Plasma Physics group is a notable asset anchored by our OFES-funded FRX-L project. The field of plasma and fusion sciences is at a crossroads because of our graying workforce. In 5–10 years the loss of essential knowledge will become overwhelming. We need to pass on our knowledge and experience in fusion science to the next generation of scientists and engineers before the exodus begins. We use a formal educational approach: summer school lectures by research staff, research projects mentored by research staff, and occasional workshops.[3] We encourage work-study semesters at LANL, *i.e.*, longer than a summer stay. This benefits the students, who get a continuous research experience. This has resulted in 1–2 first author undergraduate student publications per year. It also allows the long learning and training curve (2 months or more) necessary for sophisticated work in a national laboratory environment. We also send students to conferences and symposiums where they not only present their work, but they network with their

---

[3]Described in the following websites: `http://wsx.lanl.gov`,
`http://wsx.lanl.gov/RSX/summer-school/Summer_school_homepage.htm`,
`http://education.lanl.gov/newEPO/CS/critical_skills.html`.
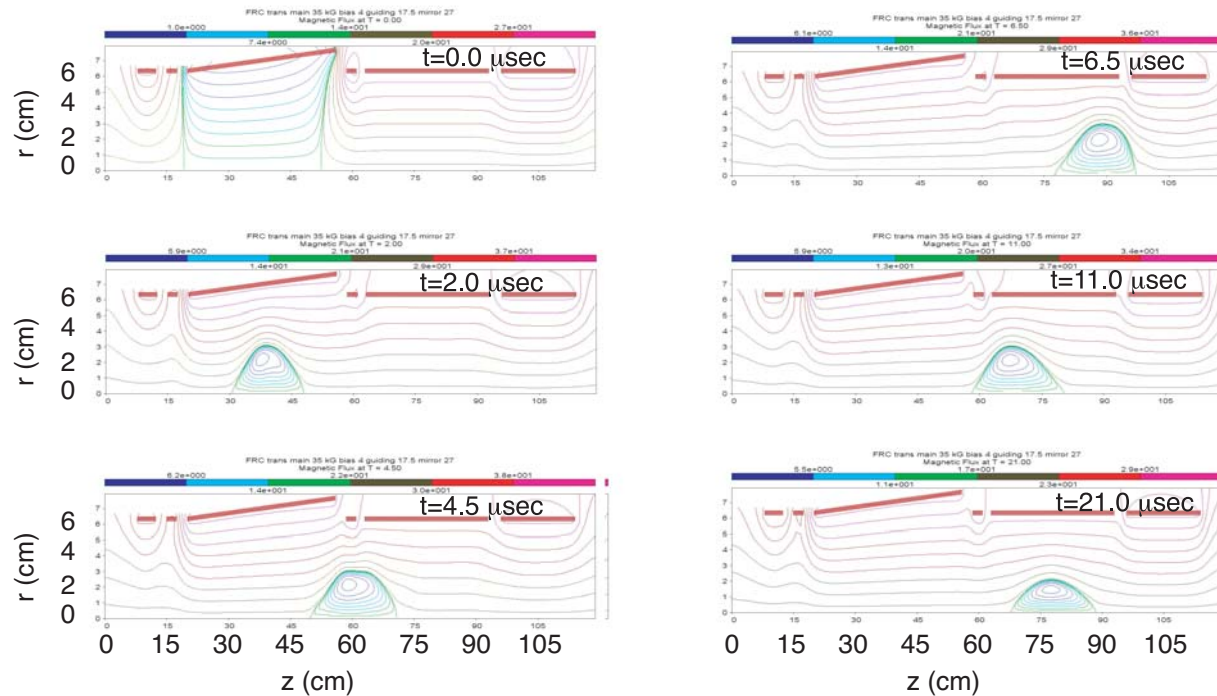
Figure 18: Six frames of a MOQUI simulation (with guidance from R. Milroy, Univ. Washington) done at LANL for typical experimental parameters and existing conical coil design. The frames start with formation in the conical θ-coil at $t = 0$ μs, acceleration at $t = 2$ μs, expulsion at $t = 4.5$ μs, and translation at $t = 6.5$ μs through a guide field region, after which it collides with a large mirror field on the right hand side. A subsequent bounce leads to leftward motion at $t = 11.0$ μs and final stagnation and dissipation shown by the frame at $t = 21.0$ μs. Travel speed is thus ≈ 15 cm/μs, and total elapsed time requires a formation time of about 3 μs plus the translation time. (Full movie at `http://wsx.lanl.gov/moqui.htm`)

peers, win awards, and attract more students to LANL. The large, continuing, year-round student population of our student program has attracted many students (> 100 in 5 years) to plasma physics and fusion science and sent some to graduate school in this field (Univ. Wisconsin, UCLA, Univ. Nevada-Reno). Many ($> 60\%$) students return, and some intend to start their careers here. Our student program has been recognized for excellence by the LANL Physics division and the UPOP engineering internship program at MIT. We bring in over \$100k/year of outside support (DOE Office of University Partnerships) to help fund our student programs, and we also attract many summer students every year who bring their own externally funded fellowships (*e.g.*, NASA and DOE-OFES).

5 Proposed research

The primary research goal during the present funding cycle (FY04-FY07) is to demonstrate the first integrated liner-on-plasma scientific demonstration for MTF. The three key goals are:

- Optimize the plasma performance of our high density and pressure FRC in FRX-L

- Translate the FRC into a mock liner region (at LANL) and to diagnose the translated plasma
- Design (mostly complete), fabricate, and perform an integrated liner-on-plasma experiment at AFRL, which we will call Shiva-FRC.

This project involves parallel experimental and engineering work at LANL and AFRL, and experimental collaborations with Univ. New Mexico and Univ. Washington. Below we give a detailed research plan and project schedule for the proposed four-year funding cycle FY06–09.

5.1 Synopsis, milestones, schedule

Here, we give a detailed plan for the entire project funding period (FY06–FY09). Tasks are indicated as LANL (funded by this proposal) and/or AFRL (funded by separated AFRL proposal with J. Degnan as PI).

- Year 1 (FY06):

    - Improve FRC lifetime by achieving more trapped flux via systematic scans of timing, bias/PI fields, gas fill pressure, PI/PPI schemes, and better diagnosis. (LANL)
    - Implement FRC translation design to do FRC translation experiments into a mock liner at LANL. (LANL)
    - Diagnostic additions/improvements for FRC formation and translation experiments, includes UNM collaboration. (LANL)
    - Fabrication of integrated experiment at AFRL, based on our nearly complete engineering design. (AFRL)
    - Migrate MDS-Plus data acquisition and archive from Solaris UNIX to LINUX operating systems on faster computers. (LANL)
    - Significant LANL personnel time at AFRL. (LANL)

- Year 2 (FY07):

    - Translation experiments on FRX-L. (LANL)
    - Test of multipole stabilization with Univ. Washington collaboration support (LANL and UW)
    - MOQUI modeling of FRC formation/translation. (LANL)
    - Refinement of Z-pinch liner hardware. (AFRL)
    - Deliver from LANL to AFRL 6 compressor bank modules and PI transmission line/switches to AFRL, commission hardware. (LANL)
    - Integrate and commission liner-on-plasma implosion experiment; clone most of LANL FRX-L experiment for configuration/installation at AFRL. (LANL and AFRL)
    - Perform first liner-on-plasma "shakedown" experiments at AFRL. (LANL and AFRL)

- Year 3 (FY08):

    - Perform first liner-on-plasma experiments at AFRL. (LANL and AFRL)

– Test multipole stabilization of $n = 2$ mode at AFRL (LANL and AFRL)

- Year 4 (FY09):

    – Continue liner-on-plasma experiments at AFRL. (LANL and AFRL)
    – Characterize compressed FRC and interface between plasma and imploding liner. (LANL and AFRL)

5.2   Detailed goals

5.2.1   Optimization of FRC formation on FRX-L

We want to increase the trapped flux in FRX-L by a factor of 2–3. The important experimental adjustments available include trigger timing scans, increasing gas pre-fill pressure p_0 from 50 to 80 mTorr, increasing B_{bias} from 3 to 4.5 kG, increasing the PI bank voltage so we can still zero cross the initial bias field during startup, and exploration (in collaboration with University of Washington) of other PI/pre-PI (PPI) and flux trapping schemes.

Increasing bias field and trapped flux: A design feature of FRX-L is a large E_θ due to the small θ-coil circumference. The θ-coil voltage is difficult to increase because we are already close to the maximum practical voltage standoff without oil insulation. For standard θ-pinch FRC formation, B_{GN} limits the scaling of the bias, lift-off, and trapped flux, and scales with neutral pressure $B_{\text{GN}}(\text{kG}) \approx 1.88[E_\theta(\text{kV/cm})]^{1/2}[A_i p_0(\text{mTorr})]^{1/4}$. Increasing p_0 is one way to increase B_{GN}, and hence gain the payoff from increased B_{bias}. More capacitance to upgrade the PI bank will be helpful, along with another complementary PPI system to reduce the requirements on the θ-pinch PI, in collaboration with J. Slough of University of Washington. Techniques to increase the ionization efficiency and uniformity include microwaves, Z-pinch discharges, multi-pole magnetic barrier fields, and other forms of inductive coupling. Consistent with FRC experiments worldwide, these details (especially timing) are important for improving the flux retention fraction of the θ-pinch formed FRC.

Pulsed power systems: We also are designing and building improvements in the pulsed power hardware, in addition to the completed upgraded crowbar. In place of our present flux excluder plates that shield the 16-turn cusp/mirror coils from θ-coil flux, we will use clad coils to protect them from mutual induced voltages. Increased use of lucite panels and plastic bags to contain SF_6 will reduce surface flashover risk in some of small clearance regions of the conductors. The design process for the translation and implosion magnetics benefits from MOQUI, an FRC simulation code, and time dependent eddy-current calculations that calculate mutual inductance matrices that include each combination of coils and conducting boundaries.

Experimental campaigns: A series of experimental campaigns are planned to scan the important parameters, and we will continue to bring more diagnostics online. The systematic scans all are likely to overlap with each other but fall under the following categories.

1. bias field amplitude
2. PI amplitude and timing
3. crowbar trigger timing
4. Different PPI scenarios and hardware
5. Gas pre-fill pressure possible gas puff schemes

6. Cusp/mirror amplitude and interaction with flux excluder plate location

7. Interactions of timing between scans 1,2, and 3.

From the foregoing list of scan parameters, a 6×6 matrix of scan permutations is possible. We will try to slowly increase B_{bias} and p_0 by exploring a judicious set of scan priorities. The first priority will be to increase B_{bias} beyond 3 kG until the PI system cannot break down the gas. Once the FRC formation has been optimized and B_{bias} limits are reached at $p_0 \approx 70$ mTorr, we will need to scan other parameters at this bias setting, starting with PI bank voltage.

5.2.2 FRC translation into a mock liner

The goal is to translate the FRC as fast as possible without compromising (too much) the pre-translated FRC parameters. MOQUI simulations (Milroy & Brackbill, 1982) suggest that an FRC can be easily translated in a few microseconds from the formation to the "implosion" section of the experiment. J. Park has carried out a survey of possible FRC formation and translation scenarios to help us choose among myriads of design options. Figure 18 shows the time history of FRC formation in a conical θ-coil, propulsion, and then translation to the right. We expect the construction of the translation section to be complete in FY06, with first experiments begun in late FY06. A "fake liner" with diagnostic holes on its side for vacuum radial access and another capacitor bank to power the mirror/guide coils will be used. The actual coils already exist. Translation into a vacuum instead of gas pre-fill chamber may be preferred, so we are developing gas puff dynamic fueling system with fast gas valves. This way we can tailor the neutral gas inventory locally to our requirements for separate formation and translation regions.

We will take advantage of the fast translation speed and try to insert electrostatic and magnetic probes in the path of the FRC since the contact time for any given probe with plasma is likely to be several μs at most. If the heat flux incident on the probes can be reduced sufficiently, or the probes designed robustly enough, *this may allow unprecedented internal measurements of magnetic, flow, electric, particle, and wave characteristics inside a high density FRC.* A time history corresponding to axial structure would be the ideal result.

The eventual integrated plasma/liner implosion experiment at AFRL will be much more difficult to diagnose because access in a real liner is severely limited to one view down the axis and neutron counting elsewhere. The translation experiment will be attached to one end of the FRX-L vessel. We will use an aluminum vessel with similar dimensions to the liner that will be used for the liner-on-plasma experiment at AFRL, but it will be enclosed inside a vessel so it does not need to hold off vacuum. This liner will be perforated with several radial ports so we can diagnose the FRC plasma as it translates through the liner region. It will be resistive enough to allow the magnetic guide and stopping mirror fields to soak through on their own time scales. We already have fabricated additional magnet pancake coils for the solenoid and mirror fields. They will be powered with pulse power equipment that is already operational for the cusp/mirror coils. Combinations of our 20 pancake coils and separate switched circuits will allow an asymmetric mirror, a uniform solenoid region, and a mirror on the far end of the liner region.

5.2.3   Design and construction of plasma-on-liner experiment at AFRL

An integrated liner-on-plasma MTF experiment is being designed and will be constructed at AFRL using the 9 MJ Shiva-Star capacitor bank to drive aluminum cylindrical liners. The details of this work are detailed in the separate LAB 05-09 proposal submitted by J. Degnan of AFRL.

Some of the existing LANL experiment will be copied and moved to AFRL with one significant change: the tube axis will need to be vertical to make a good low inductance connection to the Shiva-Star capacitor transmission line. In order to reduce the technical risk and expense, we will duplicate much of the LANL experiment. New design and engineering have been carried out for the front end/header which is the interface between FRX-L and the Shiva-Star FRC experiment.

This effort is likely to take 12–18 months. Construction starts in FY05. LANL will be responsible for delivering FRC formation/translation capability in support of the compression experiments in year two of the proposed research. The major subsystems that are part of the design include:

- New front end/header design for Shiva-FRC, the interface between the Shiva-Star bank and vacuum insulated transmission line, and the θ-coil. It provides for bias, PI, and main bank connections, as well as large Shiva bank connections for liner drive. (LANL)
- Z-pinch deformable liner design and experimentation. (AFRL)
- Build control system for Shiva-FRC. This will be a clone of the LANL version that uses open source MDS-Plus for data archives and LINUX operating systems on inexpensive computing hardware. Elements include programmable logic control using LabView FieldPoint for real time monitoring and control and air and optical interfaces from control room to high-bay equipment. (LANL)
- Build new front end/header for Shiva-FRC (at AFRL)
    - Stop FRX-L operation at LANL to move critical elements to Shiva-Star.
    - Move bias and cusp modules to Shiva-Star.
    - Cable connections, installation for 3-module main bank (700 kJ) at Shiva-FRC.
    - Transmission line installation for Shiva-Star liner drive bank (9 MJ) at Shiva-FRC.
- FRC plasma experiments at Shiva with static liner (no implosion), prepare for the first (destructive) implosion experiment.
- Field a subset of LANL FRX-L diagnostics for formation and translation at AFRL.
- Implement diagnostics that are capable of seeing down the bore of the imploding cylinder. The plasma will be very dense and optically thick to all radiation softer than X-Ray.

If resources permit, we will keep a smaller physics experiment alive at LANL to support the FRC formation/translation efforts at AFRL.

5.2.4   First integrated liner-on-plasma experiments at AFRL

In FY07 we plan the first shots for the integrated liner-on-plasma MTF experiments.

Exercising FRC, liner, diagnostic systems: Initial experiments at Shiva-FRC will exercise the systems by firing FRC's into a static liner. Multiple capacitor bank, triggers, data acquisition, and diagnostic systems need to function reliably and simultaneously in a very noisy electrical environment. Some liner shots onto vacuum or seed magnetic field will likely be necessary as well. Diagnostics for the imploding plasma will be implemented, including carrying over ones from present efforts and building several specialized ones. For liner-on-plasma shots, LANL will supply absolutely calibrated indium (DD) and copper (DT) activation neutron measurements, and also time resolved ZnS-Ag proton recoil scintillator neutron detector. Chordal, and even imaging end-on soft X-ray emission will be useful before the final moments of compression (when the liner closes off even the axial view). Protecting diagnostics from blast damage will be an issue if they are to be reused. Also, dynamic range, as the density goes up a factor of 100 and the temperature goes up a factor of 30, will be a big problem and will at the very least require dual digitizer channels for even the simplest diagnostic.

Liner-on-plasma experiments: The first integrated FRC plasma/solid liner shots will provide an opportunity to characterize FRC plasma behavior, its effects on the liner, the liner impact on the plasma, and plasma/implosion performance. We discuss briefly below some of the experimental considerations.

As the liner converges on the plasma, the radius is predicted to contract at a nearly constant speed. Figure 19 shows radius versus time data for an imploding cylindrical aluminum shell in a recent experiment at Shiva-Star (Intrator *et al.*, 2002). These dimensions were chosen to be close to what will be required in the real integrated experiment. The radial implosion in this case was onto vacuum with small embedded magnetic field. An implosion around a plasma core would experience plasma pressure pushing back on the liner, and the radius would stagnate at the last 1 μs with a radius of approximately 0.5 cm or less. But for the first 10 μs there would be a bore that decreased from a 5 to 1 cm radius. Adiabatic compression of elongated FRC equilibria can be shown to scale in a simple way (Spencer *et al.*, 1983; Tuszewski, 1988a). For liner compression, r_c contracts while $x_s \approx$ constant, and the FRC plasma volume then decreases as $r^{-2.4}$ and density increases as $r^{2.4}$. The viewing geometry and plasma density/temperature would all be accessible to conventional MFE diagnostics, including interferometers with blue lasers, which can look down the axis of the liner-compressed plasma. Faraday rotation can measure chord-averaged magnetic field for most of the experimental duration up until the last μs. Diagnostics for the imploding liner and plasma regions will be implemented. For the liner-on-plasma shots, both absolute and time-resolved neutron detectors will provide performance information. Soft X-ray emission down the axis of the FRC will also provide some information about the plasma conditions inside it. Flash hard X-ray source are typically used to image the liner at multiple times. Doping the liner surface to generate emission lines in the soft X-ray region, or crenulating the liner surface may provide some information about the mixing at the interface between plasma and imploding liner. External optical fiber Faraday-sensitive detectors can measure the liner current with minimal noise problems from the pulsed power systems.

Stabilization of $n = 2$ mode: Our first order plan is to maximize the FRC lifetime (only 1 μs is needed at final compression, consistent with a 1 μs maximum burn time) without stabilizing the $n = 2$ instability. It is not desirable to further complicate either the FRC conical source region or the liner region with additional coils, unless they are absolutely required. Nevertheless, the $n = 2$ mode is a consideration for MTF implosion
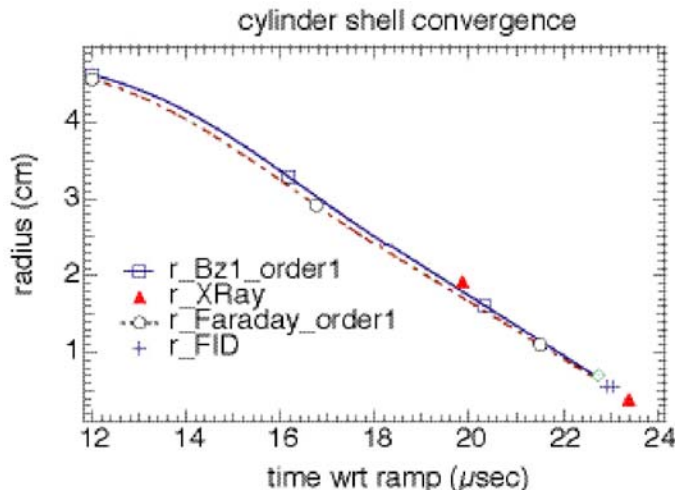
Figure 19: Time history of the convergence of a liner. Full implosion at Shiva-Star occurs in 24 μs.

performance. The FRC stability lifetime prior to the onset of toroidal mode number $n = 2$ modes has been empirically shown to be approximately $\tau_{\mathrm{N}} \approx R^2/\rho_{\mathrm{ie}}$, where ρ_{ie} is the ion gyro radius referenced to the external B field, and R is the major radius at the O-point. The quantity R^2 scales with trapped flux, and thus increased lifetime and trapped flux are desirable. Theory suggests, but it has never been experimentally confirmed, that an edge gradient parameter $\alpha = \omega_{\mathrm{rotn}}/\omega_{\mathrm{Di}} > 1.2-1.4$ from Eq. 5 indicates the threshold for rotational instability. Unlike flux compression, wall compression proceeds with fairly constant x_{s} values, but the edge gradient could increase by factors of 2–3. On the other hand, other issues are likely to compete with this for MTF. Angular momentum loss will likely be a factor, as particles and flux are lost. Also the liner material is likely to mix with the FRC scrape off layer, and viscous damping may occur. None of this is understood, and we intend to investigate and develop better understanding of these issues. We plan to address this issue, as part of our collaboration with University of Washington (J. Slough), during formation by increased trapped flux and multipole stabilization. Quadrupole or octupole "Ioffe bars" can be installed in axial holes bored in the θ-coil. This will produce field ripple on the order of 6–7% and reduce rotation by clamping the FRC in the formation region. The translation region could also be fitted with similar multipole conductors, but we believe that once the FRC is rotating, it will require more complicated hardware to decelerate the FRC than what will be required in the formation region.

Zero-D FRC models and radiation balance: A scaling law model of the FRC has been used to predict the essential formation and equilibrium parameters (Tuszewski, 1988b). These are coupled to atomic physics, excitation, emission, and radiation balance, and a connection to experimental measurements is straightforward (Rej & Tuszewski, 1984). A code used for FRX-C by D. Rej is available to us.

5.2.5 Diagnostics

Multi-chord interferometry, SXR diodes, bolometers, visible light tomographic arrays, flux loops, edge magnetic probes, VUV and visible spectroscopy, and end-on framing cameras are

already in use. Our implementation of a Thomson scattering system has had difficulties with plasma light, but in principal still has a chance to work on the pre-compression plasma. We don't intend to move it, or the 8-chord interferometer (which won't fit) to AFRL. At Shiva-Star, a few chords of interferometry will be useful in the formation region, and perhaps an end-on density schlieren/Faraday rotation imaging laser diagnostic (Qi *et al.*, 1998; Gribble *et al.*, 1967) with a red or blue laser. Other diagnostics will be improved or added as summarized in Table 4.

Diagnostic	Quantity measured
Internal probes (translation)	B, n
neutron detector	T_i
soft X-ray detectors	FRC axis and liner-plasma emissions
Thomson scattering	T_e, n_e (pre-compression)
laser holography	$\int n\mathrm{d}Z$, particle inventory
end-on laser Faraday rotation	I, B
fast camera	symmetry, instabilities
VUV spectroscopy	T_i, rotational velocity
soft X-ray array	fluctuations, impurity evolution
visible light array, tomography	emission profile
bolometers	total radiation budget, power balance

Table 4: Summary of diagnostics.

6 Budget

6.1 DOE Budget Pages (Form 4620.1)

DOE F 4620.1		**U.S. Department of Energy**		OMB Control No.	
(04-93)		**Budget Page**		1910-1400	
All Other Editions Are Obsolete		(See reverse for Instructions)		OMB Burden Disclosure Statement on Reverse	

ORGANIZATION Los Alamos National Laboratory				Budget Page No: 1 (Rollup)	
PRINCIPAL INVESTIGATOR/PROJECT DIRECTOR Thomas Intrator				Requested Duration: 48 (Months)	

A. SENIOR PERSONNEL: PI/PD, Co-PI's, Faculty and Other Senior Associates (List each separately with title; A.6. show number in brackets)	DOE Funded Person-mos.			Funds Requested by Applicant	Funds Granted by DOE
	CAL	ACAD	SUMR		
1. Tom Intrator, Technical Staff Member	34.97			413,784.00	
2. Glen Wurden, Technical Staff Member	14.76			184,898.00	
3. Scott Hsu, Technical Staff Member	18.59			187,550.00	
4. Jaeyoung Park, Technical Staff Member	18.59			171,393.00	
5.					
6. ( ) OTHERS (LIST INDIVIDUALLY ON BUDGET EXPLANATION PAGE)					
7. (4) TOTAL SENIOR PERSONNEL (1-6)	86.91			957,625.00	0.00
B. OTHER PERSONNEL (SHOW NUMBERS IN BRACKETS)					
1. (2) POST DOCTORAL ASSOCIATES	62.56			401,636.00	
2. (2) OTHER PROFESSIONAL (TECHNICIAN, PROGRAMMER, ETC.)	96.00			524,836.00	
3. (1) GRADUATE STUDENTS				98,723.00	
4. ( ) UNDERGRADUATE STUDENTS					
5. ( ) SECRETARIAL - CLERICAL					
6. ( ) OTHER					
TOTAL SALARIES AND WAGES (A+B)				1,982,820.00	0.00
C. FRINGE BENEFITS (IF CHARGED AS DIRECT COSTS)				543,065.00	
TOTAL SALARIES, WAGES AND FRINGE BENEFITS (A+B+C)				2,525,885.00	0.00
D. PERMANENT EQUIPMENT (LIST ITEM AND DOLLAR AMOUNT FOR EACH ITEM.)					
TOTAL PERMANENT EQUIPMENT					
E. TRAVEL 1. DOMESTIC (INCL. CANADA AND U.S. POSSESSIONS)					
2. FOREIGN					
TOTAL TRAVEL				0.00	0.00
F. TRAINEE/PARTICIPANT COSTS					
1. STIPENDS (Itemize levels, types + totals on budget justification page)					
2. TUITION & FEES					
3. TRAINEE TRAVEL					
4. OTHER (fully explain on justification page)					
TOTAL PARTICIPANTS ( ) TOTAL COST				0.00	0.00
G. OTHER DIRECT COSTS					
1. MATERIALS AND SUPPLIES				717,935.00	
2. PUBLICATION COSTS/DOCUMENTATION/DISSEMINATION					
3. CONSULTANT SERVICES					
4. COMPUTER (ADPE) SERVICES					
5. SUBCONTRACTS					
6. OTHER					
TOTAL OTHER DIRECT COSTS				717,935.00	0.00
H. TOTAL DIRECT COSTS (A THROUGH G)				3,243,820.00	0.00
I. INDIRECT COSTS (SPECIFY RATE AND BASE) Indirect on Labor includes Infrastructure Tax (.20), Division Tax (.455), Prog OH (.0172) and G&A (.36) Indirect on Travel and Other Direct includes G&A (.36) TOTAL INDIRECT COSTS				3,026,180.00	
J. TOTAL DIRECT AND INDIRECT COSTS (H+I)				6,270,000.00	0.00
K. AMOUNT OF ANY REQUIRED COST SHARING FROM NON-FEDERAL SOURCES					
L. TOTAL COST OF PROJECT (J+K)				6,270,000.00	0.00

DOE F 4620.1	U.S. Department of Energy	OMB Control No.
(04-93)	**Budget Page**	1910-1400
All Other Editions Are Obsolete	(See reverse for Instructions)	OMB Burden Disclosure Statement on Reverse

ORGANIZATION Los Alamos National Laboratory					Budget Page No:	2 (FY06)
PRINCIPAL INVESTIGATOR/PROJECT DIRECTOR Thomas Intrator					Requested Duration:	12 (Months)

A. SENIOR PERSONNEL: PI/PD, Co-PI's, Faculty and Other Senior Associates (List each separately with title; A.6. show number in brackets)	DOE Funded Person-mos.			Funds Requested by Applicant	Funds Granted by DOE
	CAL	ACAD	SUMR		
1. Tom Intrator, Technical Staff Member	8.74			96,286.00	
2. Glen Wurden, Technical Staff Member	3.69			43,027.00	
3. Scott Hsu, Technical Staff Member	4.65			43,646.00	
4. Jaeyoung Park, Technical Staff Member	4.65			39,883.00	
5.					
6. ( ) OTHERS (LIST INDIVIDUALLY ON BUDGET EXPLANATION PAGE)					
7. (4) TOTAL SENIOR PERSONNEL (1-6)	21.73			222,842.00	0.00
B. OTHER PERSONNEL (SHOW NUMBERS IN BRACKETS)					
1. (2) POST DOCTORAL ASSOCIATES	15.64			93,464.00	
2. (2) OTHER PROFESSIONAL (TECHNICIAN, PROGRAMMER, ETC.)	24.00			122,131.00	
3. (1) GRADUATE STUDENTS				22,974.00	
4. ( ) UNDERGRADUATE STUDENTS					
5. ( ) SECRETARIAL - CLERICAL					
6. ( ) OTHER					
TOTAL SALARIES AND WAGES (A+B)				461,411.00	0.00
C. FRINGE BENEFITS (IF CHARGED AS DIRECT COSTS)				126,374.00	
TOTAL SALARIES, WAGES AND FRINGE BENEFITS (A+B+C)				587,785.00	0.00
D. PERMANENT EQUIPMENT (LIST ITEM AND DOLLAR AMOUNT FOR EACH ITEM.)					
TOTAL PERMANENT EQUIPMENT					
E. TRAVEL 1. DOMESTIC (INCL. CANADA AND U.S. POSSESSIONS)					
2. FOREIGN					
TOTAL TRAVEL				0.00	0.00
F. TRAINEE/PARTICIPANT COSTS					
1. STIPENDS (Itemize levels, types + totals on budget justification page)					
2. TUITION & FEES					
3. TRAINEE TRAVEL					
4. OTHER (fully explain on justification page)					
TOTAL PARTICIPANTS ( ) TOTAL COST				0.00	0.00
G. OTHER DIRECT COSTS					
1. MATERIALS AND SUPPLIES				196,664.00	
2. PUBLICATION COSTS/DOCUMENTATION/DISSEMINATION					
3. CONSULTANT SERVICES					
4. COMPUTER (ADPE) SERVICES					
5. SUBCONTRACTS					
6. OTHER					
TOTAL OTHER DIRECT COSTS				196,664.00	0.00
H. TOTAL DIRECT COSTS (A THROUGH G)				784,449.00	0.00
I. INDIRECT COSTS (SPECIFY RATE AND BASE) Indirect on Labor includes Infrastructure Tax (.20), Division Tax (.455), Prog OH (.0172) and G&A (.36) Indirect on Travel and Other Direct includes G&A (.36)					
TOTAL INDIRECT COSTS				715,551.00	
J. TOTAL DIRECT AND INDIRECT COSTS (H+I)				1,500,000.00	0.00
K. AMOUNT OF ANY REQUIRED COST SHARING FROM NON-FEDERAL SOURCES					
L. TOTAL COST OF PROJECT (J+K)				1,500,000.00	0.00

DOE F 4620.1	U.S. Department of Energy	OMB Control No.
(04-93)	**Budget Page**	1910-1400
All Other Editions Are Obsolete	(See reverse for Instructions)	OMB Burden Disclosure Statement on Reverse

ORGANIZATION Los Alamos National Laboratory				Budget Page No:	3 (FY07)
PRINCIPAL INVESTIGATOR/PROJECT DIRECTOR Thomas Intrator				Requested Duration:	12 (Months)

A. SENIOR PERSONNEL: PI/PD, Co-PI's, Faculty and Other Senior Associates (List each separately with title; A.6. show number in brackets)	DOE Funded Person-mos.			Funds Requested by Applicant	Funds Granted by DOE
	CAL	ACAD	SUMR		
1. Tom Intrator, Technical Staff Member	8.74			100,911.00	
2. Glen Wurden, Technical Staff Member	3.69			45,093.00	
3. Scott Hsu, Technical Staff Member	4.65			45,739.00	
4. Jaeyoung Park, Technical Staff Member	4.65			41,797.00	
5.					
6. ( ) OTHERS (LIST INDIVIDUALLY ON BUDGET EXPLANATION PAGE)					
7. (4) TOTAL SENIOR PERSONNEL (1-6)	21.73			233,540.00	0.00
B. OTHER PERSONNEL (SHOW NUMBERS IN BRACKETS)					
1. (2) POST DOCTORAL ASSOCIATES	15.64			97,948.00	
2. (2) OTHER PROFESSIONAL (TECHNICIAN, PROGRAMMER, ETC.)	24.00			127,993.00	
3. (1) GRADUATE STUDENTS				24,076.00	
4. ( ) UNDERGRADUATE STUDENTS					
5. ( ) SECRETARIAL - CLERICAL					
6. ( ) OTHER					
TOTAL SALARIES AND WAGES (A+B)				483,557.00	0.00
C. FRINGE BENEFITS (IF CHARGED AS DIRECT COSTS)				132,439.00	
TOTAL SALARIES, WAGES AND FRINGE BENEFITS (A+B+C)				615,996.00	0.00
D. PERMANENT EQUIPMENT (LIST ITEM AND DOLLAR AMOUNT FOR EACH ITEM.)					
TOTAL PERMANENT EQUIPMENT					
E. TRAVEL 1. DOMESTIC (INCL. CANADA AND U.S. POSSESSIONS)					
2. FOREIGN					
TOTAL TRAVEL				0.00	0.00
F. TRAINEE/PARTICIPANT COSTS					
1. STIPENDS (Itemize levels, types + totals on budget justification page)					
2. TUITION & FEES					
3. TRAINEE TRAVEL					
4. OTHER (fully explain on justification page)					
TOTAL PARTICIPANTS ( ) TOTAL COST				0.00	0.00
G. OTHER DIRECT COSTS					
1. MATERIALS AND SUPPLIES				182,975.00	
2. PUBLICATION COSTS/DOCUMENTATION/DISSEMINATION					
3. CONSULTANT SERVICES					
4. COMPUTER (ADPE) SERVICES					
5. SUBCONTRACTS					
6. OTHER					
TOTAL OTHER DIRECT COSTS				182,975.00	0.00
H. TOTAL DIRECT COSTS (A THROUGH G)				798,971.00	0.00
I. INDIRECT COSTS (SPECIFY RATE AND BASE) Indirect on Labor includes Infrastructure Tax (.20), Division Tax (.455), Prog OH (.0172) and G&A (.36) Indirect on Travel and Other Direct includes G&A (.36)					
TOTAL INDIRECT COSTS				741,029.00	
J. TOTAL DIRECT AND INDIRECT COSTS (H+I)				1,540,000.00	0.00
K. AMOUNT OF ANY REQUIRED COST SHARING FROM NON-FEDERAL SOURCES					
L. TOTAL COST OF PROJECT (J+K)				1,540,000.00	0.00

DOE F 4620.1	U.S. Department of Energy	OMB Control No.
(04-93)	**Budget Page**	1910-1400
All Other Editions Are Obsolete	(See reverse for Instructions)	OMB Burden Disclosure Statement on Reverse

ORGANIZATION Los Alamos National Laboratory					Budget Page No:	4 (FY08)
PRINCIPAL INVESTIGATOR/PROJECT DIRECTOR Thomas Intrator					Requested Duration:	12 (Months)

A. SENIOR PERSONNEL: PI/PD, Co-PI's, Faculty and Other Senior Associates (List each separately with title; A.6. show number in brackets)	DOE Funded Person-mos.			Funds Requested by Applicant	Funds Granted by DOE
	CAL	ACAD	SUMR		
1. Tom Intrator, Technical Staff Member	8.74			105,757.00	
2. Glen Wurden, Technical Staff Member	3.69			47,255.00	
3. Scott Hsu, Technical Staff Member	4.65			47,933.00	
4. Jaeyoung Park, Technical Staff Member	4.65			43,805.00	
5.					
6. ( ) OTHERS (LIST INDIVIDUALLY ON BUDGET EXPLANATION PAGE)					
7. (4) TOTAL SENIOR PERSONNEL (1-6)	21.73			244,750.00	0.00
B. OTHER PERSONNEL (SHOW NUMBERS IN BRACKETS)					
1. (2) POST DOCTORAL ASSOCIATES	15.64			102,647.00	
2. (2) OTHER PROFESSIONAL (TECHNICIAN, PROGRAMMER, ETC.)	24.00			134,137.00	
3. (1) GRADUATE STUDENTS				25,231.00	
4. ( ) UNDERGRADUATE STUDENTS					
5. ( ) SECRETARIAL - CLERICAL					
6. ( ) OTHER					
TOTAL SALARIES AND WAGES (A+B)				506,765.00	0.00
C. FRINGE BENEFITS (IF CHARGED AS DIRECT COSTS)				138,795.00	
TOTAL SALARIES, WAGES AND FRINGE BENEFITS (A+B+C)				645,560.00	0.00
D. PERMANENT EQUIPMENT (LIST ITEM AND DOLLAR AMOUNT FOR EACH ITEM.)					
TOTAL PERMANENT EQUIPMENT					
E. TRAVEL 1. DOMESTIC (INCL. CANADA AND U.S. POSSESSIONS)					
2. FOREIGN					
TOTAL TRAVEL				0.00	0.00
F. TRAINEE/PARTICIPANT COSTS					
1. STIPENDS (Itemize levels, types + totals on budget justification page)					
2. TUITION & FEES					
3. TRAINEE TRAVEL					
4. OTHER (fully explain on justification page)					
TOTAL PARTICIPANTS ( ) TOTAL COST				0.00	0.00
G. OTHER DIRECT COSTS					
1. MATERIALS AND SUPPLIES				174,471.00	
2. PUBLICATION COSTS/DOCUMENTATION/DISSEMINATION					
3. CONSULTANT SERVICES					
4. COMPUTER (ADPE) SERVICES					
5. SUBCONTRACTS					
6. OTHER					
TOTAL OTHER DIRECT COSTS				174,471.00	0.00
H. TOTAL DIRECT COSTS (A THROUGH G)				820,031.00	0.00
I. INDIRECT COSTS (SPECIFY RATE AND BASE) Indirect on Labor includes Infrastructure Tax (.20), Division Tax (.455), Prog OH (.0172) and G&A (.36) Indirect on Travel and Other Direct includes G&A (.36)					
TOTAL INDIRECT COSTS				769,969.00	
J. TOTAL DIRECT AND INDIRECT COSTS (H+I)				1,590,000.00	0.00
K. AMOUNT OF ANY REQUIRED COST SHARING FROM NON-FEDERAL SOURCES					
L. TOTAL COST OF PROJECT (J+K)				1,590,000.00	0.00

DOE F 4620.1	U.S. Department of Energy	OMB Control No.
(04-93)	**Budget Page**	1910-1400
All Other Editions Are Obsolete	(See reverse for Instructions)	OMB Burden Disclosure Statement on Reverse

ORGANIZATION Los Alamos National Laboratory				Budget Page No:	5 (FY09)
PRINCIPAL INVESTIGATOR/PROJECT DIRECTOR Thomas Intrator				Requested Duration:	12 (Months)

A. SENIOR PERSONNEL: PI/PD, Co-PI's, Faculty and Other Senior Associates (List each separately with title; A.6. show number in brackets)	DOE Funded Person-mos.			Funds Requested by Applicant	Funds Granted by DOE
	CAL	ACAD	SUMR		
1. Tom Intrator, Technical Staff Member	8.74			110,830.00	
2. Glen Wurden, Technical Staff Member	3.69			49,523.00	
3. Scott Hsu, Technical Staff Member	4.65			50,232.00	
4. Jaeyoung Park, Technical Staff Member	4.65			45,908.00	
5.					
6. ( ) OTHERS (LIST INDIVIDUALLY ON BUDGET EXPLANATION PAGE)					
7. (4) TOTAL SENIOR PERSONNEL (1-6)	21.73			256,493.00	0.00
B. OTHER PERSONNEL (SHOW NUMBERS IN BRACKETS)					
1. (2) POST DOCTORAL ASSOCIATES	15.64			107,577.00	
2. (2) OTHER PROFESSIONAL (TECHNICIAN, PROGRAMMER, ETC.)	24.00			140,575.00	
3. (1) GRADUATE STUDENTS				26,442.00	
4. ( ) UNDERGRADUATE STUDENTS					
5. ( ) SECRETARIAL - CLERICAL					
6. ( ) OTHER					
TOTAL SALARIES AND WAGES (A+B)				531,087.00	0.00
C. FRINGE BENEFITS (IF CHARGED AS DIRECT COSTS)				145,457.00	
TOTAL SALARIES, WAGES AND FRINGE BENEFITS (A+B+C)				676,544.00	0.00
D. PERMANENT EQUIPMENT (LIST ITEM AND DOLLAR AMOUNT FOR EACH ITEM.)					
TOTAL PERMANENT EQUIPMENT					
E. TRAVEL 1. DOMESTIC (INCL. CANADA AND U.S. POSSESSIONS)					
2. FOREIGN					
TOTAL TRAVEL				0.00	0.00
F. TRAINEE/PARTICIPANT COSTS					
1. STIPENDS (Itemize levels, types + totals on budget justification page)					
2. TUITION & FEES					
3. TRAINEE TRAVEL					
4. OTHER (fully explain on justification page)					
TOTAL PARTICIPANTS ( ) TOTAL COST				0.00	0.00
G. OTHER DIRECT COSTS					
1. MATERIALS AND SUPPLIES				163,825.00	
2. PUBLICATION COSTS/DOCUMENTATION/DISSEMINATION					
3. CONSULTANT SERVICES					
4. COMPUTER (ADPE) SERVICES					
5. SUBCONTRACTS					
6. OTHER					
TOTAL OTHER DIRECT COSTS				163,825.00	0.00
H. TOTAL DIRECT COSTS (A THROUGH G)				840,369.00	0.00
I. INDIRECT COSTS (SPECIFY RATE AND BASE) Indirect on Labor includes Infrastructure Tax (.20), Division Tax (.455), Prog OH (.0172) and G&A (.36) Indirect on Travel and Other Direct includes G&A (.36)					
TOTAL INDIRECT COSTS				799,631.00	
J. TOTAL DIRECT AND INDIRECT COSTS (H+I)				1,640,000.00	0.00
K. AMOUNT OF ANY REQUIRED COST SHARING FROM NON-FEDERAL SOURCES					
L. TOTAL COST OF PROJECT (J+K)				1,640,000.00	0.00

6.2 Textual summary of budget

6.2.1 Personnel

The budget is dominated by salary support of the PI, senior technical staff, postdocs, and technicians. PI Tom Intrator is supported at 0.73 FTE/year, and he will provide overall project direction and oversee day-to-day operations of the project. Senior staff members Glen Wurden, Scott Hsu, and Jaeyoung Park are supported at 0.31, 0.39, and 0.39 FTE/year, respectively. They will each participate in all aspects of the project, and they will each lead various sub-tasks including diagnostic design/operation, physics analyses, and MOQUI modeling. Two postdocs, one at 1 FTE and the other at 0.3 FTE, will work on the project, including diagnostic operation and physics analysis. Two technicians and one engineer will be supported at a total of 2 FTE, to be split among the three people as the project demands. They will be involved in day-to-day operations of the project, and they will help operate experiments and provide mechanical and electrical support. We also have requested modest support ($\sim$ 0.3 FTE) for students. Even though the requested student support is only 0.3 FTE, we anticipate 2–3 FTE per year student participation. Typically, most of our student support comes from other funding sources, such as LANL student programs and external fellowships.

6.2.2 Materials and supplies (M&S)

M&S includes all non-salary costs, including but not limited to experimental equipment, computer hardware/software, travel, and publication charges. We have requested M&S amounts at approximately 10% of the total yearly budgets. This amount also includes subcontract arrangements ($\approx$ $30k/year each for Prof. Gilmore diagnostic collaboration and Dr. Miller reactor study collaboration). Table 5 summarizes our anticipated major M&S items. Hardware purchases are mostly during the first two years.

Item	cost ($k)
student/educational programs	50
Joerger digitizers CAMAC, 48 channels 40 MHz, 12 bits	24
Acquiris digitizers CAMAC, 64 channels 100 MHz, 14 bits	50
Spellman DCPS for PI bank, 100 kV, 100 mA	22
Maxwell railgaps (set of 4)	50
machine controll computer/fiber links	8
vacuum hardware	10
guide and mirror coil HV charging supplies	20
Northstar ignitron triggers for compressor modules ($3k ea)	15
software (CAD, data analysis) licenses	21
Jorway 411 SCSI serial highway driver	8
gated intensified camera for Thompson scattering, spectroscopy	42
domestic travel	20/year
foreign travel (IAEA or CT workshops)	5/year

Table 5: Listing of major one-time and recurring M&S costs.

We emphasize that we continually practice extreme cost-cutting measures, giving OFES a significant return on investment. These measures include using old equipment from prior/extinct projects (a significant LANL asset) and doing some procurement and fabrication through AFRL (which have lower overheads than LANL).

6.2.3 Indirect costs

As can be seen in the budget pages, LANL indirect costs work out to roughly 50% of the overall budget request. These indirect costs, which are broken down in "item i" of the budget pages, include infrastructure (0.2), division (0.455), and institutional taxes (0.36). M&S is charged only the institutional tax. Larger one-time capital purchases ($> \$25k$) are charged minimal indirect tax. We generally "package" our purchases whenever possible so that it qualifies as a "capital" purchase.

Despite the high indirect costs, we have been fortunate to benefit directly from these taxes. For example Scott Hsu, who has participated part-time on this project for the past 2.5 years, has been supported (at no cost to OFES) by a LANL Reines Fellowship which is paid from institutional program taxes. And as mentioned before, significant student support (on the order of $100k/year) comes from the LANL Applied Science Internship Program, also at no cost to OFES.

7   Collaborations

There are three collaborations for the technical work described in this proposal:

1. AFRL provides pulsed power expertise for our FRC formation/optimization experiments. AFRL will also provide the Shiva-Star facility, where we will perform the integrated liner-on-plasma implosion experiments (Shiva-FRC) to reach fusion conditions. AFRL is submitting a separate proposal (PI Jim Degnan) to LAB 05-09 for the tasks they will be leading.
2. Prof. M. Gilmore (University of New Mexico) and his postdoc will work on FRX-L diagnostics, focusing on VUV spectroscopy, which will yield valuable information on impurities and ion flows. ($30k/year year-to-year)
3. Dr. Ron Miller (Decysive Systems, Escondido, CA) will continue MTF reactor studies ($30k/year year-to-year)

We also list other collaborations, which are funded independently, that contribute either to the proposed work and/or to the overall national MTF effort:

1. R. Siemon (Univ. Nevada-Reno) is collaborating on Z-pinch realizations for MTF and the wall-plasma interactions.
2. J. Slough (Univ. Washington) will collaborate with us in testing and optimizing PI and PPI schemes to improve our FRC formation.
3. J. Santarius, (Univ. Wisconsin) has looked into modeling the physics of a plasma pusher instead of a metal liner for adiabatically compressing the magnetized plasma target. This has applications for both MTF and space propulsion.

4. D. Barnes (LANL, retired) has done seminal work on FRC physics. We will continue to consult him on FRC data/physics interpretations.

5. D. Ryutov (LLNL) has investigated basic issues of stability and liner considerations relating to magnetized plasma targets for MTF. He has done an analysis of drift instabilities in a strongly collisional plasma. The analysis now covers not only previously studied regimes of $\beta \gg 1$ but also regimes with modest $\beta \sim 0.5$, which are of direct interest for FRX-L. Current-driven instabilities (*e.g.*, the lower-hybrid instability) have also been analyzed in the parameter domain typical for FRX-L.

6. P. Parks (General Atomics) has carried out investigations of edge transport and will study compression issues vital to generic MTF approaches.

8 Other current and pending support of investigators

- T. Intrator

  - currently supported full-time on OFES funded FRX-L project to demonstrate MTF (overall \$1.4M/year FY04–07)
  - currently supported on internal LANL nano-sensor initiative (\$100k FY05)
  - pending NASA proposal, "Flux ropes as building units of the solar corona plasma: experiments and simulations of flux rope dynamics in plasmas" (\$163k per year FY06–08)

- G. Wurden

  - currently supported 0.1 FTE as LANL management (OFES program manager, Physics Division)
  - currently supported 0.3 FTE on OFES-funded FRX-L.
  - currently supported 0.33 FTE on diagnostic collaborations on OFES-funded Alcator CMOD and Univ. Washington FRC
  - currently supported NSTX dust beam diagnostic collaboration (\$270k/year, supports 0.5 FTE postdoc)
  - currently supported 0.1 FTE on science-based prediction initiative (internal LANL funding, see description under S. Hsu below)

- S. Hsu

  - currently supported (thru 11/05) full-time by LANL Reines Fellowship (internal LANL funding)
  - currently leading effort to integrate LANL efforts in experimental and computational plasma physics to test paradigms of "science-based prediction" (\$250k for FY05)
  - pending 0.17 FTE support for proposal submitted to OFES LAB 05-09, "Scientific Assessment Study of a Concept Exploration Experiment to Form and Sustain a Spherical Torus with a Plasma Center Column" (total request of \$139k for FY06)

- J. Park

  - currently supported 0.5 FTE on OFES-funded experiment on Electrostatic Inertial Confinement

9 Biographical sketches

9.1 Thomas Intrator

T. Intrator joined LANL in 1999 to lead the LANL Magnetized Target Fusion FRX-L effort, which was highlighted at our US-Japan CT workshop in Santa Fe NM 2004. He started the Reconnection Scaling Experiment (RSX), a unique linear device to investigate linear and non-linear MHD plasma physics, 3D magnetic reconnection and kink stability. He is a leader for P-24 and LANL wide student programs and won (2001) a LANL Student Mentor Award. Prior work at the University of Wisconsin included basic physics tabletop experiments, magnetic mirror, tokamak, ST, RFP, engineering and teaching. He was a CNRS visiting professor at the Universit de Grenoble, France (1989) and visiting scientist at Bell Laboratories Murray Hill NJ (1987). He was a PhD. student of Raul Stern and Noah Hershkowitz at the Univ. of Colorado.

Selected publications:

Magnetized Target Fusion and technology:
- Intrator, T. *et al*, *Experimental measurements of a converging flux conserver suitable for compressing a field reversed configuration for magnetized target fusion*, Nuclear Fusion, **42**(2) pp. 211-222 (2002).
- Intrator T., Zhang S. Y., Degnan J. H. *et al*, *A high density field reversed configuration (frc) target for magnetized target fusion: First internal profile measurements of a high density frc*, (2004)Physics Plasmas **11**, 2580 (2004).
- Taccetti, J.M., Intrator TP, *et al*, *FRX-L: A field-reversed configuration plasma injector for magnetized target fusion*, Rev. Sci. Instrum. **74**, 4314 (2003).
- Wurden GA, Intrator TP, *et al*, *Diagnostics for a magnetized target fusion experiment*, Review of Scientific Instrum. , **72** (1/pt.2) pp. 552-555 (2001)

Magnetic reconnection and non linear MHD experiments:
- Furno, I.G., Intrator T. P. *et al*, *Coalescence of two magnetic flux ropes via collisional magnetic reconnection*, Phys. Plasmas **12**, 055702 (2005).
- Furno, I.G., Intrator, T. *et al*, *Finite frequency kink modes in a non lined tied plasma column*, Phys Rev Lett., submitted (2005).
- Hemsing E. W., Furno, I, Intrator, T, *Fast camera images of flux ropes during plasma relaxation*, IEEE Transactions on Plasma Science, **33**, 448-449, (2005)

Tokamak RF heating and current drive:
- Intrator, T, *et al*, *Alfven Wave Current Drive in the Phaedrus-T Tokamak*, Phys Plasmas 2, 2263 (1995).
- Intrator T., *et al*, *Alfven ion-ion hybrid wave heating in the phaedrus-t tokamak*, Physics of Plasmas, 3, 1331, (1996)

Research accomplishments:
- First experimental evidence of Alfven Wave Current Drive in a tokamak
- RF hardware, antenna and fusion physics for tokamaks, spherical tokamaks, RFP.
- First laboratory measurements of 2 dimensional magnetized Double Layers
- Field Reversed Configurations and applications to magnetized Target Fusion
- Laboratory investigations of space physics, magnetic reconnection, non linear kink stability.

Recent collaborators:
- Magnetized Target Fusion: G. Wurden, S. Hsu (LANL), J. Degnan (AFRL)
- Field Reversed Configurations: J. Slough, A. Hoffman (Univ Wash.)
- Magnetic reconnection, non-linear MHD, kinks: I. Furno, G. Lapenta, S. Hsu (LANL), D. Ryutov (LLNL), J. Chen, M. Linton (NRL), G. Fiksel (Univ Wisc)

9.2   Glen Wurden

Glen A. Wurden, presently LANL's Office of Fusion Energy Sciences Program Manager, and plasma researcher in the P-24 Plasma Physics group at LANL, was born on Sept. 9, 1955 in Anchorage, Alaska. He attended public schools in western Washington, and went to the U. of Washington with a National Merit Scholarship. There he earned three simultaneous B.S. degrees, in Physics, Mathematics, and Chemistry, summa cum laude (1977) , graduating with the highest class honors as President's Medalist. He was awarded an NSF Graduate Fellowship and chose Princeton University to specialize in Astrophysical Sciences/Plasma Physics for his M.S. (1979) and Ph.D. (1982) degrees. He is a member of Phi Beta Kappa, the APS, the AAAS, the Planetary Society, and a senior member of the IEEE. He spent the summer of 1979 as a staff physicist working on x-ray and α- particle imaging of inertial fusion targets on the Shiva laser at Lawrence Livermore Laboratory in California. Upon finishing his Ph.D. ("CO_2 Laser Scattering on Radio-Frequency Waves in the Advanced Concepts Torus") at Princeton, he won a position at Los Alamos as an Oppenheimer Postdoctoral Fellow in the CTR-8 plasma diagnostics group, and later a permanent staff position in the CTR-2 reversed field pinch experimental group. In August 1988 he moved to Germany for 16 months as a DOE exchange scientist, working in the Max Planck Institute for Plasma Physics on the ASDEX tokamak, in Garching near Munich. After his return to Los Alamos at the end of 1989, he worked on the ZTH construction project (FIR interferometer, soft x-ray arrays, pellet injection) before taking a leave of absence to the U. of Washington as an Acting Associate Professor of Nuclear Engineering in August 1990, where he developed and taught new plasma lectures and lab classes, while conducting research at the LSX and MST plasma machines. He returned to LANL in April 1992, and began working on collaborations at TFTR (Princeton), JT-60U (Naka, Japan), Alcator C-Mod (MIT), HBT-EP (Columbia University), in the design of the ATLAS pulsed power machine, and at LLNL. His present collaborations include ones at Princeton, MIT, and the U. of Washington. Locally, most of his research time is on the FRX-L plasma experiment for proving the viability of the concept of magnetized target fusion. His research interests include a wide range of plasma diagnostic techniques to understand complex processes in hot fusion plasmas. He has particular research interests in laser scattering, bolometry, spectroscopy, pellet injection, fast x-ray and visible light imaging, neutron measurements, and concept improvement in fusion devices, with the ultimate aim of controlling fusion energy for use by mankind.

Selected publications:

- Z. Wang and G. A. Wurden, "Hypervelocity dust beam injection for internal mgnetic field mapping," Rev. Sci. Instrum. **74**, 1887 (2003)
- G. A. Wurden et al., "Diagnostics for a magnetized target fusion experiment," Rev. Sci. Instrum. **72**, 552 (2001)
- G. A. Wurden et al., "Plasma Tails: Comets Hyakutake and Hale-Bopp," IEEE Trans. Plasma Sci. **27**, 142 (1999)
- G. A. Wurden et al., "Design of an imaging bolometer system for the large helical device," Rev. Sci. Instrum. **68**, 766 (1997); also US Patent #5,861,625, June 19, 1999.
- G. A. Wurden and D. O. Whiteson, "High-Speed Plasma Imaging: A Lightning Bolt," IEEE Trans. Plasma Sci. **24**, 83 (1996)

- G. A. Wurden et al., "Scintillating-fiber 14 MeV neutron detector on TFTR during DT operation," Rev. Sci. Instrum. **66**, 901 (1995)
- G. A. Wurden et al., "Alpha particle detection via Helium spectroscopy in Lithium pellet cloud," LA-UR-94-667, Alpha Particle workshop, Princeton, NJ, March 2–4, 1994
- G. A. Wurden et al., "Disruption control strategies for TPX," LA-UR-93-2367, US-Japan Workshop on Steady-State Tokamaks, Kyushu, Jun 29–Jul 2, 1993
- G. A. Wurden, et al., "Initial Experimental results from the LSX field reversed configuration," 1991 EPS Conference, Berlin, Vol. 15C, part II, pp. 301–303
- G. A. Wurden et al., "Pellet refueling of the ZT-40M RFP," Nucl. Fusion **27**, 857 (1987)
- G. A. Wurden, "Soft x-ray array results on the ZT-40M RFP," Phys. Fluids **27**, 551 (1984)
- G. A. Wurden, "Ion temperature measurement via laser scattering on ion Bernstein waves," Phys. Rev. A **26**, 2297 (1982)

9.3   Scott Hsu

Dr. Scott Hsu will participate in experimental/diagnostic operation and in physics analysis of experimental results. He is currently a Reines Fellow in Experimental Sciences in the P-24 Plasma Physics Group at Los Alamos National Laboratory. He received his Ph.D. from Princeton University in January, 2000, having investigated ion heating and acceleration in magnetic reconnection experiments. Subsequently, he brought a DOE Fusion Energy Postdoctoral Fellowship to Caltech, where he performed experiments investigating the magnetic dynamics of spheromak and jet formation. He was recently elected onto the Executive Committee of the APS Topical Group in Plasma Astrophysics, and he was a co-recipient of the 2002 APS Award for Excellence in Plasma Physics Research for his work on magnetic reconnection.

Publications on magnetic helicity injection, spheromak formation, and plasma column formation experiments:
S. C. Hsu and P. M. Bellan, Phys. Plasmas **12**, 032103 (2005).
S. C. Hsu and P. M. Bellan, Phys. Rev. Lett. **90**, 215002 (2003).
S. C. Hsu and P. M. Bellan, Mon. N. Roy. Astron. Soc. **334**, 257 (2002).
S. C. Hsu and P. M. Bellan, IEEE Trans. Plasma Sci. **30**, 10 (2002).

Publications on magnetic reconnection experiments:
I. G. Furno et al., Phys. Plasmas **12**, 055702 (2005).
S. C. Hsu et al., Phys. Plasmas **8**, 1916 (2001).
H. Ji et al., Earth Planets Space **53**, 539 (2001).
S. C. Hsu et al., Phys. Rev. Lett. **84**, 3859 (2000).
M. Yamada et al., Phys. Plasmas **7**, 1781 (2000).
H. Ji et al., Phys. Plasmas **6**, 1743 (1999).
H. Ji et al., Phys. Rev. Lett. **80**, 3256 (1998).
M. Yamada et al., Phys. Plasmas **4**, 1936 (1997).
M. Yamada et al., Phys. Rev. Lett. **78**, 3117 (1997).

Publications on magnetized target fusion:
T. P. Intrator et al., Phys. Plasmas **11**, 2580 (2004).
J. M. Taccetti et al., Rev. Sci. Instrum. **74**, 4314 (2003).

Publications on diagnostic and experimental design:
Z. Wang et al., Rev. Sci. Instrum. **76**, 033501 (2005).
C. A. Romero-Talamás, P. M. Bellan, and S. C. Hsu, Rev. Sci. Instrum. **75**, 2664 (2004).

Publication on very high β tokamak equilibria:
S. C. Hsu, M. Artun, and S. C. Cowley, Phys. Plasmas **3**, 266 (1996).

Publication summarizing a Laboratory Plasma Astrophysics APS Mini-Conference:
H. Ji et al., Phys. Plasmas **11**, 2976 (2004).

Current projects:

1. Leading a LANL-funded effort to test paradigms of "Science-Based Prediction" by integrating efforts in basic laboratory plasma physics and MHD and hybrid numerical modeling of nonlinear plasma physics problems.

2. Participating on LANL internally LDRD-funded Flowing Magnetized Plasma experiment (PI: Z. Wang) to study angular momentum transport in plasmas.

3. Participating on DOE-OFES funded Magnetized Target Fusion experiment (PI: T. Intrator).

4. Collaborating with Dr. Mayya Tokman (UC-Berkeley and Lawrence Berkeley Laboratory) on MHD simulations of spheromak formation.

Recent collaborators:

1. Drs. Glen Wurden (LANL) and Tom Intrator (LANL) on Magnetized Target Fusion.

2. Dr. Zhehui Wang (LANL) on the Flowing Magnetized Plasma experiment.

3. Dr. Mayya Tokman (UC-Berkeley and Lawrence Berkeley Laboratory) on MHD simulations of spheromak formation.

4. Professor Paul Bellan (Caltech) on spheromak formation and magnetic collimation experiments.

5. Drs. Masaaki Yamada (Princeton) and Hantao Ji (Princeton) on magnetic reconnection experiments.

9.4   Jaeyoung Park

Jaeyoung Park is a Technical Staff Member in the P-24 Plasma Physics Group at LANL. He has been at LANL for the past eight years working on atmospheric pressure plasma sources, inertial electrostatic confinement systems, and high temperature plasma diagnostics for FRX-L. His recent scientific accomplishments are the following: 1) first experimental observation of periodically oscillating plasma sphere, 2) FRC translation simulations using the MOQUI code, 3) development of neutral bremsstrahlung measurement for n_e and T_e determination, and 4) carbon nano-structure production using rf high pressure plasma sources. His current research interests include neutron source development using plasma fusion devices, high temperature plasma diagnostics, and diagnostic ion beam development. He has extensive research experiences in plasma diagnostic development using spectroscopy (UV, visible, and laser), rf and microwave, and electrostatic and magnetic probes. His works also include experiments and numerical modeling of plasma-neutral interactions, gas and surface chemistry in plasma environment, and theory of collisional-radiative (CR) model for plasma spectroscopy. He received his Ph.D. (1997) and M.A. (1993) in Astrophysical Sciences from Princeton University and his B.S. in Physics from Korea Advanced Institute of Science and Technology (KAIST) in 1991. He has written 12 first-authored papers in peer-reviewed journals and two US patents, and has given numerous presentations at technical conferences including an invited talk at the 1999 and 2004 IEEE ICOPS meeting, and the 2004 APS/DPP meeting. He shared an R&D 100 award (1999) for development of the APPJ technology and was a recipient of a Merit Prize ($1,500) from Princeton University in 1991.

Selected Publications/Patents:

1. J. Park et al.,"Experimental Observation of Periodically Oscillating Plasma Sphere (POPS) Oscillation in a Gridded Inertial Electrostatic Confinement Device," Phys. Rev. Lett. **95**, 015003 (2005).

2. J. Park et al., "Periodically Oscillating Plasma Sphere (POPS)," Phys. Plasmas **12**, 056315 (2005).

3. J. Park and I. Henins, "Production of Stable, Nonthermal Atmospheric Pressure rf Capactive Plasmas using Gases other than Helium or Neon," U.S. Patent #6,909,237 (2005).

4. T. P. Intrator, J. Y. Park et al., "A High Density Field Reversed Configuration Plasma for Magnetized Target Fusion," IEEE Trans. Plasma Sci. **32**, 152 (2004).

5. J. Park et al., "Experimental studies of electrostatic confinement on the intense neutron source-electron device," Phys. Plasmas **10**, 3841 (2003).

6. J. Park et al., "Neutral Bremsstrahlung Measurement in an Atmospheric-Pressure Radio-Frequency (RF) Discharge," Phys. Plasmas **7**, 3141 (2000).

7. J. Park et al., "An Atmospheric Pressure Plasma Source," Appl. Phys. Lett. **76**, 288 (2000).

10   Facility descriptions

10.1   FRX-L

10.1.1   High-bay

The FRX-L experimental facility (Taccetti *et al.*, 2003) is distributed among three rooms including the experimental bay, the screen/control room, and a workspace/test-area. The experimental bay contains all of the pulsed power components and the experimental vessel. Its high walls and interlocked doors protect personnel, who must remain outside during operation. Figure 20 is a top-view of the 14×11.5 m (45×37') experimental high-bay drawn to scale (except for the dashed-line inset box, which shows a zoomed-in view of the coils). The principal components of the experiment are indicated on the figure: the vacuum vessel including the quartz tube and liner regions, the pulsed power components including θ-coil, transmission line, capacitor banks (PI, main, bias, cusp/mirror) and cusp/mirror coils along with flux excluder plates outboard of the θ-coil. The locations of the power supplies and triggers are also shown for reference. For clarity, we do not show safing mechanisms and diagnostics. The single turn θ-coil is segmented to allow diagnostic access and surrounds a quartz discharge tube. The bias, PI, and main banks connect to the parallel-plate transmission line via coaxial cables which feed the theta coil.
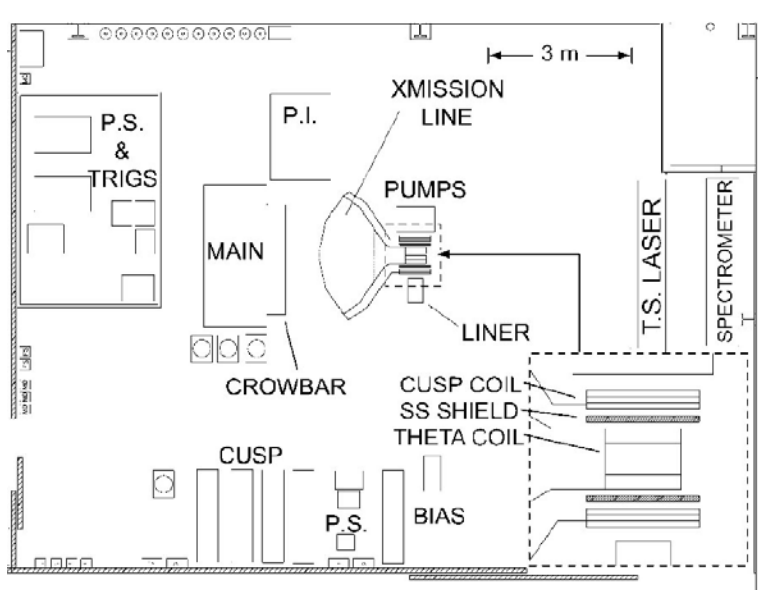

Figure 20: Layout of experimental high-bay showing primary hardware systems and zoomed inset of the θ and cusp coils.

10.1.2   Vacuum system

The vacuum chamber consists primarily of a 10.6 cm inside diameter quartz tube with 2.5 mm wall thickness located inside the θ-coil. The tube is evacuated and filled with deuterium at static pressures ranging from 10–100 mTorr. All vacuum flanges use copper gaskets except

Figure 21: FRX-L with top half of θ-coils removed, showing Kapton-wrapped quartz tube, diagnostic flux loops (white twisted cable), flux-excluder plates, and (greenish) pancake cusp coils.

for the quartz tube seals. The actual formation region can be seen in Fig. 21. A computer-controlled (LabView Field Point) real time interlock and sequencing system controls the vacuum operation. This protects against building power failures and provides the logic during shot operations to protect the vacuum sensors from voltage spikes that can occur during a shot. All vacuum sensors are physically (automatically) disconnected just before each shot to stand-off large electromagnetic pulse effects on wiring near the θ-coil.

10.1.3 Pulsed power circuits

The main capacitor bank (field-reversal bank) is a two-stage Marx bank with a maximum erected voltage of 120 kV at 36 μF yielding a quarter cycle rise time $\tau_{1/4} \approx 2.6 \mu$s into our inductive load. The crowbar switch is identical to the rail-gap array used to discharge the main bank but is situated on the output side of the main bank capacitors. The crowbar fires at maximum current and shunts the θ-coil current to ground through a low impedance circuit dominated by a long L/R decay time [Grabowski2002]. The cusp bank is a separate circuit that drives six coils. Stainless steel flux excluder plates (soak-through time $\approx 100 \mu$s) shield the cusp/mirror coils from mutual inductance coupling to the θ-coil. On the experimental time scale (20 μs) the cusp field ($\tau_{1/4} \approx 140 \mu$s) penetrates inward through the shields, but the PI and main bank fields do not diffuse out. The FRX-L circuit load is dominated by a straight (*i.e.*, no passive mirror) θ-pinch coil driven by several capacitor banks precisely timed to form, contain, and translate an FRC with the temperature, density, and lifetime appropriate for MTF. We use slow time scale active cusp/mirror coils at either end of the θ-coil. The high altitude at LANL (7300', STP = 560 Torr) requires conservative designs and unusual vigilance with high voltage systems. The timing is optimized empirically and it is important to control this to better than 100 ns. This circuit allows us to drive currents in the θ-coils. Other capacitor banks drive currents in the cusp/mirror coils at early time [Fig. 7(top)] which soaks through the flux excluder plate and creates a cusp region by canceling some of the bias field. The bias, PI, and main banks are shown with expanded time scale in Figure 10b. The θ-coil current exceeds 1.5 MA, with 70 kV on the Marxed main bank and ≈ 30 kV on the θ-coil. The crowbar is switched in at peak main bank current, and the original crowbar modulation of the main bank current is shown in Fig. 7(bottom), along with much

reduced modulation obtained with an upgraded crowbar switch (Grabowski *et al.*, 2002). The upgrade also included implementation of a fast optically coupled pre-fire detection emergency trigger system developed (Waganaar *et al.*, 2002) to mitigate pre-fire problems.

10.1.4 FRC formation scheme

A schematic of the FRC formation sequence from (Taccetti *et al.*, 2003) is shown in Fig. 22, illustrating the following steps:

1. Chamber is filled with neutral gas. The bias bank ($\tau_{1/4} \approx 140 \ \mu$s) produces a 3 kG slowly varying magnetic field B_{bias}. The PI bank triggers at the first minimum of B_{bias} ($\tau_{1/4} \approx 10 \ \mu$s) and ionizes the gas with a ringing toroidal electric field E_θ, which freezes in B_{bias}. This determines the upper limit for FRC trapped magnetic flux.

2. The θ-pinch coil current is rapidly reversed to a value 10 times the bias level ($\tau_{1/4} \approx$ 2.6 μs), driving B_{ext}. The PI plasma is pulled radially outwards by $j_\theta \times B_{\mathrm{bias}}$, and the main reversed field is driven radially inward by $j_\theta \times B_{\mathrm{ext}}$.

3. Magnetic field lines reconnect near the ends of the θ-coil and cusp region. The cusp/mirror coils, located at either end of the θ-coil, cancel out the initial B_{bias} at the θ-coil ends to form a cusp with mostly radial magnetic fields and trigger reconnection to occur repeatably at the same location and time every shot. They also create a mirror magnetic field with respect to the main bank field, centering the FRC under the θ- coil.

4. Field line tension contracts the FRC axially (Tuszewski *et al.*, 1991b) to an equilibrium with separatrix radius r_{s}. Toroidal current is induced by the jump in magnetic field. Radial shock heating rapidly drives the temperature above the radiation barrier, and dissipation of trapped flux in the presence of "anomalous" resistivity generates strong heating.

10.1.5 Control and data acquisition systems

Control (LabVIEW) and data acquisition/archival systems (Sybase, MDS-plus) are operated from within our screen room, an rf-shielded room containing digitizers, control system components, and remote (fiber-optically connected) diagnostics. From the screen room, live video views of the experimental area and personnel therein enhance the safety envelope and assist troubleshooting if things go awry. Other computer terminals make it possible for investigators to view and analyze data after each shot. Experimental "ground" can rise to many kV above earth reference for several μs during a shot, so we avoid hard electrical connections between the experiment and the screen room. Diagnostics that require contact with any part of the experiment are situated inside a separate rf-shielded enclosure which is allowed to float up in potential along with the experiment. Communication with these digitizers is done using a National Instruments GPIB fiber-optic extender. The data acquisition system is run separately from the control system. We seem to have one of nearly every digitizer known to mankind, which complicates our software systems. However, Joerger 12-bit, 16-channel, 40 Msample/sec CAMAC digitizers are gradually displacing the others.
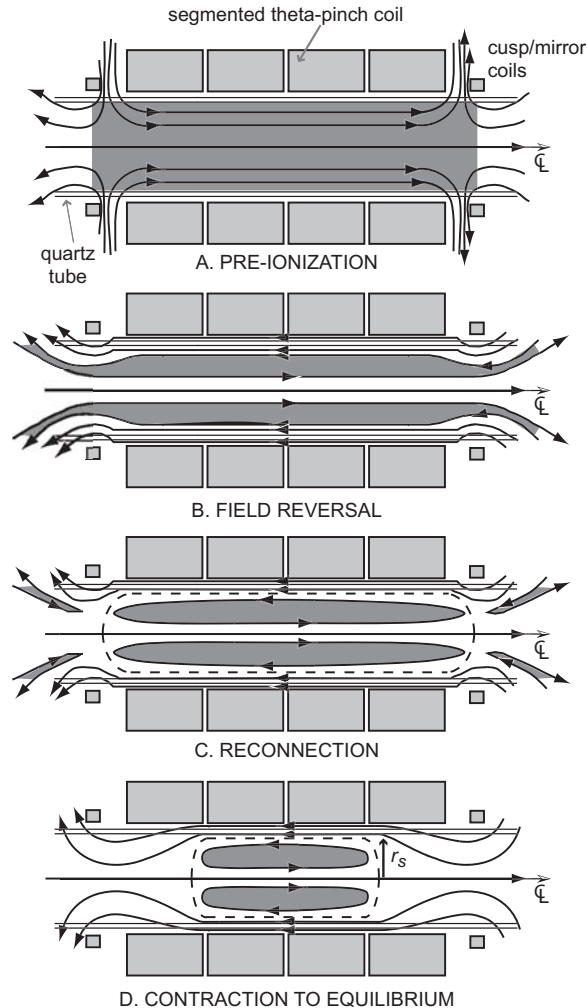
Figure 22: Cartoon of the θ-pinch FRC formation method.

10.1.6 Diagnostics presently in operation

Compared to typical MFE diagnostic suites, FRX-L diagnostics have some further constraints (Wurden *et al.*, 2001). We require access to a compact device with limited views of the plasma. The high density ($n \approx 10^{21}$ m^{-3} to 10^{23} m^{-3}), short lifetime ($\tau_{\mathrm{E}} \approx 10$–25 μs) plasma has strong transient electric and magnetic fields that create noise and ground plane troubles. FRX-L has a number of passive optical diagnostics. Generally, they include filtered photomultipliers, a 16-chord radial optical tomography array divided into two 8-chord fans positioned at 90 deg. with respect to each other, 3 time-windowed (spectral snapshots) optical spectrometers, a visible spectrometer with PMT, a VUV spectrometer with PMT, end-on bolometers, and soft x-ray detectors. The three gated, intensified visible-light spectrometers give wavelength-resolved spectra, but integrated over pre-specified time windows. Two of them (typically 10 μs average time window) are fed by single fibers (one with a radial view, and one with an axial end-on view). The third is a Roper Scientific system on loan from the U. Washington capable of measuring from six spatial positions for each snapshot in time, and either a high or low-resolution grating can be selected (typically 2 μs average). Its input fibers are positioned with central chord radial views but at 6 different axial (Z-position)

Diagnostic	Quantity measured
flux loops, magnetic probes	r_s, Φ_{exl}, $\langle\beta\rangle$
spectroscopy H_β	density during PI plasma
multi-chord laser interferometer	$\int n\,dr$, density profile, particle inventory
two 6-chord optical arrays	global tomography
framing camera	global plasma evolution
bolometer and soft X-ray detectors	radiated power (end-on)
spectroscopy OMA	impurity line spectrum snapshot
visible spectroscopy/PMT's	impurity line time evolution
closed-circuit video	pulsed power operation
pressure, voltage/current monitors	vacuum and power systems status

Table 6: Summary of existing diagnostics.

locations. Over the course of a two-month run, we have moved these fibers to different axial positions, to explore asymmetries in the plasma position control (*i.e.*, axially translating plasmas). The principal diagnostics utilized on FRX-L are summarized in Table 6.

10.2 Shiva-Star

Shiva-Star is a 9 MJ pulsed power facility located at AFRL in Albuquerque, NM. This is where we plan to field the integrated liner-on-plasma MTF implosion experiments. Details of the Shiva-Star facility are found in the LAB 05-09 proposal from AFRL (PI Jim Degnan).

A   Liner implosion background and issues

Background: The broad utility of high energy liners in Defense Programs and HEDP has led to significant investment in liner physics studies and technology advancement (Parker, 1993). High performance liners have been imploded by 5–15 MA of electric current from capacitor banks, such as the 9 MJ Shiva-Star at AFRL in Albuquerque and by greater than 100 MA from explosively powered flux compressors. MTF-relevant liner velocities of order 1 cm/μs have already been achieved, and Shiva-Star is expected to provide the necessary performance (Degnan *et al.*, 2001; Intrator *et al.*, 2002; Taccetti *et al.*, 2002) for our proposed integrated plasma-on-liner compression experiments. Axial (Z-pinch) current pinches the cylinder liner by $j_Z \times B_\theta$ forces and provides an effective and convenient configuration for driving liners using pulsed power. Relevant implosion velocities have been demonstrated while maintaining most of the liner at or above solid density and maintaining a significant fraction of the liner below ambient melt temperature (Reinovsky & Ekdahl, 1996). Because the drive pressure in the Z-pinch is applied to the outer surface of the liner, the acceleration of the lower-density outer surface interface into the higher-density metal liner gives rise to a situation analogous to the classical Rayleigh-Taylor instability. While the development of flute instabilities ($m > 0$) in the liner are inhibited by the toroidal driving field, the development of sausage instabilities ($m = 0$) on the liner surface could limit the achievable liner implosion convergence. However, because the material strength of the solid liner inhibits

instability growth, a convergence factor (~ 10) sufficient for MTF should be achievable and has been experimentally demonstrated (Degnan *et al.*, 2001; Intrator *et al.*, 2002).

Issues: Metal liners specific to FRC-implosion require larger length to diameter ratios than the liners being studied for HEDP applications. Studies including bias magnetic field and achievable compressed flux for the specific geometry of MTF are also important. Wall heating by eddy currents is severe for the Mega-Gauss fields to be used. Liner melting will reduce mechanical strength and increase electrical resistivity. These effects will limit the maximum fields that can be achieved by compression. Liner melting may also enhance the problems related to impurities. Computational models are available to quantify these concerns and will need to be used and be checked by liner experiments before integrated plasma-on-liner experiments are begun. The proposed research program will include design and proto-typing of liners appropriate for MTF based on the HEDP database. Presently, our use of aluminum solid liners provides material strength, good conductivity, and moderate melting temperatures. Other materials with higher melting point and atomic number (*e.g.*, Cu-W alloys) have been investigated (Armstrong, 1987). For a selected driver/target configuration, the demonstration of required liner properties (velocity, symmetry, shape, vacuum integrity, and uniformity) will be a prerequisite before proceeding to integrated liner-on-plasma experiments.

Integrated liner-on-plasma experiments: This proposal represents the first serious attempt to design and conduct integrated liner-on-plasma compression experiments (Lebedev *et al.*, 1993; Lindemuth *et al.*, 1978; Lindemuth & Widner, 1981; Lindemuth & Kirkpatrick, 1991). The success requires some target plasma science combined with the experience of high-energy liner implosion technology. The first integrated experiments will provide extremely interesting data on imploding MTF systems and will provide a valuable experimental check of the available computational tools. While significant advances in MTF physics will result from the initial experiments, it is not realistic to expect high fusion gain. Rather, the initial goal is to scientifically assess liner-plasma stability, impurity content and associated radiation power loss, and plasma transport under fusion-relevant implosion conditions (Drake *et al.*, 1996).

Status of liner-on-plasma experiments: A small number of FRC-wall compression experiments were done on the Tor-liner device (Alikhanov *et al.*, 1982; Es'kov *et al.*, 1981). An FRC was translated into a 5 cm radius liner with the following estimated parameters: $B_e \sim 5\,\text{kG}$, $n \sim 4 \times 10^{15}\,\text{cm}^{-3}$, $T_e \sim T_i \sim 50\,\text{eV}$, $r_s \sim 4\,\text{cm}$, and $l_s \sim 20\,\text{cm}$. These parameters correspond to $S^*/E \sim 3$. Medium-speed ($\sim 1\,\text{mm}/\mu\text{s}$), quasi-spherical liner compression (compression ratio ~ 5–10) was achieved with a shaped liner. A global neutron yield of about 2×10^8 was reported. Zero-D modeling (Es'kov *et al.*, 1983) confirmed that this yield is consistent with volume compression ratios of about 1000 and plasma temperatures of 1.5–3.5 keV, depending on assumed cross-field-line transport. Unfortunately, very few plasma measurements were reported and these encouraging results apparently were not pursued further.

Issues of liner-on-plasma experiments: A significant challenge is quantifying impurity release from the liner into the plasma during compression and its effects on power balance. Understanding of liner issues, such as metal jets produced by liner motion along the end glide-plane electrodes, will be critically tested in liner-on-plasma experiments. The issue of liner melting will also be important. Intensive studies (Gerwin & Malone, 1979) using both experimental impurity radiation measurements (Feinberg, 1976) and computational

codes will be utilized to study the effects of liner impurities before and during implosion.

B   MTF reactor considerations

Power plant perspective: Projections for mainline toroidal D-T MFE power-plant systems, based on tokamaks and stellarators, have come to be understood as steady-state plasmas with modest β ($\sim 5\%$). Plasma-facing and blanket structural materials have 14 MeV neutron fluence (10–15 MW/m^2) lifetimes that limit neutron wall loads (4–5 MW/m^2). The fusion power density in the plasma and the wall load limits tend to drive the size and cost of the fusion power core, and thus push the cost of electricity (cents/kWeh) to marginally competitive levels. Studies include the US ARIES series and the recent EU PPCS (Cook *et al.*, 2005). DT IFE systems variously include laser-drive, *e.g.*, HYLIFE-II (Moir *et al.*, 1994), heavy-ion-drive (Meier, 2005), or Z-IFE (Olson *et al.*, 2005), all characterized by pulsed fusion yield. Structural components can be protected from debris and thermal cycling by thick liquid coolant/breeder materials (*e.g.*, Li, PbLi, or Flibe). MTF operates in an intermediate regime between MFE and IFE. The MTF design space encompasses fusion yield (gain) and repetition rate, which can be traded against each other to generate a target net power output in a generating station containing one or more fusion power cores. The cost of remanufacture of front-end apparatus as a contributor to the projected cost of electricity [COE, cents/kWeh(net)] raises concern. Opportunities for direct conversion of fusion-product α-particle kinetic energy to electricity may exist. Recent experimental progress on the particular approach of interest is summarized in (Intrator *et al.*, 2004). FRX-L produces an FRC magnetized target plasma, which is to be translated into a region where an imploding flux-conserving metal shell (liner) compresses the plasma. Modeling at the level of (Quimby *et al.*, 1981), using an approximation for liner compressibility from (Gerwin & Malone, 1979), is presently in progress. External FRC formation and translation was invoked in the LINUS design (Turchi *et al.*, 1980; Robson, 1980), contrasting with *in situ* plasma formation for the Fast Liner Reactor (FLR) (Moses *et al.*, 1979; Ribe *et al.*, 1981) and the recent Z-IFE (Olson *et al.*, 2005). The FRC is also of interest as a MFE approach (Hoffman *et al.*, 1986; Moir *et al.*, 2001).

Sacrificial cartridge: The front-end apparatus of both the Fast Liner Reactor (FLR) (Moses *et al.*, 1979) and Z-IFE (Olson *et al.*, 2005) is suspended from a current leads assembly, which has come to be known as a Recyclable Transmission Line (RTL). For this MTF application, the leads assembly would additionally be configured as a cylindrical annulus to generate an axial guide magnetic field, along which an FRC plasmoid would be translated from an external plasma formation device (*e.g.*, θ-pinch coil) to the liner apparatus, which is removed a suitable distance from the inside surface of a blast-confining chamber. The liner apparatus is expected to be destroyed by the energetic fusion yield, together with a length of the RTL, denoted as a "cartridge." Moving away from the liner apparatus, the level of damage to the cartridge would diminish from vaporization or melting to mechanical distortion, leaving a stump. The cartridge provides standoff protection of the inner surface of the blast-confining chamber, which is also protected from cartridge shrapnel by a spray/fall of the primary coolant (*e.g.*, liquid Li, PbLi, or Flibe). The spray/fall of coolant for this MTF application need not be as carefully configured or controlled as would be the case for the HYLIFE (Moir *et al.*, 1994) IFE case, where converging beam paths must be accommodated.

Debris from the liner apparatus and the destroyed cartridge would have to be recovered from the primary-coolant pool at the bottom of the blast-confinement chamber (to prevent fouling of the downstream steam generators) for remanufacture into subsequent cartridges. There are a number of operational concerns associated with the cartridge, which might be avoided altogether by the Slow Liner (*e.g.*, LINUS) approach.

Cartridge remanufacture: It must be shown that the costs associated with the remanufacture of a cartridge are a suitably small fraction of the revenue generated by the sale of electric energy produced in the pulse, corrected for the duty cycle. This is the classic "kopeck problem." Recycling of sacrificial materials using automated '"rapid-prototyping" methods (*e.g.*, laser/plasma-arc forming or spray casting) as adapted from aerospace and other sources for use in the ARIES-ST study (Waganer *et al.*, 2003) can be considered. Methods for additive fabrication of aluminum components are summarized in Table 1 of (Sercombe & Schaffer, 2003), which introduces an approach involving laser sintering, nitridation, and infiltration. Additive methods would be expected to save steps and cost relative to the methods invoked for the Z-IFE. Cartridge parts made from AlLi alloys may be of interest for MTF applications, more for the presence of tritium-breeding Li than from the need for high strength, as is the rationale for aerospace AlLi alloys. This AlLi option has not yet been developed as a fusion breeder/coolant in terms of environment, safety, or materials compatibility.

Direct conversion: Twenty percent of the fusion energy released in DT fusion pulse is associated with 3.5 MeV α-particle fusion products. Depending upon the relative magnitudes of the α thermalization time, the α confinement time, and the liner dwell time, some of the α's may escape the liner front end and be conducted along the guide field to a zone where their kinetic energy can be directly converted to electricity at an efficiency higher than that of the thermal cycle. Similarly, plasma end losses might escape the blast chamber along the cartridge guide field. Examples of the conversion mechanism include a grid collector (Harms, 2000) or an MHD generator. A single-end cartridge cuts the available loss population in half (to first order). A two-ended cartridge (illustrated as Option C in Fig. III-9 of (Moses *et al.*, 1979) but set aside in the FLR work) might allow capture of much more of the charged-particle energy. In either case, the particles must escape before the cylindrical liner ends close off. Time of flight considerations suggest that the charged-particle pulse along the cartridge will be preceded by a 14 MeV neutron pulse, which may begin to disrupt the cartridge before fast α or plasma end losses can emerge. To minimize the loss of neutrons from the blast chamber, a curved cartridge designed to eliminate the line of sight from the liner to the cartridge access hole might be a useful variant. We believe that pulsed power driven MTF with an FRC target is the most expeditious way of testing the MTF concept, whether or not this ultimately turns out to be the best realization of this approach. This can be carried out on the existing 9 MJ Shiva-Star capacitor bank at AFRL.

C Peer-reviewed journal publications from this project

1. G. Wurden et al., "Diagnostics for a magnetized target fusion experiment," Rev. Sci. Instrum. **72**, 552 (2001).
2. J. Degnan et al., "Implosion of solid liner for compression of field reversed configuration," IEEE Trans. Plasma Sci. **29**, 93 (2001).

3. C. Grabowski et al., "Development of a high-current low-inductance crowbar switch for FRX-L," IEEE Trans. Plasma Sci. **30**, 1905 (2002).

4. T. Intrator et al., "High sensitivity Faraday rotation technique for measurements of magnetic fields with immunity to x-ray effects," Rev. Sci. Instrum. **73** 141 (2002).

5. T. Intrator et al., "Experimental measurements of a converging flux conserver suitable for compressing a field reversed configuration for magnetized target fusion," Nucl. Fusion **42**, 211 (2002).

6. M. Taccetti et al., "Magnetic field measurements inside a converging flux conserver for magnetized target fusion applications," Fusion Sci. Tech. **41**, 13 (2002).

7. M. Taccetti et al., "FRX-L: a field-reversed configuration plasma injector for magnetized target fusion," Rev. Sci. Instrum. **74**, 4314 (2003).

8. T. Intrator et al., "A high-density field reversed configuration plasma for magnetized target fusion," IEEE Trans. Plasma Sci. **32**, 152 (2004).

9. T. Intrator et al., "A high density field reversed configuration (FRC) target for magnetized target fusion: first internal profile measurements of a high density FRC," Phys. Plasmas **11**, 2580 (2004).

10. S. Zhang et al., "Separatrix radius measurement of field-reversed configuration plasma in FRX-L," Rev. Sci. Instrum. **75**, 4289 (2004).

11. T. Intrator et al., "Summary of US-Japan Exchange 2004: New directions and physics for compact toroids," J. Fus. Energy **23**, 175 (2005).

12. S. Zhang et al., "Confinement analyses of the high density field reversed configuration plasma in the field reversed configuration experiment with a liner," Phys. Plasmas **12**, 052513 (2005)

D   Time-dependent magnetic design considerations

We attach a design document written by Dr. Leonid Dorf.

MAGNETIC SYSTEM:

MAIN CONSIDERATIONS AND PROPOSED DESIGN

The entire FRX-L construction must comprise three stages – formation stage, translation stage, and implosion stage. We shall now dwell upon most important issues that need to be taken into account when designing the magnetic system of FRX-L.

The formation stage is realized by a set of five single-turn "theta" coils made out of stainless steel (Fig. D1). During FRC formation, these coils are first used to create a slow-varying "bias" field rising on a characteristic time-scale of $T_{rise} \sim 200 - 250$ μ sec. This field creates azimuthal plasma currents. After that, the voltage applied to the theta coils rapidly reverses the polarity, and the coils produce a fast-varying "main" field ($T_{rise} \sim 3 - 4$ μ sec). Together with the plasma field, this main field creates the magnetic field configuration – FRC – that confines the plasma. After the "plasma torus" is formed, it needs to be expelled out of the formation (theta-coil) region. Thus, almost purely axial "main" field should indeed have a mirror-like configuration, with the axial component reducing toward the exhaust, i. e. the end of the formation region, through which we want the plasma to leave. To create proper plasma currents prior to the field reversal, the magnetic field should have cusps (zeros of the field on the axis) at both ends of the formation region. These cusp fields can vary in time as slow as or slower than the bias field. These fields become mirror fields after the theta-field reversal.

After plasma is expelled out of the formation region, it needs to be translated to the implosion region. Along this translation stage, as well as the implosion region where the aluminum liner is located, the field needs to be almost constant. We refer to this field as to the "guide" field, and it can be realized by a set of several identical guide coils. Along these translation and implosion stages, the radius of the closest to the plasma cylindrical metal surface, R_m, should also be kept constant, and similar to that in the formation region. This prevents FRC plasma from expanding, and thus decreases the wall losses. In the implosion region, the radius of this metal surface is determined by the inner radius of the implosion liner. Along the translation stage, a different metal liner (made

out of Al or SS-304) can be used to keep R_m constant. When plasma translates across the implosion liner, it needs to be reflected, to return to the implosion region. A mirror coil placed above the implosion liner can be used for this purpose.

The axial field along the translation and implosion stages is created by the coils placed outside the metal cylinders – translation and implosion liners. This field increases in time, reaches its maximum, and then decreases to the zero level again. Such pulsed magnetic field creates eddy currents in a wall of the cylinder, which prevent it from penetrating inside and filling up the volume. The diffusion time for an infinitely fast magnetic pulse can be estimated as $\tau_{fill-up}[\text{msec}] = \dfrac{2\pi \cdot \Delta[\text{cm}] \cdot R_{in}[\text{cm}]}{\eta[\mu\Omega \cdot \text{cm}]}$, where Δ is the wall thickness, R_{in} is the inner radius of the cylinder, and η is the resistivity of the wall material. For an aluminum liner, this time is 1.2 msec, while for a stainless steel one it is 47 μ sec. Thus, for the guide and mirror coils in the implosion region, the voltage on the coils should not rise to the maximum faster than in about 1.2 msec, while for the guide coils in the translation stage, the applied voltage can be varied as fast as the bias field, if the translation liner is made out of SS-304.

The design of the entire FRX-L experiment, including the magnetic coils system, is shown in Fig. D1. Note that currents in the two power transmission lines do not create axial magnetic field, and thus do not affect the total magnetic field in any of the above three stages of the experiment. More importantly, it is necessary to protect the regular multi-turn cusp and first guide coil from the fast-rising main field that can induce a very large voltage and current across these coils, causing irreversible damage. These coils are designed to produce the slow-varying cusp and guide fields during the "field preparation stage" that precedes the rapid field reversal and FRC translation/implosion processes. One of the ways to prevent the fast main field, which is required only in the formation stage, from diffusing into the slow coils is to use metal "flux excluder plates" (FEPs) shown in Fig. D2. The guide/cusp coils are designed to withstand a voltage from a magnetic field of ~ 1T rising in ~ 100 μ sec. The main theta field in our design rises in about 3-4 μ sec, so theta field at the locations of the cusp/guide coils should be no more then ~ 0.03-0.04T, i.e ~ 100 times smaller then theta field in the formation region (which

CRYO-PUMP

2004 TAPERED TALL LINER
30 cm TALL
ri = 4.89 cm, t = 1.1 mm
(Identical liner to 2003 shot)

Power Transmission Line
(for liner implosion)

Mirror Coil

Giude Field Coils

Acrylic flange

Blast Shield
(should not be
flux excluder)

Diagnostic Flanges Spool

Giude Field Coils

Power Transmission Line
(for theta coils)

Translation Liner

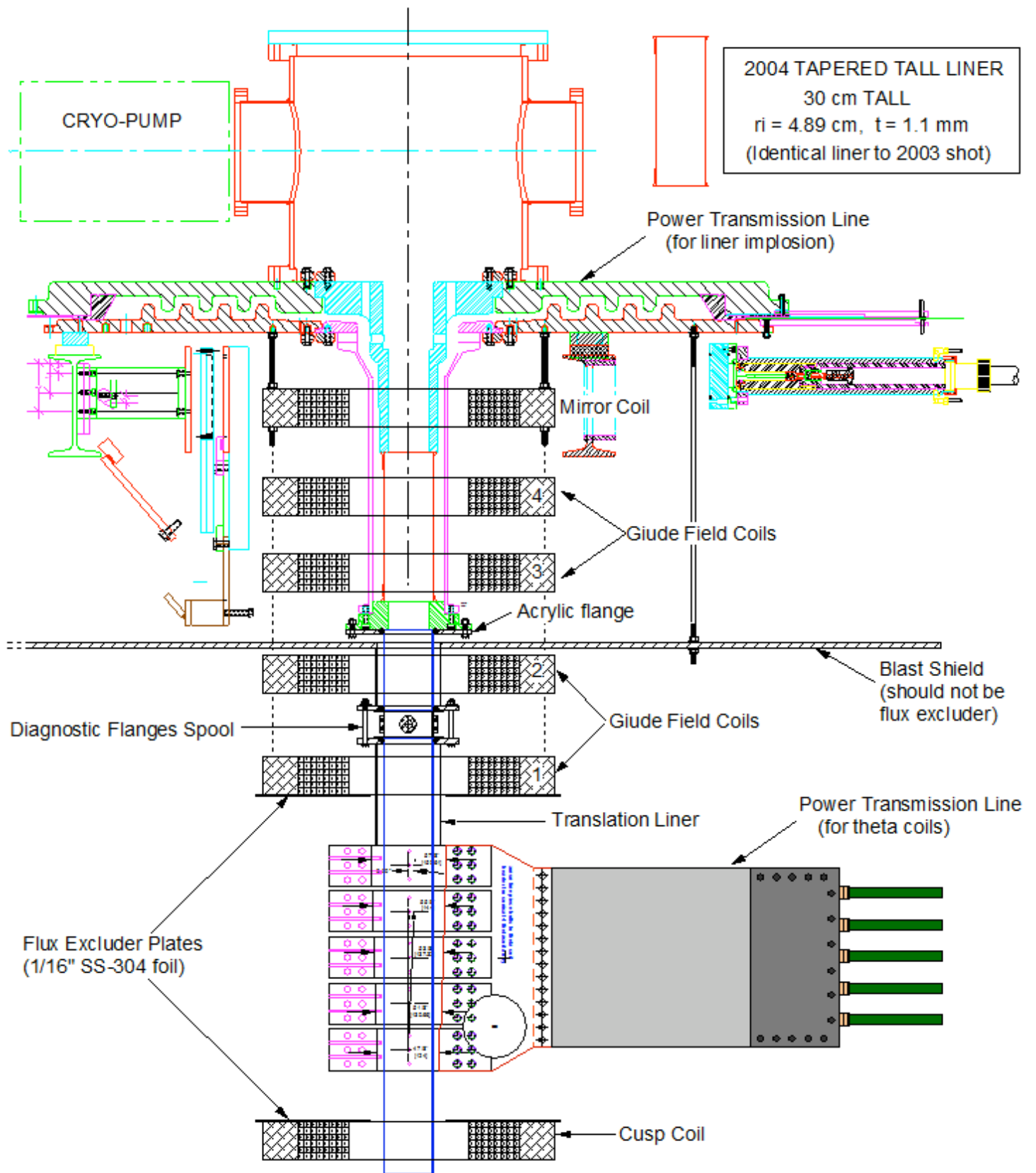Flux Excluder Plates
(1/16" SS-304 foil)

Cusp Coil

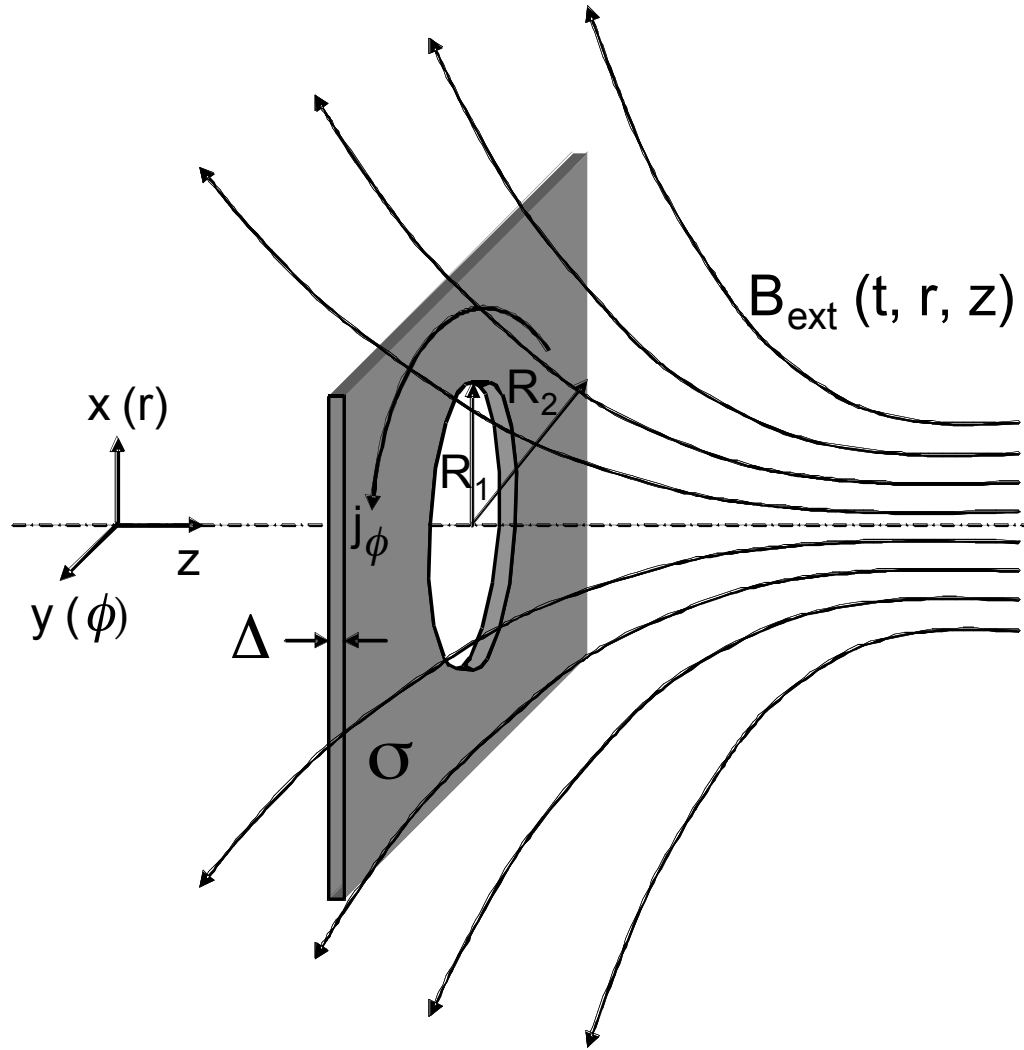Figure D1. Suggested design of formation, translation and implosion stages of FRX-L.

Figure D2. Flux excluder plate in the external time-dependent magnetic field.

in our current design is $\sim 3T$). It can be estimated that due to geometrical separation, theta field drops by about a factor of ≥ 10 at these locations. So we need FEPs to provide another factor of 10 in field reduction. These plates should be designed so that not to affect the slow-varying cusp, bias, and guide fields. It is useful to consider the FEP problem separately.

We have obtained the approximate expressions for the magnetic field on the axis, created by a thin disk ($\Delta << \tilde{R}$) with an aperture, placed in an axysimmetric monochromatic magnetic field changing with the time frequency f.

$$\frac{B^{FEP}(z, r=0)}{B_0} = -\frac{(1-g)}{R_2}\left(\frac{2z^2 + R_2^2}{\sqrt{z^2 + R_2^2}} - \frac{2z^2 + R_1^2}{\sqrt{z^2 + R_1^2}}\right) \xrightarrow{z \gg R_{1,2}}$$

$$(1-g)\frac{(R_2 - R_1)}{2R_2}\frac{(R_1 + R_2)(R_1^2 + R_2^2)}{z^3}$$

(1)

where the field attenuation factor for an infinite plate without an aperture, $g(f)$, is shown in Fig. D3 for a stainless steel plate with $R_1 = 3" = 7.62\,\text{cm}$, $R_2 = 9" = 22.86\,\text{cm}$, $\tilde{R} = (R_1 + R_2)/2 = 15.24\,\text{cm}$, and $\Delta = 1/16" = 0.16\,\text{cm}$. The general shape of this curve will be true for any $\tilde{R}$ and Δ, as long as $\tilde{R} > 25\Delta$. In eq. (1), B_0 is the magnitude of the external magnetic field in the center of the disk, $z = 0$, $r = 0$.
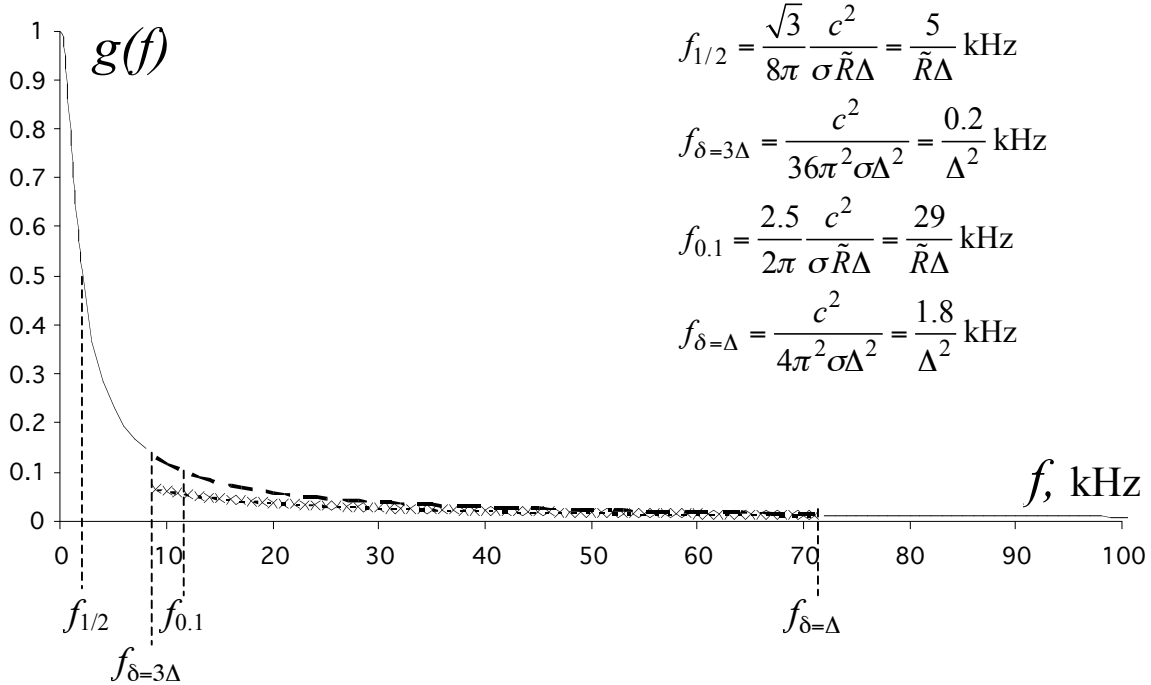

$$f_{1/2} = \frac{\sqrt{3}}{8\pi}\frac{c^2}{\sigma \tilde{R}\Delta} = \frac{5}{\tilde{R}\Delta}\,\text{kHz}$$

$$f_{\delta=3\Delta} = \frac{c^2}{36\pi^2\sigma\Delta^2} = \frac{0.2}{\Delta^2}\,\text{kHz}$$

$$f_{0.1} = \frac{2.5}{2\pi}\frac{c^2}{\sigma \tilde{R}\Delta} = \frac{29}{\tilde{R}\Delta}\,\text{kHz}$$

$$f_{\delta=\Delta} = \frac{c^2}{4\pi^2\sigma\Delta^2} = \frac{1.8}{\Delta^2}\,\text{kHz}$$

Figure D3. Field attenuation factor, $g(f)$, versus field frequency, f, for $\Delta = 0.16\,\text{cm}$.

In Fig. D3, $f_{1/2}$ and $f_{0.1}$ refer to the frequencies, at which $g = 1/2$ and 0.1, respectively, and $\delta = c/(2\pi\sqrt{\sigma f})$ is the frequency-dependent skin-depth, and σ is the conductivity of the plate material. We can make the following conclusions from eq. (1):

(1) In the center of the aperture, the external field is attenuated by a factor $g' = R_1 / R_2 + (1 - R_1 / R_2) g(f)$.

(2) In the case of the perfect screening, $g(f) \ll 1$, the ratio of the total field in the center of the aperture to the external field is $g' = R_1 / R_2$. Thus, a finite non-zero part of the external field soaks through the aperture, regardless of the field frequency.

(3) A thin conductive disk with an aperture perturbs the external field in the vicinity of its location on the characteristic scale $L \sim \sqrt[3]{(R_1 + R_2)(R_1^2 + R_2^2)}$.

Now consider a $\cap$-shaped time-pulse of the external field. There can be two different cases:

(A). *Slow-varying field.* The characteristic width of the attenuation factor versus frequency curve, $g(f)$, can be used to estimate the diffusion time, τ_{diff}, i. e. characteristic time required for the magnetic field with a step-like time dependence to soak (diffuse) through the conductive plate. If the external magnetic field rises to its maximum value on a time-scale longer than or of the order of the diffusion time, $T_{rise} > \tau_{diff}$, eddy-currents in the plate follow the time-pattern of the external field, and we can apply eq-n (1) with $g(f)$ shown in Fig. D3 to estimate the field produced by the FEP, substituting $1/(4T_{rise}) \rightarrow f$. For previously considered $R_1 = 3"$, $R_2 = 9"$, and $\Delta = 1/16"$, we can estimate $\tau_{diff} \sim 1/f_{0.1} - 1/f_{1/2} = 84 - 500 \mu sec$. Thus, for an external field rising on a scale $T_{rise} \sim 250\ \mu sec$, which is characteristic for the cusp, bias, and guide fields in FRX-L, we can roughly apply eq-n (1) with $f \sim 1$ kHz to obtain: $g' \sim 0.85$. For $R_2 = 12"$ we have $g' \sim 0.78$. From these examples we conclude that the FEP with the above dimensions will not significantly perturb the slow-varying bias, guide, or cusp fields in FRX-L. The strongest effects of the FEPs in our design will be on the field produced by the first guide coil and the cusp coil, because these coils are located right next to the corresponding FEPs. The FEPs can affect the fields produced by these coils by ~20%. The simplest way to take into account the effects of these FEPs is to increase the currents

in the cusp and/or the first guide coils by ~25%. Whether this measure is required can be decided later, in the course of the actual experiments.

(B). *Fast-varying field*. If, on the contrary, the external field rises on a very short time scale, $T_{rise} << \tau_{diff}$, the eddy-currents in the plate will not have sufficient time to distribute properly in the plate, and will be induced over the entire plate thickness. The external field will not diffuse through the plate effectively, and the total screened field in the center of the plate will not rise even to the level of $g'B_0$. In this case, we can roughly estimate the effective attenuation factor in the center of the plate as $g'' = \dfrac{T_{rise}}{\tau_{diff}} g'$. Then, the field produced by the plate on the axis can be approximated as:

$$\frac{B^{FEP}(z, r = 0)}{B_0} \sim -\left(1 - \frac{T_{rise}}{\tau_{diff}} g'\right) G(z), \tag{4}$$

where $G(z) = \dfrac{1}{(R_2 - R_1)}\left(\dfrac{2z^2 + R_2^2}{\sqrt{z^2 + R_2^2}} - \dfrac{2z^2 + R_1^2}{\sqrt{z^2 + R_1^2}}\right)$.

For an external field rising on a scale $T_{rise} \sim 4\,\mu sec$, which is characteristic for the main FRC field, and the previously considered parameters of the plate we obtain $g'' \sim 0.0027 - 0.016$ for $R_2 = 9"$, and $g'' \sim 0.002 - 0.012$ for $R_2 = 12"$ (which is actually used in the design shown in Fig. D1). Thus, we conclude that the FEP with such parameters should be able to provide sufficient protection for the cusp and the first guide coils from the fast rising main (theta) field. Note that such field reduction is realized not only at the centers of the FEPs, which in our design clad the protected cusp/guide coils, but also at the distance of about $\pm R_2$ from the centers of the FEPs. In our design that means protection at about $\pm 12"$, while the thickness of the protected coils is only 3".

With all of the above in mind, we can calculate the axial profiles of the magnetic field produced by all coils and FEPs on the axis of the FRX-L during the field preparation stage and the field reversal stage [Figs. E4 (a) and (b)]. Note that FEPs create considerable fields only during the fast field reversal stage, when the field produced by the theta coils changes the polarity within several microseconds, while the fields produced by all other coils remain almost unchanged.
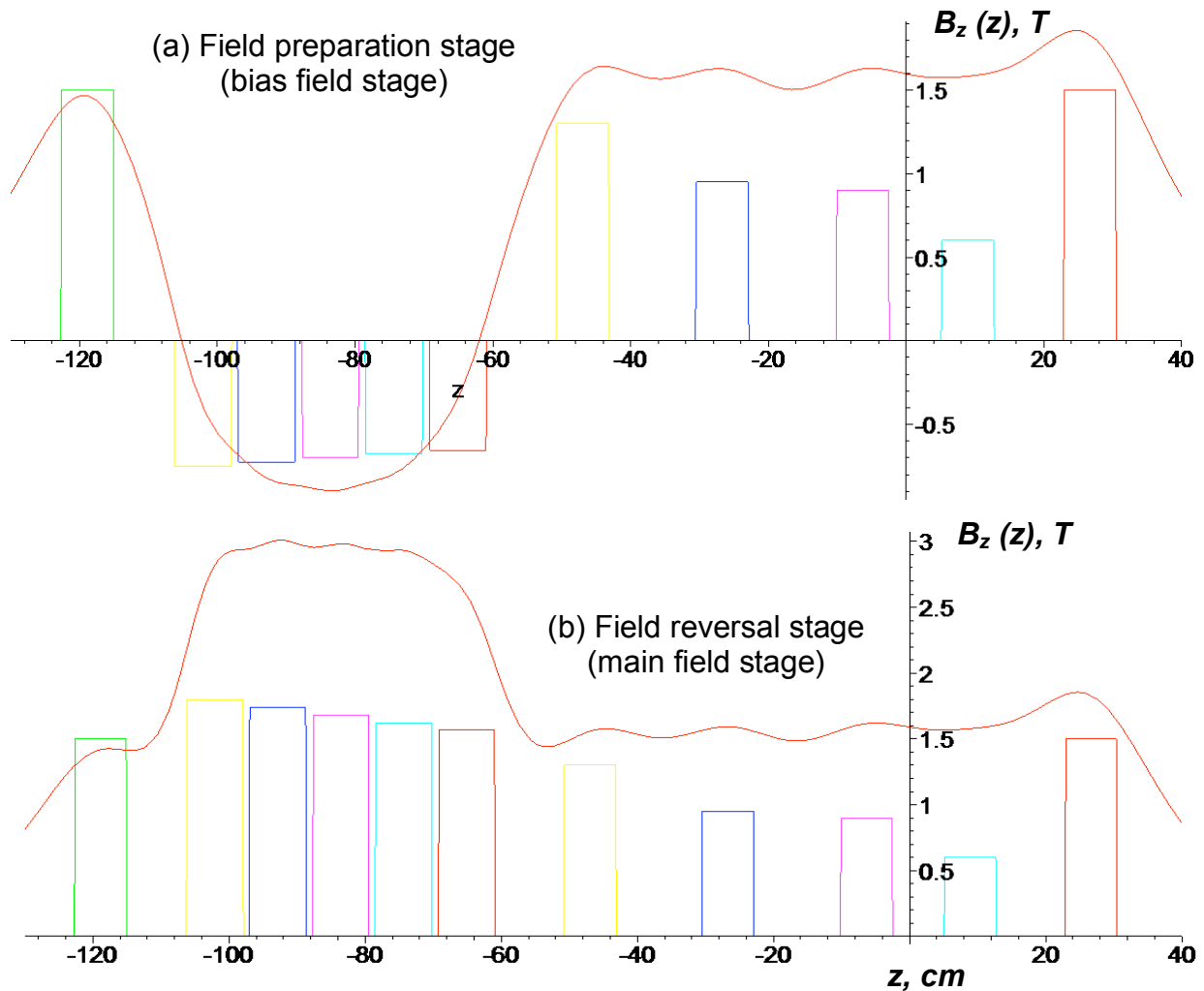
Figure E4. The axial profile of the magnetic field on the axis of FRX-L, at some point in time during (a) field preparation stage, and (b) immediately following field reversal stage. The width and location of the bars indicate those of the actual magnetic coils, and the height of each bar indicates the field produced by the corresponding coil in its center.

Note that during the field reversal stage, the FEPs reduce the main field and protect the cusp and the first guide coils without producing a considerable dip in the magnetic field profile. This is an important benefit, as the dip in $Bz(z)$ would prevent FRC from translating towards the implosion region.

In conclusion, as can be seen from Figs. E4 (a) and (b), the proposed design of the magnetic coils system provides the magnetic field profile that fulfills all major requirements for successful formation, translation, and implosion of the FRC plasma.

References

ALIKHANOV, S. G., BAKHTIN, V. P., ES'KOV, A. G., KURTMULLAEV, R. KH, SEMENOV, V. N., STRIZHOV, E. F., KOZLOV, N. P., KHVESYUK, V. I., & YAMINSKIJ, A. V. 1982. Three-dimensional plasma compression in a Z-pinch liner system-transport and compression of a compact torus by a quasi-spherical liner. *Page 319 of: Proc. 9th IAEA Intl. Conference on Plasma Physics and Controlled Nuclear Fusion Research*, vol. 3.

ARMSTRONG, W. T. MORGAN, J.A. 1987. Liner-compression of magnetically-confined, FRC plasmas. *Page 683 of:* FOWLER, C.M., CAIRD, R.S., & ERICKSON, D.J. (eds), *Megagauss Technology and Pulsed Power Applications*. New York, NY: Plenum Press.

ARMSTRONG, W. T., LINFORD, R. K., LIPSON, J., PLATTS, D. A., & SHERWOOD, E. G. 1981. Field-reversed experiments (FRX) on compact toroids. *Physics of Fluids*, **24**, 2068.

ARMSTRONG, W. T., COCHRANE, J. C., COMMISSO, R. J., LIPSON, J., & TUSZEWSKI, M. 1981b. Theta -pinch ionization for field-reversed configuration formation. *Applied Physics Letters*, **38**, 680.

ARMSTRONG, W. T., HARDING, D. G., CRAWFORD, E. A., & HOFFMAN, A. L. 1982. Flux-trapping during the formation of field-reversed configurations. *Physics of Fluids*, **25**, 2121.

BARNES, D. C. 2002. Stability of long field-reversed configurations. *Physics of Plasmas*, **9**, 560.

BARNES, D. C., & SEYLER, C. E. 1979. Compact torus theory - MHD equilibrium and stability. *Page 110 of: Proc. of the US-Japan Joint Symposium on Compact Tori and Energetic Particle Injection*. Princeton, NJ: PPPL.

BARNES, D. C., SCHWARZMEIER, J. L., LEWIS, H. R., & SEYLER, C. E. 1986. Kinetic tilting stability of field-reversed configurations. *Physics of Fluids*, **29**, 2616.

BHATTACHARYYA, R., JANAKI, M. S., & DASGUPTA, B. 2001. Field-reversed configuration (FRC) as a minimum-dissipative relaxed state. *Physics Letters A*, **291**, 291.

COMMISSO, R. J., ARMSTRONG, W. T., COCHRANE, J. C., EKDAHL, C. A., LIPSON, J., LINFORD, R. K., SHERWOOD, E. G., SIEMON, R. E., & TUSZEWSKI, M. 1980. *The initial ionization stage of FRC formation*. Tech. rept. LA-8700-C. Los Alamos National Laboratory.

COOK, I., MAISONNIER, D., TAYLOR, N. P., WARD, D. J., SARDAIN, P., DI PACE, L., GIANCARLI, L., HERMSMEYER, S., NORAJITRA, P., FORREST, R., & TEAM, PPCS. 2005. European fusion Power Plant studies. *Fusion Science and Technology*, **47**, 384.

DEGNAN, J. H., TACCETTI, J. M., CAVAZOS, T., CLARK, D., COFFEY, S. K., FAEHL, R. J., FRESE, M. H., FULTON, D., GUEITS, J. C., GALE, D., HUSSEY, T. W.,

INTRATOR, T. P., KIRPATRICK, R. C., KIUTTU, G. H., LEHR, F. M., LETTERIO, J. D., LINDEMUTH, I., McCULLOUGH, W. F., MOSES, R., PETERKIN, R. E., REINOVSKY, R. E., RODERICK, N. F., RUDEN, E. L., SHLACHTER, J. S., SCHOENBERG, K. F., SIEMON, R. E., SOMMARS, W., TURCHI, P. J., WURDEN, G. A., & WYSOCKI, F. 2001. Implosion of solid liner for compression of field reversed configuration. *IEEE Transactions on Plasma Science*, **29**, 93.

DRAKE, R. P., HAMMER, J. H., HARTMAN, C. W., PERKINS, L. J., & RYUTOV, D. D. 1996. Submegajoule liner implosion of a closed field line configuration. *Fusion Technology*, **30**, 310.

EBERHAGEN, A., & GROSSMANN, W. 1971. Theta pinch experiments with trapped antiparallel magnetic fields. *Z. Physics*, **248**, p. 130.

ES'KOV, A. G., KITAEV, M. I., KURTMULLAEV, R. KH, NOVIKOV, V. M., SEMENOV, V. I., & STRIZHOV, E. F. 1981. Experiments in the 'Tor-Liner' device. *Pages L–5/319–22 of: 10th European Conference on Controlled Fusion and Plasma Physics*. Petit-Lancy, Switzerland: European Phys. Soc.

ES'KOV, A. G., KOZLOV, N. P., KURTMULLAEV, R. KH, SEMENOV, V. N., KHVESYUK, V. I., & YAMINSKII, A. V. 1983. Energy balance in a system with quasispherical liner compression. *Pis'ma v Zhurnal Tekhnicheskoi Fizika*, **9**, 38.

FAEHL, R. J., SHEEHEY, P. T., REINOVSKY, R. E., LINDEMUTH, I. R., BUYKO, A. M., CHERNYSHEV, V. K., GARANIN, S. F., MOKHOV, V. N., & YAKUBOV, V. B. 1997. Modeling and analysis of the high energy liner experiment, HEL-1. *Digest of Technical Papers-IEEE International Pulsed Power Conference*, **2**, 1375.

FEINBERG, B. 1976. Experimental study of hot plasma in contact with a cold wall. *Plasma Physics and Controlled Fusion*, **18**, 265.

GERWIN, R. A., & MALONE, R. C. 1979. Adiabatic plasma heating and fusion-energy production by a compressible fast liner. *Nuclear Fusion*, **19**, 155.

GRABOWSKI, CRIS, DEGNAN, JAMES H., GALE, DONALD G., INTRATOR, TOM P., TACCETTI, J. MARTIN, WURDEN, GLEN A., CAVAZOS, T., GILMAN, C., SOMMARS, W., WAGANAAR, B., & SIEMON, R. E. 2002. Development of a high-current low-inductance crowbar switch for FRX-L. *IEEE Transactions on Plasma Science*, **30**, 1905.

GREEN, T. S. 1962. Investigation of theta pinch using magnetic pick-up loops. *Nuclear Fusion*, **2**, 92.

GREEN, T. S., & NEWTON, A. A. 1966. Diffusion of antiparallel bias magnetic field during initial stages of theta-pinch. *Physics of Fluids*, **9**, 1386.

GRIBBLE, R. F., LITTLE, E. M., & QUINN, W. E. 1967. Faraday rotation measurement on the SCYLIA IV theta-pinch. *In: Proc. APS Topical Conference on Pulsed High-Density Plasmas*.

HARMS, H. F. 2000. Using wire grid structures in the combination of uniform geometric theory of diffraction and method of moments for near-field analysis. *Radio Science*, **35**, 639.

HOFFMAN, A. L., & SLOUGH, J. T. 1993b. Field reversed configuration lifetime scaling based on measurements from the Large s Experiment. *Nuclear Fusion*, **33**, 27.

HOFFMAN, A. L., MILROY, R. D., SLOUGH, J. T., & STEINHAUER, L. C. 1986. Formation of field-reversed configurations using scalable, low-voltage technology. *Fusion Technol*, **9**, 48.

INTRATOR, T., TACCETTI, M., CLARK, D. A., DEGNAN, J. H., GALE, D., COFFEY, S., GARCIA, J., RODRIGUEZ, P., SOMMARS, W., MARSHALL, B., WYSOCKI, F., SIEMON, R., FAEHL, R., FORMAN, K., BARTLETT, R., CAVAZOS, T., FAEHL, R. J., FORMAN, K., FRESE, M. H., FULTON, D., GUEITS, J. C., HUSSEY, T. W., KIRKPATRICK, R., KIUTTU, G. F., LEHR, F. M., LETTERIO, J. D., LINDEMUTH, I., MCCULLOUGH, W., MOSES, R., PETERKIN, R. E., REINOVSKY, R. E., RODERICK, N. F., RUDEN, E. L., SCHOENBERG, K. F., SCUDDER, D., SHLACHTER, J., & WURDEN, G. A. 2002. Experimental measurements of a converging flux conserver suitable for compressing a field reversed configuration for magnetized target fusion. *Nuclear Fusion*, **42**, 211.

INTRATOR, T., ZHANG, S.Y., DEGNAN, J.H., FURNO, I., GRABOWSKI, C., HSU, S.C., RUDEN, E.L., SANCHEZ, P.G., TACCETTI, J.M., & TUSZEWSKI, M. 2004. A high density field reversed configuration (FRC) target for magnetized target fusion: first internal profile measurements of a high density FRC. *Physics of Plasmas*, **11**, 2580.

ISHIDA, A., KANNO, R., & STEINHAUER, L. C. 1992. Tilt stability of a gyroviscous field-reversed configuration with realistic equilibria. *Physics of Fluids B*, **4**, 1280.

JARBOE, T. R. 1994. Review of spheromak research. *Plasma Physics and Controlled Fusion*, **36**, 945.

KALECK, A., KEVER, H., KOENEN, L., NOLL, P., SUGITA, K., WAELBROECK, F., & WITULSKI, H. 1967 (1967). *Study of trapped reversed field configurations in a linear theta pinch experiment.* Tech. rept. LA-3770. Los Alamos National Laboratory.

KALECK, A., KONEN, L., NOLL, P., SUGITA, K., WAELBROECK, F., WATANABE, K., & WITULSKI, H. 1969. Limitation of the confinement of plasma in a linear theta-pinch with trapped reverse magnetic field. *Plasma Physics and Controlled Fusion*, 581.

KEVER, H. 1962. Theory of dynamical behavior of plasmas with internal magnetic fields during magnetic compression - Comparison with experiments. *Nuclear Fusion*, 613.

KIRKPATRICK, R. C., LINDEMUTH, I. R., & WARD, M. S. 1995. Magnetized target fusion: An overview. *Fusion Technology*, **27**, 201.

KUTUZOV, M. I., SEMENOV, V. N., & STRIZHEV, V. F. 1981. Trapping of magnetic flux in the formation of a compact toroid. *Fizika Plazmy*, **7**, 943.

LEBEDEV, A. I., NIZOVTEV, P. N., & RAEVSKII, V. A. 1993. *Computational, theoretical and experimental investigations of Rayleigh-Taylor instability in solids.* presented at the 4th International Workshop on the Physics of Compressible Turbulent Mixing in Cambridge, England.

LINDEMUTH, I., & KIRKPATRICK, R. 1991. *The promise of magnetized fuel: high gain in inertial confinement fusion.* Tech. rept. LA-UR-91-2498. Los Alamos National Laboratory.

LINDEMUTH, I. R., & WIDNER, M. M. 1981. Magnetohydrodynamic behavior of thermonuclear fuel in a preconditioned electron beam imploded target. *Physics of Fluids*, **24**, 746.

LINDEMUTH, I. R., PETTIBONE, J. S., STEVENS, J. C., HARDING, R. C., KRAYBILL, D. M., & SUTER, L. J. 1978. Unstable behavior of hot, magnetized plasma in contact with a cold wall. *Physics of Fluids*, **21**, 1723.

LINDEMUTH, I. R., REINOVSKY, R. E., CHRIEN, R. E., CHRISTIAN, J. M., EKDAHL, C. A., GOFORTH, J. H., HAIGHT, R. C., IDZOREK, G., KING, N. S., KIRKPATRICK, R. C., LARSON, R. E., MORGAN, G. L., OLINGER, B. W., OONA, H., SHEEHEY, P. T., SHLACHTER, J. S., SMITH, R. C., VEESER, L. R., WARTHEN, B. J., YOUNGER, S. M., CHERNYSHEV, V. K., MOKHOV, V. N., DEMIN, A. N., DOLIN, Y. N., GARANIN, S. F., IVANOV, V. A., KORCHAGIN, V. P., MIKHAILOV, O. D., MOROZOV, I. V., PAK, S. V., PAVLOVSKII, E. S., SELEZNEV, N. Y., SKOBELEV, A. N., VOLKOV, G. I., & YAKUBOV, V. A. 1995. Target plasma formation for magnetic compression/magnetized target fusion. *Physical Review Letters*, **75**, 1953.

MCLEAN, E. A., ANDERSON, A. D., & CRIEM, H. R. 1967 (1967). *Measurement of plasma density and particle losses in a large theta pinch.* Tech. rept. LA-3770. Los Alamos National Laboratory.

MEIER, W. R. 2005. Update on progress and current research in the development of heavy ion fusion. *Fusion Science and Technology*, **47**, 616.

MILROY, R. D., & BRACKBILL, J. U. 1982. Numerical studies of a field-reversed theta-pinch plasma. *Physics of Fluids*, **25**, 775.

MOIR, R. W., BIERI, R. L., CHEN, X. M., DOLAN, T. J., HOFFMAN, M. A., HOUSE, P. A., LEBER, R. L., LEE, J. D., LEE, Y. T., LIU, J. C., LONGHURST, G. R., MEIER, W. R., PETERSON, P. F., PETZOLDT, R. W., SCHROCK, V. E., TOBIN, M. T., & WILLIAMS, W. H. 1994. HYLIFE-II: a molten-salt inertial fusion energy power plant design-final report. *Fusion Technology*, **25**, 5.

MOIR, R. W., BULMER, R. H., GULEC, K., FOGARTY, P., NELSON, B., OHNISHI, M., RENSINK, M., ROGNLIEN, T. D., SANTARIUS, J. F., & SZE, D. K. 2001. Thick liquid-walled, field-reversed configuration-magnetic fusion power plant. *Fusion Technology*, **39**, 758.

MONTGOMERY, D., & PHILLIPS, L. 1990. Minimum dissipation states and vortical flow in MHD. *Physical Review Letters*, **38**, 2953.

MOSES, R., KRAKOWSKI, R. A., & MILLER, R. L. 1979. *A conceptual design of the fast-liner reactor for fusion power.* Tech. rept. LA-7686-MS. Los Alamos National Laboratory.

NIBLETT, G. B. F., & GREEN, T. S. 1959. Radial hydromagnetic oscillations. *Proceedings of the Physical Society of London*, **74**, 737.

OLSON, C., ROCHAU, G., SLUTZ, S., MORROW, C., OLSON, R., CUNEO, M., HANSON, D., BENNETT, G., SANFORD, T., BAILEY, J., STYGAR, W., VESEY, R., MEHLHORN, T., STRUVE, K., MAZARAKIS, M., SAVAGE, M., POINTON, T., KIEFER, M., ROSENTHAL, S., COCHRANE, K., SCHNEIDER, L., GLOVER, S., REED, K., SCHROEN, D., FARNUM, C., MODESTO, M., OSCAR, D., CHHABILDAS, L., BOYES, J., VIGIL, V., KEITH, R., TURGEON, M., CIPITI, B., LINDGREN, E., DANDINI, V., TRAN, H., SMITH, D., MCDANIEL, D., QUINTENZ, J., MATZEN, M. K., VANDEVENDER, J. P., GAUSTER, W., SHEPHARD, L., WALCK, M., RENK, T., TANAKA, T., ULRICKSON, M., MEIER, W., LATKOWSKI, J., MOIR, R., SCHMITT, R., REYES, S., ABBOTT, R., PETERSON, R., POLLOCK, G., OTTINGER, P., SCHUMER, J., PETERSON, P., KAMMER, D., KULCINSKI, G., EL-GUEBALY, L., MOSES, G., SVIATOSLAVSKY, I., SAWAN, M., ANDERSON, M., BONAZZA, R., OAKLEY, J., MEEKUNASOMBAT, P., DE GROOT, J., JENSEN, N., ABDOU, M., YING, A., CALDERONI, P., MOREY, N., ABDEL-KHALIK, S., DILLON, C., LASCA, C., SADOWSKI, D., CURRY, R., MCDONALD, K., BARKEY, M., SZAROLETTA, W., GALLIX, R., ALEXANDER, N., RICKMAN, W., CHARMAN, C., SHATOFF, H., WELCH, D., ROSE, D., PANCHUK, P., LOUIE, D., DEAN, S., KIM, A., NEDOSEEV, S., GRABOVSKY, E., KINGSEP, A., & SMIMOV, V. 2005. Development path for Z-pinch IFE. *Fusion Science and Technology*, **47**, 633.

PARKER, J. 1993. *A Primer on liner implosions with particular application to the Pegasus II capacitor bank.* Tech. rept. Athena No. 1. Los Alamos National Laboratory.

QI, N. S., FULGHUM, S. F., PRASAD, R. R., & KRISHNAN, M. 1998. Space and time resolved electron density and current measurements in a dense plasma focus Z-pinch. *IEEE Transactions on Plasma Science*, **26**, 1127.

QUIMBY, D. C., HOFFMAN, A. L., & VLASES, G. C. 1981. LINUS cycle calculations including plasma transport and resistive flux loss. *Nuclear Fusion*, **21**, 553.

REINOVSKY, R. E., & EKDAHL, C. A. 1996. Development of imploding liners with kinetic energies > 100 MJ and their applications. *Page 646 of:* CHERNYSHEV, V. K., SELEMIR, V. D., & PLYASHKEVICH, L. N. (eds), *Proc. 7th International Conference on Megagauss Field Generation and Related Topics.* Sarov, Russia: VNIIEF.

REJ, D. J., & TUSZEWSKI, M. 1984. A zero-dimensional transport model for field-reversed configurations. *Physics of Fluids*, **27**, 1514.

REJ, D. J., ARMSTRONG, W. T., CHRIEN, R. E., KLINGNER, P. L., LINFORD, R. K., McKENNA, K. F., SHERWOOD, E. G., SIEMON, R. E., TUSZEWSKI, M., & MILROY, R. D. 1986. Experimental studies of field-reversed configuration translation. *Physics of Fluids*, **29**, 852.

REJ, D. J., TAGGART, D. P., BARON, M. H., CHRIEN, R. E., GRIBBLE, R. J., TUSZEWSKI, M., WAGANAAR, W. J., & WRIGHT, B. L. 1992. High-power magnetic-compression heating of field-reversed configurations. *Physics of Fluids B*, **4**, 1909.

RIBE, F. L., SHERWOOD, A. R., & TELLER, E. 1981. Fast-liner-compression fusion systems. London, UK: Academic Press.

ROBSON, A. E. 1980. A conceptual design for an imploding-liner fusion reactor. *Pages 425–436 of:* TURCHI, P. J. (ed), *Proc. 2nd International Conference on Megagauss Magnetic Field Generation and Related Topics*. New York, NY, USA: Plenum.

RYUTOV, D. D., & SIEMON, R. E. 2001. Magnetized plasma configurations for fast liner implosions: A variety of possibilities. *Comments On Modern Physics*, **2**, C185.

SERCOMBE, T. B., & SCHAFFER, G. B. 2003. Rapid manufacturing of aluminum components. *Science*, **301**, 1225.

SIEMON, R., LINDEMUTH, I., & SCHOENBERG, K. F. 1999. Why magnetized target fusion offers a low-cost development path for fusion energy. *Comments On Plasma Physics Controlled Fusion*, **18**, 363.

SIEMON, R. E., ARMSTRONG, W. T., BARNES, D. C., BARTSCH, R. R., CHRIEN, R. E., COCHRANE, J. C., HUGRASS, W. N., KEWISH, R. W., JR., KLINGNER, P. L., LEWIS, H. R., LINFORD, R. K., McKENNA, K. F., MILROY, R. D., REJ, D. J., SCHWARZMEIER, J. L., SEYLER, C. E., SHERWOOD, E. G., SPENCER, R. L., & TUSZEWSKI, M. 1986. Review of the Los Alamos FRX-C experiment. *Fusion Technology*, **9**, 13.

SLOUGH, J. T., & HOFFMAN, A. L. 1993. Stability of field-reversed configurations in the large s experiment (LSX). *Physics of Fluids B*, **5**, 4366.

SLOUGH, J. T., & HOFFMAN, A. L. 1997. Acceleration of a field reversed configuration for central fueling of ITER. *Proceeding Series of the International Atomic Energy Agency*, 237.

SLOUGH, J. T., HOFFMAN, A. L., MILROY, R. D., CRAWFORD, E. A., CECIK, M., MAQUEDA, R., WURDEN, G. A., ITO, Y., & SHIOKAWA, A. 1992. Confinement and stability of plasmas in a field-reversed configuration. *Physical Review Letters*, **69**, 2212.

SLOUGH, J. T., HOFFMAN, A. L., MILROY, R. D., MAQUEDA, R., & STEINHAUER, L. C. 1995. Transport, energy balance, and stability of a large field-reversed configuration. *Physics of Plasmas*, **2**, 2286.

SPENCER, R. L., TUSZEWSKI, M., & LINFORD, R. K. 1983. Adiabatic compression of elongated field-reversed configurations. *Physics of Fluids*, **26**, 1564.

STEINHAUER, L. C. 1992. Electron thermal confinement in the edge plasma of a field-reversed configuration. *Physics of Fluids B*, **4**, 4012.

STEINHAUER, L. C., & ISHIDA, A. 1997. Relaxation of a two-species magnetofluid. *Physical Review Letters*, **79**, 254.

TACCETTI, J. M., INTRATOR, T. P., WYSOCKI, F. J., FORMAN, K. C., GALE, D. G., COFFEY, S. K., & DEGNAN, J. H. 2002. Magnetic field measurements inside a converging flux conserver for magnetized target fusion applications. *Fusion Science and Technology*, **41**, 13.

TACCETTI, J. M., INTRATOR, T. P., WURDEN, G. A., ZHANG, S. Y., ARAGONEZ, R., ASSMUS, P. N., BASS, C. M., CAREY, C., DEVRIES, S. A., FIENUP, W. J., FURNO, I., HSU, S. C., KOZAR, M. P., LANGNER, M. C., LIANG, J., MAQUEDA, R. J., MARTINEZ, R. A., SANCHEZ, P. G., SCHOENBERG, K. F., SCOTT, K. J., SIEMON, R. E., TEJERO, E. M., TRASK, E. H., TUSZEWSKI, M., WAGANAAR, W. J., GRABOWSKI, C., RUDEN, E. L., DEGNAN, J. H., CAVAZOS, T., GALE, D. G., & SOMMARS, W. 2003. FRX-L: a field-reversed configuration plasma injector for magnetized target fusion. *Review of Scientific Instruments*, **74**, 4314.

THIO, Y. C. F., PANARELLA, E., KIRKPATRICK, R., KNAPP, C. E., WYSOCKI, F., & SCHMIDT, G. R. 1999. Magnetized target fusion in a spheroidal geometry with standoff drivers. *In:* PANARELLA, E. (ed), *Current Trends in International Fusion Research: Proceedings of the Second Symposium*. Ottawa, Canada: National Research Council Canada.

TURCHI, P. J., COOPER, A. L., FORD, R., & JENKINS, D. J. 1976. Rotational stabilization of an imploding liquid cylinder. *Physical Review Letters*, **36**, 1546.

TURCHI, P. J., COOPER, A. L., FORD, R. D., JENKINS, D. J., & BURTON, R. L. 1980. Review of the NRL liner implosion program. *Page 375 of:* TURCHI, P. J. (ed), *Proceedings of the Second International Conference on Megagauss Magnetic Field Generation and Related Topics*. New York, NY: Plenum.

TUSZEWSKI, M. 1988a. Field reversed configurations. *Nuclear Fusion*, **28**, 2033.

TUSZEWSKI, M. 1988b. A semiempirical formation model for field-reversed configurations. *Physics of Fluids*, **31**, 3754.

TUSZEWSKI, M., BARNES, D. C., CHRIEN, R. E., COBB, J. W., REJ, D. J., SIEMON, R. E., TAGGART, D. P., & WRIGHT, B. L. 1991a. Observations of tilt instabilities in field-reversed configurations of a confined plasma. *Physical Review Letters*, **66**, 711.

TUSZEWSKI, M., TAGGART, D. P., CHRIEN, R. E., REJ, D. J., SIEMON, R. E., & WRIGHT, B. L. 1991b. Axial dynamics in field-reversed theta pinches. II. Stability. *Physics of Fluids B*, **3**, 2856.

WAGANAAR, W. J., COCHRANE, J. C., HOSACK, K. W., INTRATOR, T., SANCHEZ, P. G., TACCETTI, J. M., THOMPSON, M. C., & GRABOWSKI, C. 2002. *Design and*

performance of the prefire detection system for the FRX-L main capacitor bank. Tech. rept. LA-UR-02-7660. Los Alamos National Laboratory.

WAGANER, L. M., DEUSER, D. A., SLATTERY, K. T., WILLE, G. W., ARCELLA, F., & CLEVELAND, B. 2003. Ultra-low cost coil fabrication approach for ARIES-ST. *Fusion Engineering and Design*, **65**, 339.

WIRA, K., & PIETRZYK, Z.A. 1990. Toroidal field generation and magnetic field relaxation in a conical theta pinch generated configuration. *Physics of Fluids B*, **2**, 561–573.

WURDEN, G. A., SCHOENBERG, K. F., SIEMON, R. E., TUSZEWSKI, M., WYSOCKI, F. J., & MILROY, R. E. 1998. Magnetized target fusion: a burning FRC plasma in an imploded metal can. *Pages 238–41 of:* IGUCHI, H., SATO, T., TOMITA, Y., & ISHIGURO, S. (eds), *9th International Toki Conference on Plasma Physics and Controlled Nuclear Fusion.* Nagoya, Japan: Japan Soc. Plasma Sci. & Nucl. Fusion Res.

WURDEN, G. A., INTRATOR, T. P., CLARK, D. A., MAQUEDA, R. J., TACCETTI, J. M., WYSOCKI, F. J., COFFEY, S. K., DEGNAN, J. H., & RUDEN, E. L. 2001. Diagnostics for a magnetized target fusion experiment. *Review of Scientific Instruments*, **72**, 552.

WURDEN, G. A., INTRATOR, T. P., ZHANG, S. Y., FURNO, I. G., HSU, S. C., PARK, J., KIRKPATRICK, R., RENNEKE, R. M., SCHOENBERG, K. F., TACCETTI, M. J., TUSZEWSKI, M. G., WAGANAAR, W. J., WANG, Z., SIEMON, R. E., DEGNAN, J. H., GALE, D. G., GRABOWSKI, C., RUDEN, E. L., SOMMARS, W., FRESE, M. H., COFFEY, S., CRADDOCK, G., FRESE, S. D., & RODERICK, N. F. 2004. FRC plasma studies on the FRX-L plasma injector for magnetized target fusion. *In: Proc. 20th IAEA Fusion Energy Conference.* Vilamoura, Portugal: IAEA.

ZHANG, S. Y., TEJERO, E. M., TACCETTI, J. M., WURDEN, G. A., INTRATOR, T. P., WAGANAAR, W. J., & PERKINS, R. 2004. Separatrix radius measurement of field-reversed configuration plasma in FRX-L. *Review of Scientific Instruments*, **75**, 4289.

ZHANG, S. Y., INTRATOR, T.P., WURDEN, G.A., WAGANAAR, W.J., TACCETTI, J.M., RENNEKE, R., GRABOWSKI, C., & RUDEN, E. 2005. Confinement analyses of the high density field reversed configuration plasma in the field reversed configuration experiment with a liner. *Physics of Plasmas*, **12**, 052513.